CORTICOFUGALLY INDUCED *c-fos* EXPRESSION, SYNCHRONIZED OSCILLATION AND ITS PROPAGATION IN THE THALAMUS

GUO YIPING

SUPERVISOR: PROFESSOR JUFANG HE

A thesis submitted in partial fulfillment of the requirements for the Degree of Doctor of Philosophy

Department of Rehabilitation Sciences
The Hong Kong Polytechnic University

June 2008

CERTIFICATE OF ORIGINALITY

I hereby declare that this thesis is my own work and that, to the best of my knowledge and belief, it reproduces no material previously published or written, nor material that has been accepted for the award of any other degree or diploma, except where due acknowledgement has been made in the text.

_____(Signature of Candidate)

_____(Name of Candidate)

Abstract of thesis entitled "Corticofugally induced c-fos expression, synchronized oscillation and its propagation in the thalamus" submitted by Guo Yiping for the degree of Doctor of Philosophy at the Hong Kong Polytechnic University in January 2008

Abstract

A variety of fast and slow rhythmic brain oscillations have been revealed to occur spontaneously during different behavioral states. Fast rhythms are associated with cognition, and slow rhythms (e.g. spindle, 7-15 Hz; delta, 1-4 Hz; slow oscillation, 0.3-1 Hz) define the slow-wave sleep. However, the precise cellular and synaptic mechanisms underlying these different rhythms remain unclear and much controversial despite intensive investigations in the past two decades. Even little evidence is available in the auditory system.

The present study investigated the mechanisms underlying the generation, synchronization and propagation of the spontaneous slow rhythms (< 15 Hz) in the corticothalamic networks within a given modality and across different modalities in animals under anesthesia by using multi-channel extracellular recordings and immunohistochemical method.

In an attempt to study the contribution of the corticofugal projection to thalamic neurons in the ascending auditory circuitry by using Fos as an activity marker, we ascertained for the first time, the presence of dense Fos positive neurons in the ventral division (MGv) of medial geniculate body (MGB) after the auditory cortex (AC) was activated by injection of bicuculline methobromide (BIM), a $GABA_A$ receptor antagonist. We further investigated the relationship between *c-fos* expression in the MGB and corticofugal activation, as well as its pathway

and related neurotransmitters and receptor-types. The result indicated that *c-fos* expression in the MGv was triggered by corticofugal projections, specific to the cortitothalamic activation. *C-fos* expression could be elicited in the MGB with direct injection of glutamate in certain conditions, but never with acetylcholine. Moreover, direct injections of antagonists for all three glutamate receptor types, NMDA, AMPA and metabotropic glutamate receptors into MGB, have a determining effect in eliminating the cortically induced *c-fos* expression in the MGv.

Multiple electrode recordings showed that BIM injection in the AC triggered synchronized oscillatory activities (0.3-3 Hz, mainly in 1-3 Hz) with burst firing patterns recurring sequentially in the AC and MGB. The animals with the thalamic reticular nucleus (TRN) lesioned by kainic acid, showed no difference in the slow synchronized oscillation in both the thalamus and the neocortex, when compared to that of the un-lesioned animals. Cortically induced *c-fos* expression in the MGv was not affected by the TRN lesion, either. These results indicated that the corticothalamic synchronized oscillation evoked by cortical hyperactivity was not mediated by a pathway involving the TRN. The results would probably provide us more thought about the traditional notion that all the thalamic oscillations are associated with the hyperpolarizations derived from TRN.

We examined MGv neurons under three different conditions: repeatedly acoustically-stimulated, directly chemically-evoked and corticofugally evoked.

Only animals with cortical activation showed *c-fos* expression in the MGv, though MGv neurons showed similar firing rate for all three conditions. The present results concluded that *c-fos* expression in the MGv was not simply associated with firing rate, but with the firing pattern. The synchronized corticothalamic activities with burst firings were proposed to lead *c-fos* expression in the MGv because of the strong association between them. The bicuculline-induced bursts were different from the spindle LTS bursts. The association between *c-fos* expression in the principle thalamic nuclei and the synchronized slow oscillations in the corticothalamic network was also envisioned in other sensory corticothalamic circuitry, e.g. visual and somatosensory systems.

We next investigated the propagations of slow rhythms in the corticothalamic networks *in vivo* within a given modality and across different modalities. Sleep- or anesthesia- related slow rhythms and the bicuculline-induced slow oscillations were considered in the present study. We found that slow oscillations typically propagated along the rostrocaudal direction in the dorsal thalamus when the cortex was activated with BIM injection. The same propagation in the corticothalamic network was also observed from animals under anesthesia without cortical BIM injection. During this process, the activity in cerebral cortex is always preceding that of the thalamic sites, at least within the same modality. The slow oscillations can be of global distributions, showing nearly-simultaneous EEG or burst discharges in the bilateral hemispheres, or

more local events of modality-dependence, recurring independently in different modality systems. However, this modality-specific asynchrony is seldom observed among the TRN sites of different modalities, indicating strong intranuclear connections within the TRN. The results would propose that common principles probably governed the spatiotemporal patterns of different oscillation types.

In summary, the present study revealed that *c-fos* expression in the MGB could be triggered by corticofugal activation. Cortically induced *c-fos* expression in the MGB was not mediated by the pathway via the TRN. *C-fos* expression in MGv was not simply associated with the firing rate, but the firing pattern. Burst-firings of possibly high-threshold calcium spikes that were synchronized with the cortical oscillation are proposed to lead *c-fos* expression in the MGB. Slow oscillations in the corticothalamic network typically propagated along the rostrocaudal direction in the dorsal thalamus. The common principles probably governed the spatiotemporal patterns of different oscillation types. All in all, experimental evidence provided by the present study would further our understanding on the generation and propagation of synchronized excitability within the corticothalamic network of specific modality and across modalities.

Relevant Publications

Journal papers:

Guo YP, Sun X, Li C, Wang NQ, Chan Y-S, He J. Corticothalamic synchronization leads to *c-fos* expression in the auditory thalamus. **Proc Natl Acad Sci USA**. 2007 104(28):11802-7.

Sun X, **Guo YP**, Chan Y-S, He J. Cortical activation induced Fos expression and neuronal activity in auditory thalamus and midbrain at different timings after bilateral cochlear ablation (submitted).

Conference papers:

Guo YP, Sun X, Li C, Wang NQ, Chan Y-S, He J. Fos expression in the auditory thalamus is triggered by corticofugal projections. *The 36th annual meeting of Society for neuroscience, Atlanta, Georgia, United States, October 14-18, 2006.*

Li C, **Guo YP**, Chan Y-S, He J. Postnatal development of corticofugal modulation in the auditory thalamus in rats. *The 36th annual meeting of Society for neuroscience, Atlanta, Georgia, United States, October 14-18, 2006.*

Guo YP, Li C, Wang NQ, Sun X, Chan Y-S, He J. Cortically derived highly synchronized oscillation (0.3-3 Hz) in the auditory thalamus is via the direct excitatory pathway rather than the thalamic reticular nuclei. *The 4th Congress of Federation of Asian-Oceanian Neuroscience Societies, Hong Kong, November*

30-December 2, 2006

Li CH, **Guo YP**, Meng XK, Chan Y-S, He J. The oscillations in the thalamic reticular nucleus, auditory thalamus and cortex. *The 37th annual meeting of Society for neuroscience, San Die*go, *California, United States, November 3-7, 2007.*

Acknowledgements

The lines of this text are to all those who helped to make this thesis possible.

First of all, I would like to thank my supervisor, Dr. Jufang He, for his constructive guidance and support for this research. Without his encouragement, knowledge and perceptiveness I would never have finished my study. Thanks to my examiners, for managing to read the whole thing so thoroughly and providing all the advice and suggestions.

I sincerely thank Simon S.M. Chan and Kimmy F.L. Tsang of the University of Hong Kong for their excellent technical assistances.

Thanks to Ms. Liu Chunhua, Ms. Zhang Zhuo, Mr. Wang Ningqian, Dr. Li Chuan and all the other people that I have worked with, in the laboratory, during the course of my studies. Thanks also to all my friends in Hong Kong and elsewhere, for keeping me company and encouraging me through the difficult times that came my way.

I heartily thank my experimental animals. Their sacrifice is priceless in terms of the contribution to our understanding of neuroscience, which has undoubtedly formed the foundation for future human studies.

Most importantly, I would like to thank my wife, my parents and my sister, for their love, patience and continuous support during the whole PhD period.

The study summarized in this thesis was supported by the Hong Kong Polytechnic University.

Guo Yiping

Jan. 2008

Table of Contents

List of figures and tables

List of abbreviations

5-HT: serotonin

Ach: acetylcholine

AHP: after-hyperpolarization

AC: auditory cortex

AI: Primary auditory field

AII: secondary auditory cortical field

AIII: third auditory cortical field

AAF: anterior auditory field

AMPA: alpha-amino-3-hydroxy-5-methyl-4-isoxazole propionic acid

AP-V: (2*R*)-amino-5-phosphonovaleric acid, also APV

BIM: bicuculline methobromide

CF: characteristic frequencies

CNQX: 6-cyano-7-nitroquinoxaline-2,3-dione

CT: corticothalamic

EEG: electroencephalography

MEG: magnetoencephalography

EPSP: excitatory postsynaptic potential

FPP: fast prepotential

FRB: fast rhythmic bursting

GABA: γ-aminobutyric acid

HA: histamine

IC: inferior colliculus

IGL: intergeniculate leaf,

I_h: hyperpolarization-activated current

$I_{Na(p)}$: persistent Na^+ current

I_T: low threshold Ca^{2+} or T-current

i.p.: intraperitoneal

IPSP: inhibitory postsynaptic potential

KA: kainic acid

LDT: laterodorsal tegmental nucleus

LFP: local field potential

LGN: lateral geniculate nucleus

dLGN: dorsal division of LGN

vLGN: ventral division of LGN

LTS: low threshold calcium spikes

MGB: medial geniculate body

MGv: ventral division of MGB

MGd: dorsal division of MGB

MGm: medial division of MGB

NE: norepinephine

NMDA: *N*-methyl *D*-aspartate

PPT: pedunculopontine tegmental nucleus

REM: rapid-eye-movement

NREM: non-REM

SC: somatosensory cortex

s.c.: subcutaneous

SPL: sound pressure level

SWS: slow-wave sleep

TRN: thalamic reticular nucleus

TC: thalamocortical

VB: ventrobasal nucleus

VPL: ventroposterolateral nucleus

VC: visual cortex

Vm: membrane potential

Chapter 1

Introduction

1.1 Background of the study

The brain electrical activity has been widely explored in mammalians and humans for a long time. Multi-site, extracellular and intracellular recordings from the neocortex and thalamus during different states of vigilance revealed a variety of fast and slow rhythmic oscillations spontaneously occurring in the corticothalamic network. These neural activities are state-dependent: three slow rhythms[1] (spindle, 7-15 Hz; delta, 1-4 Hz; slow oscillation, 0.3-1 Hz) define the slow-wave sleep (SWS), and two fast rhythms (beta, 20-30 Hz; gamma, 30-60 Hz) are prevalent during the brain-active states of waking and rapid-eye-movement (REM) sleep (Steriade et al., 1993b; Contreras and Steriade, 1996; Steriade et al., 1996a; Amzica and Steriade, 1997).

Far from being epiphenomena, it appears that spontaneous brain rhythms during different states of vigilance may lead to increased responsiveness and plastic changes in the strength of connections among neurons, a mechanism through which information is stored (Lee and Wilson, 2002; Steriade and Timofeev, 2003; Ji and Wilson, 2007; Rasch and Born, 2007; Rasch et al., 2007). Slow wave sleep, which was previously regarded as associated with global inhibition of the

[1] Slow rhythms in this thesis are defined as rhythms of a frequency less than 15 Hz.

cerebral cortex and annihilation of consciousness, shows unexpectedly high levels of spontaneous neuronal activities when using intracellular recordings of cortical and thalamic cell types in naturally sleeping animals (Steriade et al., 2001). Although the thalamic gates are closed for signals from the outside world during SWS, the intracortical dialogues are maintained and even increased (Timofeev and Steriade, 1996). These data suggest that SWS, which was commonly regarded as complete brain quiescence, actually is highly coordinated and regulated, and may serve important cerebral functions, among which is the consolidation of memory traces acquired during wakefulness (Steriade and Timofeev, 2003, Rasch and Born, 2007; Lee and Wilson, 2002; Ji and Wilson, 2007; Rasch et al., 2007).

Although it has been a long time since the brain rhythms were first unraveled, it is until the recent two decades that their distinct cellular and synaptic mechanisms were not intensively investigated and elucidated, due to the introduction of simultaneous multi-site extra- and intracellular recordings from various brain areas. Studies have shown that to a certain extent, the great variety in wave frequencies and patterns is ascribed to different intrinsic and synaptic properties of cortical and thalamic neurons. The thalamus relays sensory information to the cerebral cortex with an exception of olfaction, and in return, receives massive feedback projections from the cortex (Jones, 1985; Winer and Larue, 1987; Ojima, 1994; Steriade et al., 1997). The importance of the corticothalamic projections is emphasized by the abundance of corticothalamic

axons, about one order of magnitude larger than that of thalamocortical fibers (White and Hersch, 1982). The corticothalamic projections are suggested to provide a gain-control mechanism on the transmission of sensory information (Murphy and Sillito, 1987; Villa et al., 1991; He, 2003a) and to play an important role in the generation of neural oscillations (Steriade et al., 1993a; Golshani and Jones, 1999; Bal et al., 2000).

The thalamic reticular nucleus (TRN) is situated between the cerebral cortex and the dorsal thalamus, playing an important role in controlling the flow of information between them, and is particularly well suited for the generation of spindles. All sleep-related slow rhythms are associated with prolonged hyperpolarizations of thalamic or cortical neurons, which are effective in inhibiting the transmission of afferent signals (Steriade et al., 1997). In the thalamus of rodents, the hyperpolarizations of the thalamic neurons are proven to derive from the TRN (Steriade et al., 1985). It seems that TRN stands a very central position in the thalamus functions. However, whether the TRN is really dispensable in the generations of thalamic rhythms is yet to be further investigated.

Another important feature of slow rhythms is the sustained long-range synchronization across different cortical and thalamic nuclei. Although some isolated neurons can oscillate by virtue of their intrinsic properties, in the intact brain, these different oscillations coalesce into complex and less stereotyped

rhythmic patterns due to the neuronal interactions in the corticothalamic network. Maping of slow oscillations may provide a functionally useful probe in the study of highly integrative brain functions. The orderly propagation of correlated activities along a certain pathway may play a role in the spike timing-dependent synaptic plasticity (Meister et al., 1991; Wong et al., 1993; Abbott and Nelson, 2000; Steriade and Timofeev, 2003; Rasch and Born, 2007; Rasch et al., 2007).

However, the distribution and coherence of oscillations are far more complicated and elusive than we had thought. Previous studies regarding the propagation of neuronal oscillations showed a great discrepancy. Some (Kim et al., 1995; Massimini et al., 2004) showed a high degree of spatiotemporal variability from one spindle sequence to the next, while others (Contreras et al., 1996, 1997) demonstrated that spindle sequences occurred nearly simultaneously even in distant cortical fields. The cortical-generated slow oscillations (< 1 Hz) have the virtue of grouping the other two sleep rhythms arising in the thalamus within slowly recurring wave–sequence due to the high power of the corticothalamic projections (Steriade et al., 1993c; Contreras and Steriade, 1995).

Although great progress in the study of the brain rhythms has been obtained in recent decades, little evidence is available in terms of the auditory system. A 10 Hz tone-evoked oscillation was reported in the auditory cortex (AC), medial geniculate body (MGB) and auditory TRN neurons (Cotillon et al., 2000, 2003). Recent studies from our laboratory (He, 2003b) also confirmed that the auditory corticothalamic network participates in the state-dependent forebrain rhythms.

Since the oscillation is a whole-brain activity, it is not reasonable to explore the propagation of the oscillations excluding the auditory system.

1.2 Aims of the study

Basically, the present study, by using multi-channel extracellular recordings and immunohistochemical method, seeks to investigate the mechanisms underlying the generation，synchronization and propagation of the spontaneous slow rhythms (< 15 Hz) in the corticothalamic network within a given modality (e.g. auditory) and across different modalities in animals under anesthesia.

The first specific aim of this study is to examine the effect of corticofugal modulation from the auditory cortex on the spontaneous activities of the auditory thalamus. Previous studies have shown that the ventral of the MGB (MGv) neurons never showed *c-fos* expression when activated by the ascending pathway. In present study, the corticofugal volleys, arising from cortical bicuculline injections, succeed in inducing dense *c-fos* expression in the MGv, which was associated with synchronized oscillations in the corticothalamic network. We further investigated related neurotransmitter-receptor types, and the contribution of TRN to this synchronized corticothalamic oscillation type.

The second specific aim of this study is to investigate the propagations of spontaneous slow rhythms *in vivo* in the corticothalamic network within a given modality (e.g. auditory) and/or across different modalities. Sleep- or anaestheia-

related slow rhythms (<15Hz, mainly spindle oscillations) and the bicuculline-induced slow oscillations were considered in the present study. The common principles behind the spatiotemporal patterns of different oscillation types will be discussed.

1.3 Significance of the study

The present study will provide novel insight into the mechanisms of the generation and propagation of the oscillations in the corticothalamic network, which are of fundamental role to understand the highly integrative brain processes. The study across different modalities can also offer a more general view on the brain rhythms. Basically, different brain rhythms define different states of vigilance, such as sleep and wakefulness. The results of this study can benefit us to better understand the mechanism of arousal as well as how the outside signals are blocked when sleep. Together with our previous knowledge from intracellular recordings, the present study will provide a blueprint of the excitability and connectivity in the corticothalamic network of mammals, and lead us to the entrance of understanding the organization and functional significance of the slow oscillations in the corticothalamic network.

1.4 Outline of the thesis

There are six chapters in this thesis.

Chapter 1 introduces the background and objective of this study. The significance of the present study is also mentioned in this chapter.

Chapter 2 provides a literature review of basic anatomic and physiological knowledge of corticothalamic network. The molecular, cellular and circuit or network mechanisms for the generations and synchronizations of the sleep-related oscillation types are also described.

Chapter 3 lists the methodology employed in this thesis. It explains what the primary data sources were, how data were collected, and how they were processed and interpreted.

Chapter 4 illustrates the cortical-bicuculline-induced *c-fos* expression in the MGB and its associated synchronized oscillations in the corticothalamic network. The related neurotransmitter-receptor types, and the contribution of TRN to this synchronized corticothalamic oscillation type are further explored.

Chapter 5 demonstrates the propagations of spontaneous slow rhythms *in vivo* in the corticothalamic network within modality and across modalities in terms of sleep-related slow rhythms and the bicuculline-induced slow oscillations.

Chapter 6 summarizes the findings and leads to the conclusions of the present study.

Chapter 2

Literature review

Multi-site, extracellular and intracellular recordings of the cerebral cortex and thalamus during different behavioral states reveal a variety of electrically synchronized oscillations in the corticothalamic network, including the fugacious and spatially restricted fast rhythms (20-60Hz) during arousal and REM sleep, the sustained, long-range synchronized sleep-related slow rhythms: and the abnormally increased synchrony of cortical and thalamic neurons during paroxysmal state. This chapter first describes the anatomy and physiology of the corticothalamic network, then moves to the possible molecular, cellular and circuit or network mechanisms for the generations and synchronizations of the sleep-related oscillations, as well as their functional implications.

2.1 Introduction

The cerebral cortex is constantly active, even during slow-wave sleep. Multi-site, extracellular and intracellular recordings from the neocortex and thalamus during different states of vigilance revealed a variety of electrical oscillation in the corticothalamic network (Steriade et al., 1991b; Steriade et al., 1993a; Steriade et al., 1994; Amzica and Steriade, 1995a, 1995b; Contreras and Steriade,

1995, 1996; Steriade et al., 1996a; Timofeev and Steriade, 1996; Steriade et al., 1997; Timofeev and Steriade, 1997). These neural activities are state-dependent, and spontaneously occur during different behavioral states. Three slow rhythms (spindle, 7-15 Hz, Figure 2.1, 2.2; delta, 1-4 Hz; slow oscillation, 0.3-1 Hz, Figure 2.2) define the slow-wave sleep (SWS), and two fast rhythms (beta, 20-30 Hz; gamma, 30-60 Hz, Figure 2.2) are prevalent during the brain-active states of waking and rapid-eye-movement (REM) sleep. When the brain falls asleep, electroencephalography (EEG) recordings shift from low-amplitude, high-frequency rhythms to large amplitude slow oscillations. Far from being epiphenomena, these fast and slow-frequency oscillations in the forebrain have been hypothesized to play a role in highly integrative brain functions, e.g., consciousness, attentive perception, as well as synapse plasticity and memory.

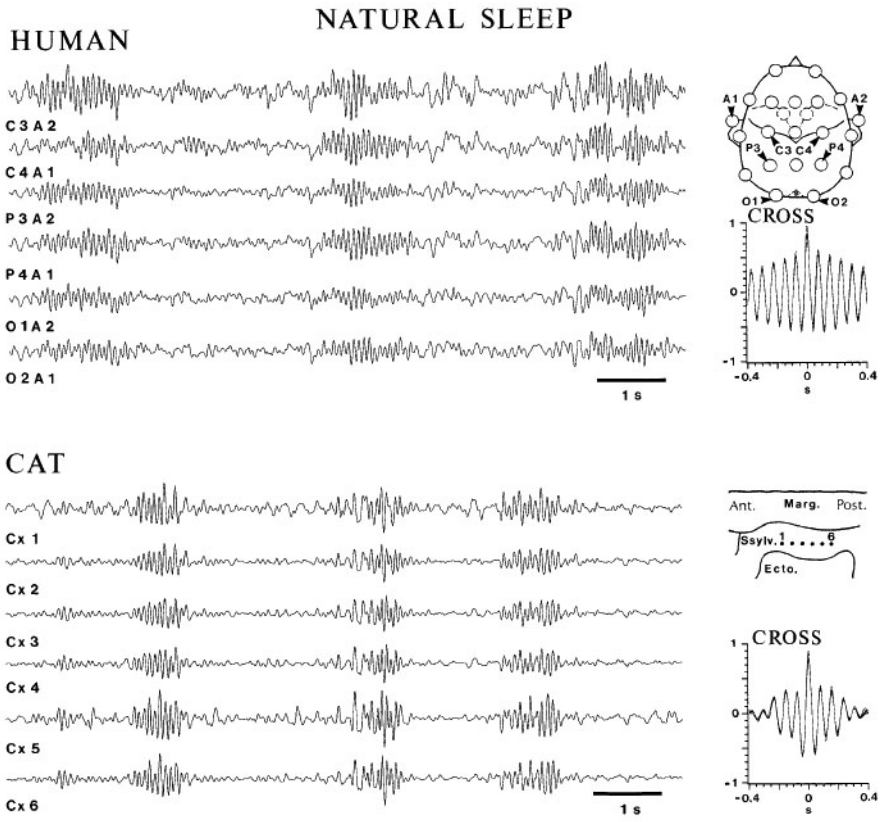

Figure 2.1 Cortical spindle waves during natural sleep of humans and cats (Contreras et al., 1997)

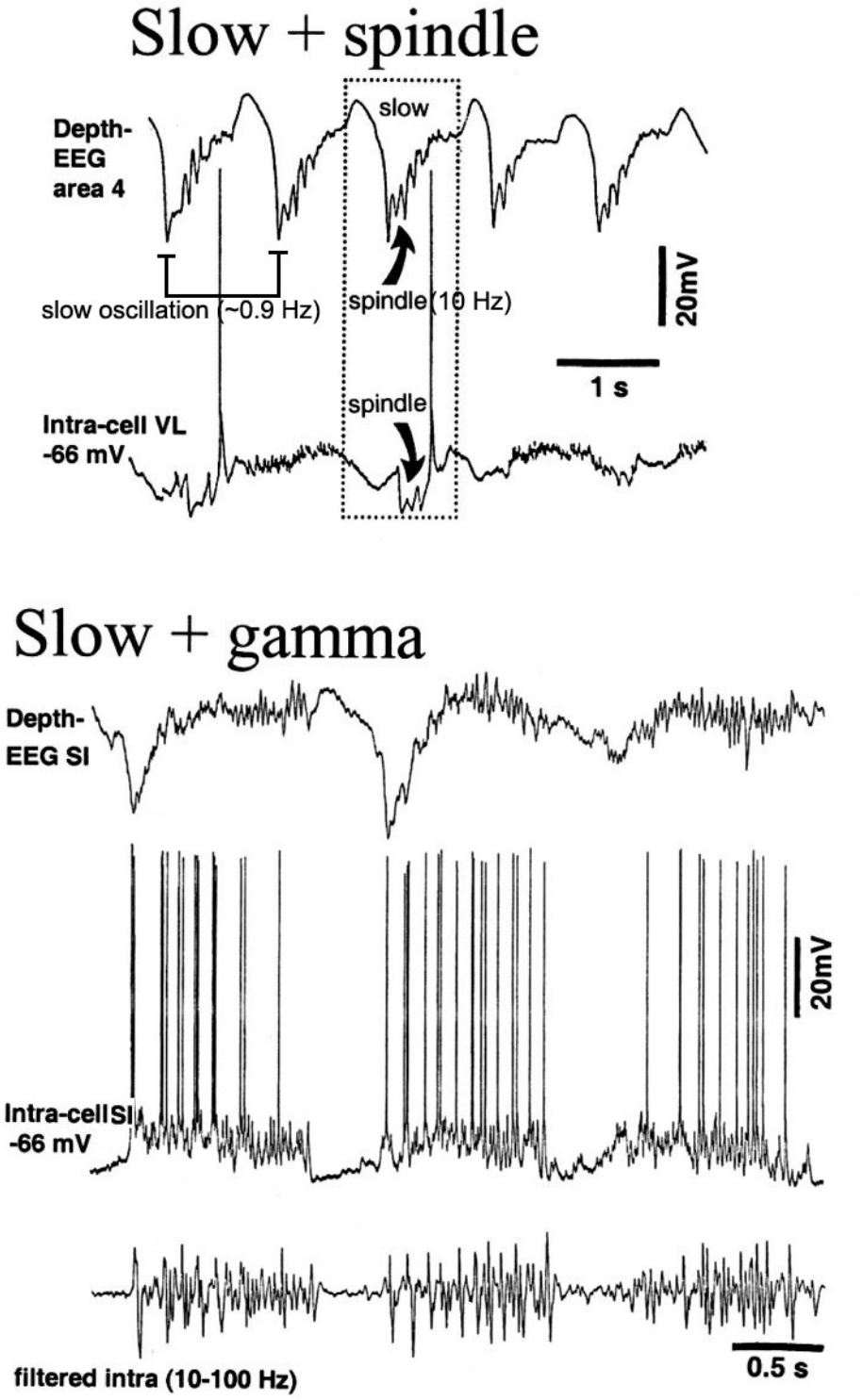

Figure 2.2 Coalescence of slow oscillation with spindle and gamma rhythms. Intracellular recordings from cortical and thalamic neurons in cats. Note the spindle (~10 Hz, up) and fast gamma rhythms (~40 Hz, bottom) during the

depolarizing phase (from the onset of the negative trough of EEG) of the slow oscillations. Modified from (Steriade, 2006).

Slow-wave sleep (SWS), which is characterized by synchronized low-frequency rhythms (<15 Hz), was previously regarded as associated with global inhibition of the cerebral cortex and the annihilation of consciousness. However, recent studies, by using intracellular recordings of cortical cell types in naturally sleeping animals, showed unexpectedly high levels of spontaneous neuronal activities during SWS. Although the thalamic gates are closed for signals from the outside world during SWS, the intracortical dialogues are maintained and even increased (Timofeev and Steriade, 1996). These data suggest that SWS, which was commonly regarded as complete brain quiescence, actually is highly orchestrated and regulated, and may serve important cerebral functions, among which is the consolidation of memory traces acquired during wakefulness (Lee and Wilson, 2002; Steriade and Timofeev, 2003; Ji and Wilson, 2007; Rasch and Born, 2007; Rasch et al., 2007).

By contrast, during brain-active states of waking and REM sleep, slow-frequency rhythms are suppressed, and synchronized fast rhythms within the frequency band of 20-60Hz (within the beta/gamma frequency bands)occur (Steriade et al., 1991b; Steriade et al., 1996a; Steriade et al., 1996b). These fast rhythms are synchronized among cortical foci, within intrathalamic network, as well as between cortical areas and related thalamic nuclei. The coherent fast rhythms have distinct spatial and temporal features, when compared with those of low-frequency oscillations. These data challenged the conventional notion,

which postulated a completely desynchronized activity in thalamocortical network during brain-active states of waking and REM sleep. Instead, they demonstrated different degrees of synchronization among neurons during various functional modes of behavioral states. Further study found that fast rhythms (20-60Hz) are also superimposed upon the depolarizing components of the slow (<1 Hz) oscillation (Steriade and Amzica, 1996; Steriade et al., 1996a).The fast rhythms, which are present in the background electrical activity during the brain-activated states of waking and REM sleep, are also thought to enhance temporal coherence of responses and firing probability of cortical neurons.

It appears that spontaneous brain rhythms during different states of vigilance may lead to increased responsiveness and plastic changes in the strength of connections among neurons, through which information is stored (Steriade and Timofeev, 2003, Rasch and Born, 2007; Rasch et al., 2007).

Previous studies have shown that, to a certain extent, the genesis of brain rhythms and the impact they exert on target structures depend on the intrinsic properties of thalamic and neocortical neurons, and synaptic connections among them. Thus, before entering into the core of spontaneous brain oscillations, it is necessary to make a few introductions on the intrinsic properties of the neurons and connections in the corticothalamic network.

2.2 The organizations and properties of the corticothalamic network

The thalamus and cerebral cortex, undissociable in both structure and function, should be considered as a unified entity or an oscillatory machine (Steriade et al., 1997). The interconnections and functional interactions between the thalamus and cerebral cortex are of great interest, because they are not only the physical basis of sensory information processing, but also the foundation upon which the state-dependent network activities of the forebrain are built.

The thalamus and cerebral cortex, the two major components of the corticothalamic network, are intimately linked by means of reciprocal thalamocortical (TC) –corticothalamic (CT) projections (Steriade et al., 1997). The corticothalamic network mainly consist of neocortical, thalamic reticular (TRN) and TC neurons (Figure 2.3), meanwhile subject to the inhibitory and facilitatory modulation arising from the brain stem and other related forebrain structures (Pape and McCormick, 1989; McCormick and Wang, 1991; McCormick and von Krosigk, 1992; Steriade et al., 1997; Monckton and McCormick, 2002). TC neuron, one neuron type of the dorsal thalamus, which relays sub-cortical inputs to the cerebral cortex, is also called thalamic relay neurons. The other thalamic neuron type in the dorsal thalamus is the local inhibitory interneurons. The thalamic interneurons are greatly different in numbers across species, and are unlikely to play an active role in the generations of forebrain oscillations, which are common in all mammals. TRN neuron, the GABAergic inhibitory neuron and the only neuron type in TRN, which is the

most prominent part of the ventral thalamus.

2.2.1 The thalamus

The thalamus is at the crossroads of the brainstem, basal ganglia and telencephalic circuits. It is the major gateway for the flow of information toward the cerebral cortex, these signals including inputs from both the periphery and from the intrinsic brain structure. In all sensory systems except olfaction, the cerebral cortex receives sensory signals from the thalamus. The thalamus actively implicates in shaping afferent signals through the CT feedback, and is the first station at which the incoming signals can be blocked by synaptic inhibition during sleep.

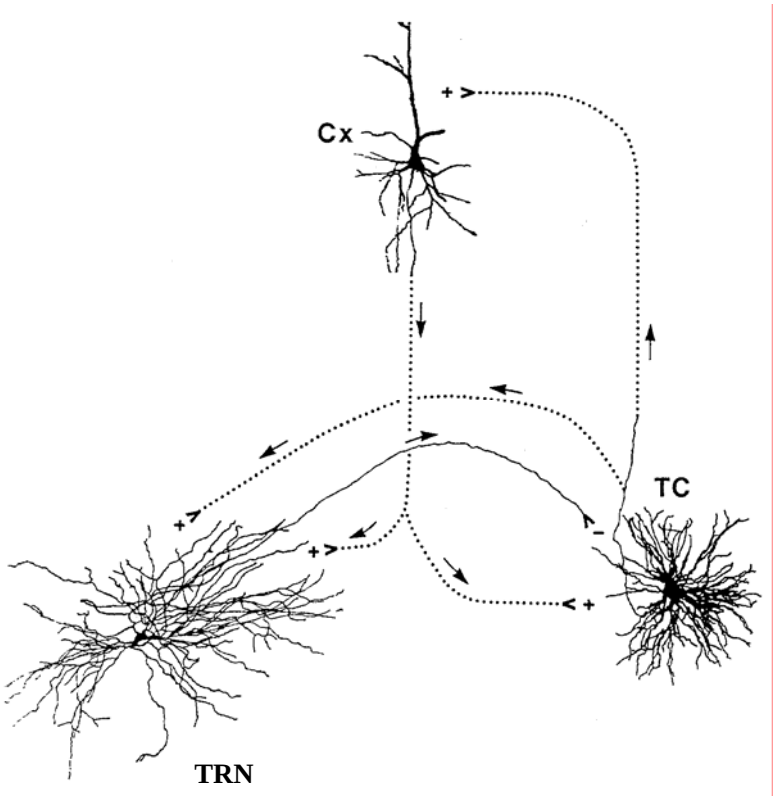

Figure 2.3 The oscillatory network in thalamocortical systems basically consist of pyramidal-shaped long-axoned cortical neurons, TRN GABAergic neurons, and TC neurons. Direction of axons is indicated by the arrows and excitatory or

inhibitory effects are indicated by + or -. Modified from Steriade et al.(Steriade et al., 1993d; Steriade et al., 1993a; Steriade et al., 1993b, 1993c).

Moreover, the thalamus participates in the intracortical propagations via cortico-thalamo- cortical loops. Therefore, it could not be regarded merely as a simple passive relay that communicates afferent impulses to the cerebral cortex, but rather, a component of an elaborate circuit, which is designed to perform the complicated computation for sensory signals processing. In addition to shaping the signals and "switching off" the unwanted signals like a filter, another important role of the CT feedback projections is to affect the firing mode of the thalamus, which is associated with the behavioral states or the functional mode of the neocortex. The corticothalamic network participates in the highly complex integrative functions, and is crucial for shifting the functional mode of the brain in a continuous way between an adaptive behavioral state, open to the outside world, and a disconnected state when thalamic gates are closed (Steriade et al., 1997).

2.2.1.1 Dorsal thalamus: TC neurons

When speaking of the thalamus, it usually refers to the dorsal thalamus, the largest and most prominent component of the diencephalon. The dorsal thalamus contains a number of distinct nuclei, each associated with a separate sensory, motor or limbic function, e.g. the medial geniculate body (MGB) for auditory system, the lateral geniculate nucleus (LGN) for visual system, and the ventrobasal nucleus (VB) for somatosensory (Figure 2.5). TC neurons across

functional systems share common principle with respect to the synapse organizations and topographic distributions (Jones, 2002). With regard to sensory nuclei, the ascending projections from the thalamus can be segregated into two parallel pathway, known as lemniscal (primary) and non-lemniscal (secondary) pathway (Hu et al., 1994; Sherman and Guillery, 2001; Jones, 2002). Accordingly, the TC neurons can be divided into two distinct classes, namely principal and non-primary nuclei. In auditory system, the lemniscal core of MGB is the tonotopically organized ventral division (MGv). Neurons in the MGv have extremely uniform properties, which include sharp frequency tuning, and the shortest latency (8-15 ms) responses to acoustic stimuli. Neurons in non-lemniscal MGB, the dorsal division (MGd) and medial division (MGm), however, show broader or less well-tuned frequency response properties, more variable firing patterns, longer latencies, non-tonotopic organization, and integrative features for multisensory afferent inputs (Calford and Webster, 1981; Calford, 1983).

2.2.1.2 Ventral thalamus: TRN neurons

The most prominent part of the ventral thalamus is the TRN, a thin sheet of exclusively GABAergic neurons, forming a shell of the thalamus between the thalamus and cerebral cortex, through which thalamocortical and corticothalamic fibers pass (Jones, 2002). The main inputs of the TRN are the collateral projections of TC and CT fibers. Unlike dorsal thalamus, ventral thalamus does not project to cortex but instead targets the dorsal thalamus. TRN

is the main inhibitory source of the corticothalamic network in many mammalian species, e.g. rodents (Arcelli et al., 1997), making inhibitory synapses with TC neurons.

On one hand, neurons in different TRN sectors are devoted to different sensory modalities, show modality-specific and a topographic connections with the dorsal thalamus and cortex, though the extensive overlap of dendrite of TRN neurons make it unlikely that the topographic maps are very accurate just like dorsal thalamus and primary cortex. In rats (Figure 2.4), the auditory sector of the TRN is located in the caudoventral region of the nucleus, with the visual sector situated dorsally to the auditory part, and the somatosensory sector rostrally to them (Jones, 1975; Shosaku and Sumitomo, 1983). More details about the precise topographic arrangements in visual (Montero et al., 1977; Crabtree and Killackey, 1989), auditory (Conley et al., 1991), and somatosensory (Shosaku et al., 1984; Pinault et al., 1995) systems (for review, see Mitrofanis and Guillery (1993)) were illustrated in different species.

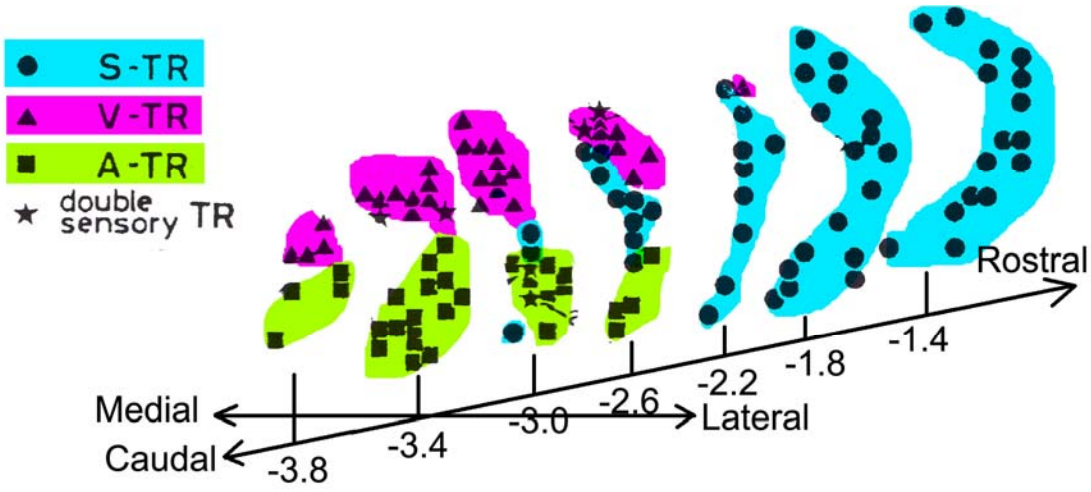

Figure 2.4 Sequential coronal sections through the right TRN of the rat, based on data from (Shosaku and Sumitomo, 1983). Different symbols and colors represent recorded neurons of different modalities and the range of the corresponding modality. The numbers represent distance (in mm) from bregma (based on our unpublished data). S-TR: somatosensory TRN, V-TR: visual TRN, A-TR: auditory TRN.

On the other hand, the TRN neurons extend dendrite trees within the thin reticular sheet, which enable them receive from a widespread cortical and thalamic regions and project to a widespread area in the dorsal thalamus (Liu et al., 1995, Yu et al., unpublished data), Recent studies show that the TRN is likely involved in the intrathalamic pathways allowing modality-related and cross-modality switching in the dorsal thalamus (Crabtree, 1998; Crabtree and Isaac, 2002).

More details about TRN neuron, please refer to 2.3.2.1.

2.2.1.3 The intrinsic properties of the TC and TRN neurons

Intra- and extracellular recordings *in vivo* and *in vitro* have revealed that thalamic neurons have two basic modes of action potential generation: single spike activity and rhythmic burst generation (for review see Steriade and Deschenes (1984); Steriade and Llinas (1988)). Single spike activity is prevalent during “brain activated” states e.g. wakefulness and REM sleep. Rhythmic burst firing is dominant during the periods of low vigilance, such as SWS, deep anesthesia, or absence seizures (McCarley et al., 1983; Steriade et al., 1993d; Steriade et al., 1993a; Steriade et al., 1993c, 1993b; Neckelmann et al., 1998; Steriade and Amzica, 1998; Steriade et al., 1998; Steriade and Contreras, 1998).

I*n vivo* and *in vitro* intracellular recordings have revealed that bursting firing is due to the activation of low threshold Ca^{2+} or T-current (I_T)(Jahnsen and Llinas, 1984a, 1984b, 1984c; Steriade and Deschenes, 1984; Crunelli et al., 1989). The T-current is a Ca^{2+} current that is activated by depolarization of the membrane positively to approximately -80mV after membrane hyperpolarization and progressively inactivated by depolarization. That inactivation is complete at around -60mV. Then this Ca^{2+} current activate a high frequency discharge of between 1 and 8 typical Na^+ and K^+ mediated fast action potentials at frequencies of 250-500 Hz (Jahnsen and Llinás,1984a). The transition from rhythmic burst firing in SWS to single spike activity during waking and REM sleep is associated with substantial depolarization of the membrane potential, which inhibits neuronal burst firing through inactivation of I_T and promotes single spike activity by moving the membrane potential closer to the single spike firing threshold (approximately -55mV).

Both TC neurons and TRN neurons are endowed with this calcium-dependent electrogenic mechanism that leads to generation of phasic bursts of high frequency spike discharge (Deschenes et al., 1982; Llinas and Jahnsen, 1982; Mulle et al., 1986; Shosaku et al., 1989), but not local circuit inhibitory interneurons (Pape and McCormick, 1989), which is why the latter group of neurons do not appear to participate to any significant degree of synchronous thalamic network activity (Bal et al., 1995b). The ability to fire high frequency burst of spikes depends on the expression of sufficient numbers of the T-type

low-threshold calcium channel (Huguenard, 1996).

Membrane hyperpolarization, resulting from either long-lasting neuromodulatory action (e.g. removal of the cholinergic inputs on TC neurons originating from the pedunculopontine tegmental (PPT) and laterodorsal tegmental (LDT) nuclei) (McCormick and Prince, 1987; McCormick and Wang, 1991), or brief inhibitory synaptic events (e.g. compound inhibitory postsynaptic potential (IPSP) with $GABA_A$ and $GABA_B$ component on TC relay neurons arising from TRN)(Steriade and Deschenes, 1984; Crunelli et al., 1988; von Krosigk et al., 1993; Huguenard and Prince, 1994b, 1994a), enable burst firing through deinactivation or repriming of the T-type channels (Steriade et al., 1997).

One consequence of burst firing is that the associated depolarization, which lasts approximately 20-100ms, can result in activation of secondary voltage- and calcium-dependent conductances that in turn have long lasting effects on excitability. In each cell type the secondary conductance is altered (either activated or inactivated) by the burst itself, resulting in a subsequent hyperpolarization that leads to repriming of T-type channels and ultimately to secondary and tertiary burst responses, etc (Steriade et al., 1997). The difference is that, TC relay neurons tend to oscillate around 4 Hz due to an interaction between a hyperpolarization-activated current (I_h) and the calcium-dependent burst response (McCormick and von Krosigk, 1992; Steriade et al., 1997), while TRN neurons can oscillate at higher frequencies (~8Hz) as a result of a large

calcium-dependent after-hyperpolarization (AHP) which follows each burst (von Krosigk et al., 1993).

In summary, TC neurons and TRN neurons can fire calcium-dependent burst responses after membrane hyperpolarizations, and both cell types have the capability of auto-rhythmicity under appropriate conditions.

2.2.2 The sensory cerebral cortex

2.2.2.1 Anatomy and physiology of sensory cortex

Similar to the dorsal thalamus, the different sensory cortices show a commonality of organization, and can be divided into primary and non-primary areas. Take the auditory cortex as an example, the primary auditory cortex (AI) is the main target of the lemniscal ascending pathway from MGv, with tonotopic organization, sharp frequency tuning, and short latency (Winer, 1992). Neurons with similar characteristic frequencies (CF) occupy cortical bands. In many species, at least one other auditory field with a regular topography is found adjacent to AI, forming mirror images of AI. The number of non-primary auditory fields varies across species, including the secondary or third auditory cortex (AII/ AIII). At the borders of different sensory cortices are multisensory association areas, in which neurons receive visual or somatosensory in addition to auditory inputs (Toldi, 1986; Clarey and Irvine, 1990).

2.2.2.2 The Intrinsic properties of CT neurons[2]

[2] Cortical neurons sending projections to thalamus, is called corticothalamic (CT) neurons

In neocortex, four basic electrophysiological subtypes of neurons have been identified, including the regular spiking cells (predominant in middle layers), burst spiking cells (mainly in deep layers), fast spiking cells (interneurons) and fast rhythmic bursting (FRB) cells (sometimes called "chattering cells", morphologically identified as spiny layer II/III pyramidal neurons)(Cunningham et al., 2004).

Since neurons in the deep layers contribute to the corticofugal pathway, the burst spiking cells in the deep layers have been proposed to play an important role in the generation of rhythmic activity in the cortex. Burst firing CT neurons can generate burst of 3 to 6 action potentials either in response to a short or prolonged depolarizing input, such as excitatory postsynaptic potentials (EPSPs), in response to the offset of a hyperpolarizing input, or spontaneously in a rhythmic manner (Steriade et al., 1997). Similar to burst firing thalamic neurons, burst firing corticothalamic neurons can shift to generating trains of single action potentials upon tonic depolarization. The axons of them bifurcate repeatedly in layers V and VI.

All these physiological properties and axonal connections may allow burst firing neurons to act as the trigger or pacemaker of certain types of synchronized cortical generated activity, such as delta waves and slow rhythms.

2.2.3 The reciprocal projections and physiological interactions in the corticothalamic network

Although some isolated neurons can oscillate by virtue of their intrinsic

properties, these different oscillations coalesce and combine into complex and less stereotyped rhythmic patterns in the intact brain, due to the neuronal interactions in the corticothalamic network.

The thalamus and cerebral cortex, the two major components of the corticothalamic network, are intimately linked by means of reciprocal projections. However, it is noteworthy that the recipient area of CT projections and the originating area of TC fibers in the thalamic relay nuclei are not completely overlapped. In the rodent and monkey, the recipient of SI cortical axons in the thalamic relay nucleus was larger than the origin of TV projections (Hoogland et al., 1987).

Different areas of the cerebral cortex receive inputs from various dorsal thalamic nuclei. TC pathways begin with excitatory synapses, from TC neurons, such as the LGN, MGB, and VB neurons, mainly to neurons in layer IV of the visual, auditory, and somatosensory cortex. In return, the CT neurons of layer V and VI send the CT projections and innervate both dorsal TC neurons (as well as local interneurons) and the ventral TRN neurons, all through the same excitatory neurotransmitters- glutamate acids. The TRN neurons receive excitatory collaterals of both thalamocortical and corticothalamic fiber, and project back, however, only to the dorsal thalamus, but not to the cerebral cortex. They make inhibitory synapses with TC neurons, and also innervate other cells of the TRN (Figure 2.1, Figure 2.5).

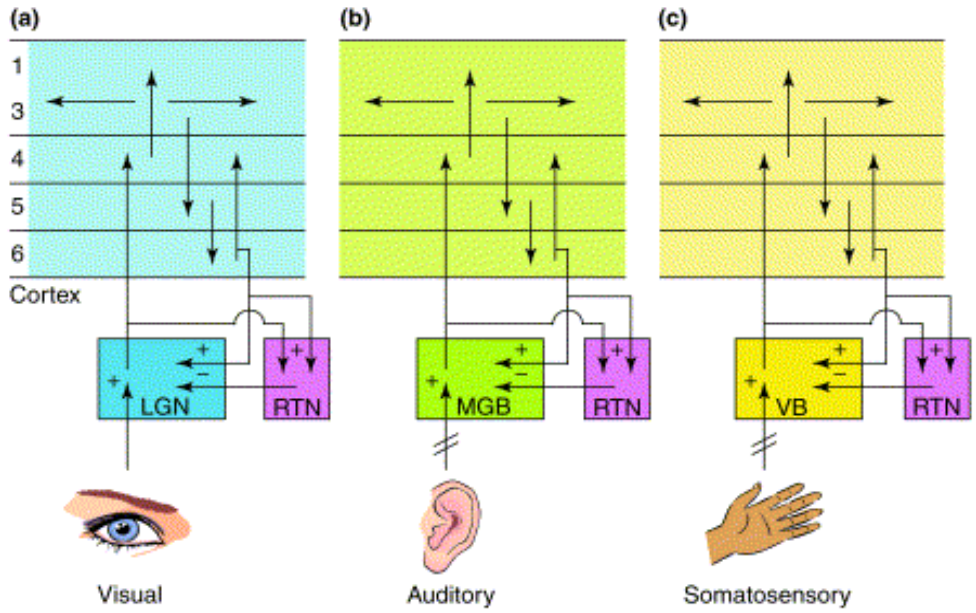

Figure 2.5 Corticothalamic circuitry in human for the **(a)** visual, **(b)** auditory, and **(c)** somatosensory systems. All three systems share a similar basic organization in mammals. TC neurons in the LGN, MGB, and VB send excitatory projections to neurons in layer IV of primary visual, auditory, and somatosensory cortex. In turn, neurons in cortical layer VI give rise to excitatory feedback to the thalamus. Corticothalamic feedback axons terminate directly onto relay neurons and interneurons in thalamic relay nuclei. Corticothalamic axons also extend collateral projections into the TRN. TRN neurons then give rise to inhibitory projections that terminate on thalamic relay neurons (Alitto and Usrey, 2003).

All these crossing and interweaving axon pathways form the foundation upon which the state-dependent network rhythmic activities of the forebrain are built, and hold the key to understand the transmission and integrative mechanism of the peripheral and intrinsic signals in the forebrain.

2.2.3.1 TC projections

The TC pathways arise from different populations of thalamic neurons terminating in different areas and layers in the cortex, common in all sensory systems. The lemniscal pathways relay sensory information from the core TC

nuclei to the primary sensory cortical areas, which typically contain a map of the sensory modality they represent and are topographically organized. The lemniscal pathways carry the main sensory information to be relayed to cortex. Projections from other non-primary thalamic nuclei are called non- primary TC pathways, which however project to multiple cortical areas, other than to the specific primary sensory cortex, including the second sensory cortex, multisensory areas, or the sensory association cortex. The non-primary TC pathways carry modulatory information, selectively gating of the sensory information through the lemniscal pathways, integrating multisensory afferents (Winer and Morest, 1983; Edeline, 1990; Edeline and Weinberger, 1992), and leaving the sensory cortex prepared for the incoming signal. In the auditory system, for example, the organization of MGB projections is quite similar in different mammals. In cats, the MGv neurons project primary to the AI, and its mirror region, the anterior auditory field (AAF)(Imig and Morel, 1984). The MGd neurons project to auditory cortical area outside the primary auditory cortex, while MGm projects to all auditory cortices including the association cortex (Winer et al., 1977; Imig and Morel, 1983). MGm also projects to the somatosensory cortex, prefrontal cortex, as well as amygdale and basal ganglia (LeDoux et al., 1990; Shinonaga et al., 1994).

2.2.3.2 CT projections

Corticothalamic fibers make excitatory synaptic contacts on the distal dendrites of thalamic principal neurons (Liu et al., 1995), as well as on inhibitory local

circuit cells of the main sensory thalamic nuclei and the TRN (Yen et al., 1985). The importance of the corticothalamic projections is emphasized by the abundance of corticothalamic axons, about one order of magnitude larger than that of thalamocortical fibers (White and Hersch, 1982; Steriade et al., 1997).

It is well known that the corticothalamic fibers originate from two distinct classes of pyramidal cells with somata located in layers V and VI respectively (Jones, 2002). The latter type (layer VI), the major part and with a narrow vertical dendritic field centered on a short apical dendrite which ends by branching in middle layers of the cortex with small terminals (<1μm), has focused projections with a specific thalamic nucleus from which its parent cortical area receives input. The layer VI neurons play an important role in the feed-back modulation of the cerebral cortex on the thalamic nucleus where it receives its main afferents in appropriate topographic order. In contrast, the layer V neurons in the same cortical area, although in smaller number but consistent, interact non-specifically with different thalamic nuclei in large terminals (2-10μm). Their projections are not restricted to the area where it cortical parent receives input, possiblly involving in feed-forward distribution of activity among different parts of the cerebral cortex (e.g. corticocortcial communication)(Steriade et al., 1997). Compared with layer VI, layer V neurons have a stout apical dendrite ascending to layer I of the cortex with a horizontal distribution of intracortical collateral. Studies also revealed that, the corticothalamic neurons in layer VI give off collaterals to TRN neurons, whereas

the axons of layer V do not. Additionally, the layer V originating axons, after giving branches to the thalamus, continue on to the tectum (Ojima, 1994), to other parts of the brainstem or the spinal cord.

CT projections also differ in regional organization. Different cortical areas receive inputs from various dorsal thalamic nuclei, and project reciprocally to them. In auditory system of cat, AI and AAF project to MGv, AII to the MGd, and all fields as well as amygdala to the MGm (Andersen et al., 1980).

2.2.3.3 Dual effects of corticothalamic pathway on relay neurons

Undoubtedly, the corticothalamic fibers produce monosynaptic excitatory effects on TC relay neurons mediated by *N*-methyl *D*-aspartate (NMDA), AMPA and metabotropic glutamate receptors (McCormick and von Krosigk, 1992; Golshani et al., 1998; von Krosigk et al., 1999). Meanwhile, the cortex exerts a disynaptic inhibitory influence on the dorsal thalamus through TRN neurons mediated by both $GABA_A$ and $GABA_B$ receptors (Jones, 2002). The corticothalamic activation can generate either inhibitory or excitatory effects, to a large extent, depending on the functional state of these neurons. When the TC relay cells are relatively hyperpolarized, as occurred during natural sleep, drowsiness, or under anesthesia, the disynaptic inhibition via TRN is normally sufficient to overcome the direct excitatory effects of the CT projections. Hyperpolarized thalamocortical neurons tend to discharge in burst firing mode after recover from TRN inhibition. The burst action potentials excite, in turn, the TRN neurons through the collaterals of the TC fibers. The re-excited TRN neurons

re-inhibit the relay neurons, which burst again, and the cycle continues as a 7-14 Hz oscillation. This is the spindle generation mechanism that we normally believe.

2.2.4 Modulatory systems

As mentioned at the beginning, the corticothalamic network are subject to the modulatory systems located in brainstem reticular formation, posterior hypothalamus and basal forebrain, which have been proved to play an important role in changing the functional mode of the corticothalamic network associated with states of vigilance. A series of studies have shown that a variety of neurotransmitters, including acetylcholine (Ach), norepinephine (NE), serotonin (5-HT), histamine(HA), and glutamate, can be released by the these modulatory systems. All these neurotransmitters help maintain the waking state. Increase of firing rate in neurons of these modulatory nuclei can predict the advent of the arousal, and decrease of their activity indicates the drowsiness and sleep. Electrical stimulation of brainstem cholinergic neurons or direct application of Ach, results in the depolarization of TC neurons and the hyperpolarization of TRN neurons (McCormick and Prince, 1986, 1987; McCormick, 1993), which is associated with the disruption of sleep rhythms.

Because animals under anesthesia can hardly display the critical facets of the fast rhythms faithfully, the fast rhythms are beyond our study with acute preparations, and therefore, will not be addressed in this literature review.

2.3 Long-range corticothalamic synchronization of sleep oscillations

Although the history of low-frequency oscillations of brain electrical activity begins with Caton (1875) who is credited with the first report on electrical currents of the brain, it is until the recent two decades that the distinct cellular bases and mechanisms of the three major types of sleep rhythms were not elucidated. Due to multi-channel simultaneous extracellular and intracellular recordings from various cortical areas as well as from the thalamus, we have learned that a variety of slow rhythms, from spindles (7-14 Hz) to delta (1-4 Hz) and slow oscillations (< 1 Hz), occur from the early stages of sleep to deeper stage. They are all associated with prolonged hyperpolarizations of TC and cortical neurons, which are effective in inhibiting the transmission of afferent signals.

The cortical-generated slow oscillations (< 1 Hz) have the virtue of grouping the other two sleep rhythms arising in the thalamus within slowly recurring wave–sequence due to the high power of the CT projections (Steriade et al., 1993c; Contreras and Steriade, 1995), which explaining some differences between the genesis and temporal sequence of spindles recorded from various thalamic foci in animal with fully preserved corticothalamic circuit as opposed to decorticated preparation. The stereotyped (clock-like) delta rhythm appeared at an increasing level of hyperpolarization of TC neurons as compared with that at which spindles appear (Steriade et al., 1991a; Nunez et al., 1992b). Delta waves are also observed in athalamic cats (Villablanca and Salinas-Zeballos,

1972), indicating that cortex is capable of generating these oscillations independently (Metherate and Ashe, 1993), and that at least two components are involved in generating delta oscillations in the normal and intact brain.

2.3.1 Cortically initiated slow oscillation (<1 Hz)

The slow oscillation was discovered by with intracellular recordings from different (sensory, motor, association) cortical areas (Steriade et al., 1993d; Steriade et al., 1993c, 1993b) of animals under different anesthetics and in unanesthetized animals with isolated forebrain. It has been further confirmed with EEG and magnetoencephalography (MEG) recordings during natural sleep of human and behaving animals (Achermann and Borbély, 1997a; Amzica and Steriade, 1997; Simon et al., 2000; Fell et al., 2002). The survival of slow oscillations after extensive thalamic lesions suggests that it is generated within the neocortex (Steriade et al., 1993c). However, the synchronization of cortical neurons is a powerful source for driving both TRN and TC neurons (Steriade et al., 1972). Therefore, the slow oscillations can be reflected in the thalamus by grouping the two other sleep rhythms arising in the thalamus, namely spindles and clock-like delta oscillations.

2.3.1.1 Cellular mechanisms of slow oscillation

The slow oscillation consists of slow depolarizing envelopes ("up" phase, lasting for 0.8-1.5 sec) with superimposed full action potentials or presumed dendritic spikes, followed by long-lasting hyperpolarizations ("down" phase, up to 1 sec).

The up phase is formed by non-NMDA-mediated EPSPs, fast prepotentials (FPPs), a persistent Na^+ current ($I_{Na(p)}$), and fast IPSPs which reflect the action of synaptically coupled GABAergic local cortical cells (Steriade et al., 1993b). NMDA components seem unlikely to contribute to the maintenance of up states, at least not essentially, because the slow oscillation is prevalent when animals are anesthetized with ketamine, a powerful blocker of NMDA receptors.

The slow inactivation of the persistent Na^+ current (Fleidervish and Gutnick, 1996), as well as the activation of Ca^{2+}- and Na^+-dependent K^+ currents (Schwindt et al., 1989) would displace the membrane potential of neurons from firing level, and the entire network would enter the hyperpolarized down state. The synaptic depression of active synaptic connections (Tsodyks and Markram, 1997; Galarreta and Hestrin, 1998), probably produced by progressive depletion of Ca^{2+} during up phase (Massimini and Amzica, 2001), would also contribute to the hyperpolarization state. However, the local cortical GABAergic interneurons (electrophysiologically identified as conventional fast-spiking neurons) do not participate in maintaining the down state, because they do not fire during the hyperpolarization phase of all other neuronal types. Model studies proposed that summation of miniature EPSPs during the down phase of the slow oscillation could activate the $I_{Na(p)}$ and depolarize the membrane of pyramidal neurons enough to generate spikes and trigger the next up phase (Timofeev et al., 2000; Bazhenov et al., 2002).

The prolonged hyperpolarizations of cortical neurons during down phases are

suggested to play a key role in the generation and synchronization of the cortical slow oscillations. The transition from the slow sleep oscillation to brain-activated behavioral states resulted from the erasure of prolonged hyperpolarizations in cortical neurons and their increased input resistance during the state of quiet wakefulness (Steriade et al., 2001). The initiation of hyperpolarizations of cortical neurons should be ascribed to the decreased release of modulatory transmitters as well as the loss of the excitatory inputs from the thalamus.

2.3.1.2 Intracortical and corticothalamic synchronization of slow oscillations

First of all, the slow oscillation is the emergent property of intracortical network, since it survives the extensive destruction of thalamus. It is synchronously distributed in distant and functionally different cortical areas. Most of the cortical neurons (88%), including the regular-spiking and intrinsically-bursting pyramidal-shaped neurons, as well as local-circuit aspiny stellate interneurons are engaged in the slow oscillation (Steriade et al., 1993b). Studies showed that the closely located cells were also closer in time, with shortest time-lags between adjacent cortical areas (such as suprasylvian area 5 and 7) about 12ms, and the caudally located neurons precede more rostral ones in 70% of cases. The time-lags between oscillatory activities from distant sites, such as motor and visual cortices, are longer, with a mean about 120ms (Amzica and Steriade, 1995a). Three pathways may contribute to the intracortical synchronization:

intracortical projections, cortico-thalamo-cortical loops and intercortical connections between bilateral hemispheres. The synchronization of oscillating cortical foci can be disrupted by reversible inactivation with lidocaine, or intracortical transections (Amzica and Steriade, 1995a, 1995b), and can fully recover after the lidocaine-induced inactivation and partially recover even after transections, of which the latter maybe due to compensatory functions exerted by the corticothalamocortical circuits or intergyral connections. However, these rather long time-lags are not necessarily due to a series of excitatory synapses, because they may be ascribed to inhibition-rebound sequences between different recorded foci (Steriade, 2002). But the precise mechanisms need further investigations.

All thalamic nuclei reflect the cortical-generated slow oscillation. The synchronization of cortical and thalamic neurons during the slow sleep oscillation, through paired intracellular recordings from these two neuronal types (Contreras and Steriade, 1995), leads to combined slow and spindle rhythms. The grouping of these two sleep oscillations, as described in animal experiments, was also illustrated in human EEG signals during stages two and three of SWS (Molle et al., 2002).

Studies have shown that the slow oscillation is absent in TRN and TC neurons which are ipsilateral to a hemi-decortication (Timofeev and Steriade, 1996), whereas the other sleep rhythms are present. However, this does not exclude the possibility that, in intact animals, the thalamus provides additional drivers to

reinforce the depolarizing component of this cortical rhythm.

2.3.2 Thalamic-generated spindle oscillations (7-15 Hz)

Spindle waves typically appear in EEG, during early sleep stages and drowsiness (Steriade and Deschenes, 1984; Steriade et al., 1993a), and are prevalent under barbiturate anesthesia. However, it should be noted that barbiturate-induced spindles are different from the natural sleep spindles (Molle et al., 2002; De Gennaro and Ferrara, 2003), as the former is unlikely associated with a K-complex. The spindles are made of rhythmic waxing and waning activity at 7-14 Hz over a 1-4 s period that recurs once every 3-10 s. They are generated in the thalamus through the interaction between the TRN and TC relay neurons (von Krosigk et al., 1993), by the combination of intrinsic membrane properties and connectivity pattern among thalamic neurons. Complete removal of the cerebral cortex leaves the spindle waves intact in the thalamus, while lesions of the thalamus result in abolished of spindle waves in the cerebral cortex (Guo et al., unpublished observation). The TRN is suggested to play a pace-making role in the genesis of spindle wave, which is demonstrated by the absence of spindle in thalamic territories disconnected by lesions or naturally devoid of input from TRN (Steriade et al., 1985; Pare et al., 1987) and the preservation of spindle rhythmicity in the isolated TRN (Steriade et al., 1987).

2.3.2.1 Mechanisms of spindle rhythms

TRN consists of a GABAergic neuronal sheet, and forms a shell of the thalamus between the thalamus and cerebral cortex, through which thalamocortical and corticothalamic fibers pass (Jones, 1985). The TRN is heavily innervated by collaterals of thalamocortical and corticothalamic fibers and in return innervates TC relay neurons in the thalamus. Thus TRN neurons form reciprocal loops with glutamatergic TC neurons, and their major source of excitation is the neocortex. The TRN neurons are inhibited by acetylcholine (Ach) released from projections of the brainstem PPT and LDT, as well as the basal forebrain. Ach hyperpolarizes TRN neurons and depolarizes TC relay neurons (McCormick and Prince, 1986, 1987; McCormick, 1993).

TRN neurons have long dendrite trees extended within the thin sheet. Spindle sequences in TRN neurons are preceded by prolonged (200-300ms) hyperpolarizing potentials (Fuentealba et al., 2004), and these hyperpolarizing potentials could have a dendritic origin, similar to the T-current in TRN neurons. Dendrodendritic synapses in TRN have been definitely recognized in cat. Indeed, G-protein-activated inwardly rectifying K^+ channels mediate this dendritic hyperpolarization (Fuentealba et al., 2005), and the candidate receptors could be $GABA_B$ receptors, as well as peptidergic receptor for somotostatin and neuropeptide Y, all of which have been identified by immunostaining in the TRN.

Spindle generation by a network of GABAergic reticular neurons is supported by *in vivo* (Steriade et al., 1987; Fuentealba et al., 2004) and *in computo*

(Destexhe et al., 1994; Timofeev et al., 2000) studies demonstrating interactions between inhibitory reticular neurons that lead to spindle sequences. During spindle, TRN neurons generate rhythmic (7-14Hz) spike-burst superimposed on a depolarizing envelope, whereas TC neurons fire rebound bursts when the IPSPs imposed by TRN neurons are hyperpolarized enough to remove inactivation of the low threshold Ca^{2+} channels.

Because corticothalamic excitatory volleys could elicit this prolonged hyperpolarization in TRN neurons, here is the whole picture of spindle rhythms generated during slow-wave sleep. The firings in cortical neuronal pools could excite TRN neurons, generating low-threshold spikes (LTS) crowned by spike bursts (at relatively hyperpolarization levels of membrane potential, as occurring in slow-wave sleep). These TRN neurons, in turn would induce prolonged hyperpolarization in adjacent and/or distant TRN neurons through dendrodendritic GABAergic synapses (Steriade et al., 1985; Fuentealba et al., 2004) and electrical coupling (Landisman et al., 2002; Fuentealba et al., 2005), generating rhythmic (7-14Hz) spike-burst, hyperpolarizing TC relay neurons to remove inactivation of the low threshold Ca^{2+} channels and resulting in the latter to rebound burst. The inhibitory actions of TRN neurons and rebound spike bursts in TC neurons are in return responsible for the transfer of spindles to the cortex. Intracellular recordings from thalamic relay neurons reveal that spindle wave is associated with barrages of inhibitory postsynaptic potentials (IPSPs) arising from the TRN neurons. These IPSPs result in the occasional generation

of rebound low threshold Ca^{2+} spikes of the TC neurons, thereby causing barrages of EPSPs in cortical neurons and generating the spindle waves of the EEG.

For the more powerful activation of TRN neurons, which depends on the enrichment of GluR4 receptor subunits at corticothalamic synapses on TRN neurons, the capacity to generate higher amplitude EPSCs in TRN neurons than in TC relay neurons (Golshani et al., 2001). These ensure that the monosynaptic EPSPs in the thalamic relay neurons are quickly overcome by the disynaptic TRN-based IPSPs. The rebound spike bursts in TC neurons after hyperpolarizations re-excite TRN neurons, thus promoting continuation of the oscillation in the spindle range. On the other hand, some studies also showed that the intrareticular inhibitory interactions, mainly mediated by $GABA_A$ receptors, could serve to dampen the recurrent excitation of TRN neurons by the bursting relay neurons (von Krosigk et al., 1993; Kim and McCormick, 1998). Synchronization of the cells is promoted by the blockade or absence of $GABA_A$ receptor–mediated inhibition in the TRN, leading to prolonged bursts and hyper-synchronized slower oscillations, which resembles absence seizures (Destexhe et al., 1996b; Destexhe, 1998; Blumenfeld and McCormick, 2000).

Notice that activation of $GABA_A$ receptors which are directly coupled to chloride ionophores, leads to rapid inhibition, while $GABA_B$ receptors are linked through G protein-dependent processes to a slower activation of potassium channels.

2.3.2.1.1 Intrathalamic interaction

The equilibrium potential for the synaptic current is quite hyperpolarized in TC relay neurons, where estimates of the E_{Cl}, the chloride equilibrium potential for $GABA_A$ mediated responses, range from -86 to -94mV, which is in the voltage range where repriming of T currents occurs quite rapidly (Coulter et al., 1989). Therefore, single IPSPs that reach a peak hyperpolarization, near -90mV, may result in rebound calcium-dependent burst firing. $GABA_B$ receptors activate a long lasting (~100-600ms) potassium conductance that results in almost complete repriming of T-type channels. Thus, the combined response of an early $GABA_A$ chloride current and a late $GABA_B$ potassium current evokes prolonged postsynaptic hyperpolarization on thalamic relay neurons and thus robust burst activation that re-excite the TRN neurons, promoting continuation of the oscillation.

Excitatory output from TC relay neurons is mediated mainly by ionotropic glutamate receptors (Huguenard and Prince, 1994a; Bal et al., 1995a), largely of the AMPA subtype (Bal et al., 1995a), although there also appears to be a component mediated by NMDA receptors (Huguenard and Prince, 1994a).

As the $GABA_B$ IPSPs are long-lasting and deeply hyperpolarizing, their activation would be a particular effective mechanism for reliable burst generation in relay neurons. The potassium-dependent synaptic potential may be responsible for activating relay neurons and recruiting them into a synchronous network oscillation. TRN intranuclear connections, mediated mainly by $GABA_A$

receptors (Ulrich and Huguenard, 1996), can actually shunt burst generation in these cells (Bal et al., 1995b). When recurrent connections are blocked, very long lasting bursts occur, and enhance the output onto TC relay neurons (von Krosigk et al., 1993; Huguenard and Prince, 1994b). The resulting de-inhibition causes enhanced GABAergic output from TRN, with resultant large $GABA_B$-dependent IPSPs in TC relay neurons that promote rebound burst responses in a large proportion of cells.

2.3.2.1.2 Corticothalamic synchronization of spindles

Spindle is distributed to cortical territories by the thalamocortical axons, and induces rhythmic EPSPs in the cortical neurons, which is the origin of the EEG spindle waves. In return, spindle wave can also be triggered by the corticothalamic volleys arising from slow-wave activity generated in the cerebral cortex (Contreras and Steriade, 1995). The synchronization of spindles over widespread thalamic and cortical territories is different *in vitro* and in *vivo*. In contrast to the nearly simultaneous spindle sequences seen in the thalamus and cerebral cortex *in vivo*, in acutely prepared animals as well as during natural slow-wave sleep in cats and humans (Contreras et al., 1996, 1997), spindles propagate along the dorsoventral axis of the lateral geniculate nucleus in slices from the visual thalamus of ferrets (Kim et al., 1995). The contrast between the simultaneity of spindle sequences in the intact brain and spindle propagation in thalamic slices might be due to the absence of the cortex in the latter, simplified preparation (Fuentealba et al., 2005). In fact, after decortication, the simultaneity

of spindle sequences throughout the thalamus is disorganized without, however, showing systematic propagation as in thalamic slices (Contreras et al., 1996). Compared with the simultaneous occurrence of spindle oscillations in the functionally intact brain, a diminished spatiotemporal coherence of spindle oscillations was observed during barbiturate anesthesia, when corticothalamic neurons display poor spontaneous activity, as well as during states of depressed cortex, produced by releasing a drop of highly concentrated K^+ acetate over the cortex (Destexhe et al., 1999b).

The decisive role of the slow oscillation in thalamic spindles is also demonstrated by the fact that the typical waxing-and-waning pattern of the spontaneous spindles waves are only envisioned under barbiturate anesthesia or isolated thalamus. Under ketamine/xylazine anesthesia, the thalamic spindles display only a waning pattern, with nearly no waxing process, because the powerful corticothalamic drive recruits almost the maximum TRN and TC neurons from the beginning of spindle sequences (Contreras and Steriade, 1996). The waxing pattern of spindle oscillation is due to a progressive entrainment of units into the oscillation until a maximum number is reached. The same reason can explain that under all anesthetics, spindles have a waning pattern when elicited by cortical stimuli, and that only waning pattern of spindles can be seen in the thalamic relay neurons when ascending pathway is activated.

2.3.2.2 Close phase relations between cortical and thalamic neuronal activities during the slow EEG oscillation

Many studies have confirmed the close time-relations between cortical and thalamic neuronal activities during anesthesia or natural sleep. Under urethane or ketamine/xylazine anesthesia, spindle sequences are grouped by a cortically generated slow oscillation and preceded by a depth-positive EEG wave that corresponded to a prolonged hyperpolarization in all three investigated (cortical, TC and TRN) cellular types (Contreras and Steriade, 1996). Cortical, TC and TRN neurons are similarly hyperpolarized during the depth-positive EEG waves and depolarized during the depth-negative (surface-positive) EEG deflections. In TC neurons, spindles consist of IPSPs, and could fire spike bursts at the onset of the EEG depth-negativity. During low-frequency oscillatory states, due to the high efficiency of the corticothalamic volley in triggering thalamic spindles (Steriade et al., 1972), the cortical and thalamic neurons display phase relations that are restricted to narrow time windows. The spontaneous transitions from less synchronized to more synchronized EEG states are marked by a simultaneous hyperpolarization, coincident with an overt depth-positive EEG wave, i.e. this synchronization results from a generalized inhibitory phenomenon (Contreras and Steriade, 1995).

2.3.3 Stereotyped delta oscillation generated in the thalamus and the delta EEG waves

That a stereotyped delta oscillation generated in the thalamus was unambiguously demonstrated in many intracellular studies of TC neurons

recorded from the dorsal division of LGN and ventroposterior nucleus slices (McCormick and Pape, 1990b, 1990a; Leresche et al., 1991) and from a variety of sensory, motor, associational, and intralaminar thalamic nuclei *in vivo* (Steriade et al., 1991a; Nunez et al., 1992a; Steriade et al., 1993d). However, delta waves are also observed in athalamic cat (Villablanca and Salinas-Zeballos, 1972), indicating that the cortex is capable of generating these oscillations independently. So thalamocortical neurons can generate stereotyped clocklike delta oscillation due to their intrinsic properties, but it can hardly account for the rather irregular polymorphous EEG delta waves. Early experiments indicated that large thalamic lesions suppressed cortical spindles, but EEG delta waves were preserved in the cortex (Villablanca and Salinas-Zeballos, 1972).

2.3.3.1 Spindle and delta

Delta oscillation is generated at a membrane potential (Vm), more negative than spindle rhythm (Steriade et al., 1991a; Nunez et al., 1992a; Steriade et al., 1993d). The transformation of spindles to delta rhythms was also obtained by means of microinjections of NMDA blockers into the thalamus (Buzsaki, 1991), likely producing a hyperpolarization of TC neurons. Delta appears during later stages of sleep than spindles. The occurrence of these two sleep oscillations at different Vm, led us to postulate a progressive hyperpolarization of TC neurons with deepening of EEG-synchronized sleep (Steriade et al., 1991a), which is due to the progressive reduction in the firing rates of brainstem cholinergic and monoaminergic cells (Steriade, 1990). Similarly, a progressive hyperpolarization

takes place in TRN. That the spindles and delta oscillations in TRN neurons occur at different Vm, like in TC neurons, is also suggested by the intracellular recordings *in vivo* showing that spindles are triggered in rostrolateral sectors of RE nucleus at the resting Vm (≈ -60 mV), while rhythmic spike bursts at delta frequency require depolarizing pulses applied at -90 mV (Steriade and McCarley, 1990; Steriade et al., 1997). These data support the idea that spindle and delta oscillations progressively develop during EEG-synchronized sleep as a consequence of Vm changes in both CT and TRN neurons. The reciprocal relation between spindles and delta oscillations found support in studies of EEG patterns recorded from the CL intralaminar thalamic nucleus in naturally sleeping cats, with spindles being maximal at sleep onset and decreasing thereafter whereas delta waves increasing gradually (Lancel et al., 1992).

2.3.3.2 Cellular mechanism of delta rhythms in TC neurons

McCormick and Pape (McCormick and Pape, 1990a) have proposed a model of delta oscillation resulting from the interplay between two membrane intrinsic currents present in thalamic neurons: (1) a hyperpolarization-activated inward (anomalous) rectifier carried by Na^+ and K^+ (I_h)(Pape and McCormick, 1989), and (2) a transient Ca^{2+} current (I_T) underlying the LTS giving rise to bursts of high-frequency, fast Na^+ action potentials (Jahnsen and Llinas, 1984a, 1984b, 1984c).

According to this model, the hyperpolarization of TC neurons activates the I_h, which depolarizes the membrane toward threshold for a Ca^{2+}-dependent LTS

crowned by a burst of Na^+ fast spikes; this depolarization inactivates the I_h and the resulting hyperpolarizing overshoot again triggers the I_h, which depolarizes the membrane toward another LTS.

The delta oscillation is generated by two currents of TC neurons when their V_m is hyperpolarized by about l0-15 mV. This alteration occurs during natural slow-wave sleep (Hirsch et al., 1983), because of the decrease in firing rates of activating cholinergic and monoaminergic brainstem neurons (Steriade and McCarley, 1990). Another factor leading to the hyperpolarization of thalamic neurons during slow-wave sleep is the decreased firing rates of CT neurons (Steriade et al., 1978). During waking, the cortical input produces a prolonged depolarization of thalamic neurons resulting from a reduction in a resting K^+ conductance, IKL, through the activation of glutamate metabotropic receptors (McCormick and von Krosigk, 1992). After removal of the powerful depolarizing impingement of cortical origin, thalamic neurons are hyperpolarized by about 10mV and, consequently, spontaneously delta oscillations are seen in virtually all recorded neurons (Steriade et al., 1993d).

Cortical cellular mechanisms of delta waves have been proposed by Metherate and Ashe (Metherate and Ashe, 1993).

2.4 Grouping of brain rhythms in corticothalamic network

Each of these brain rhythms stems from distinct neuronal network and is

generated by the interplay among different synaptic mechanisms or voltage-gated currents (reviewed in (Steriade et al., 1997)). They may be recorded in the thalamus (such as spindles) or neocortex (the slow oscillation) after their complete disconnection. However, it is encouraging to note that, in the intact brain, different brain rhythms coalesce by the virtue of the reciprocal loops between the neocortex and thalamus. The major factor behind this coalescence is the cortically generated slow oscillation. The coherent firing of cortical neurons during its depolarizing phase impinges upon the thalamus and triggers less stereotyped and complex wave-sequences, which include different types of rhythmic patterns within one oscillatory cycle. The experimental evidence for unified oscillations derived from simultaneous intracellular recordings of cortical and thalamic neurons *in vivo* (Steriade et al., 1993b). Recent studies in humans using global methods provided congruent results of grouping different types of slow and fast oscillatory activities (Achermann and Borbély, 1997a).

Another concept of unified brain rhythms is based on basic cellular mechanisms that underlie generation of brain waves. Therefore, we will not be confused when we observe a cortical slow oscillation with a frequency of > 1 Hz, which is assumedly within the delta band. Another example is the thalamic spindle and delta oscillation. They can be unified by considering hyperpolarization-rebound discharges under different membrane potentials, regardless of its frequency range.

Instead of dissecting various frequency bands of the major oscillations that characterize the brain electrical activity during states of vigilance, it is conceptually more rewarding to analyze their coalescence (Steriade, 2006).

2.5 Functional implication of sleep oscillations

Far from being epiphenomena, spontaneous brain rhythms serve highly integrative brain functions, e.g. consciousness, attentive perception, as well as synapse plasticity and memory (Lee and Wilson, 2002; Steriade and Timofeev, 2003, Rasch and Born, 2007; Rasch et al., 2007).

The cortical and thalamic neurons may use oscillations as a way to homeostatically adjust the balance of ionic currents and regulatory mechanisms (LeMasson et al., 1993). The rhythmic spike burst during sleep may provide a "search light" for a quick transition to an arousal state (Crick, 1984; Steriade et al., 1993a).

More importantly, it appears that spontaneous brain rhythms during different states of vigilance may lead to increased responsiveness and plastic changes in the strength of connections among neurons, through which information is stored. For example, it is well established that synchronized oscillations occurring in the immature retina can direct the synaptic development of visual thalamus and cortex long before the onset of vision (Meister et al., 1991; Tononi and Cirelli, 2006). Similarly, the slow-wave sleep oscillation along a certain pathways during sleep may play a role in the spike timing-dependent or activity-dependent

synaptic plasticity. Recently, evidences both from human studies by Born group (Raschet al., 2007) and from rats by Wilson group (Lee and Wilson, 2002; Ji and Wilson, 2007) strongly proposed sleep as an off-line period during which memories are spontaneously reactivated and redistributed in the absence of interfering external input (Rasch and Born, 2007). The role of slow-wave sleep oscillation in consolidating memory traces acquired during wakefulness is being explored in both experimental animals and human subjects (for review see Steriade and Timofeev (2003), Rasch and Born (2007)).

However, uncovering the function of the sleep-related oscillation will be a hard and long-standing task, just as understanding the nature of cognitive representations.

Chapter 3

Methodology

3.1 Introduction

The methods employed in this thesis consist of observational recordings and experimental designs. This chapter illustrates our animal model, surgical procedures, recording techniques, stimulation signals, histological skills and analytical processes. Some further details are described in Chapter 4 to 5 if needed.

3.2 Materials and methods

3.2.1 Animal preparation

3.2.1.1 Subjects

Adult Sprague-Dawley rats (220–380 g) and Hartley albino guinea pig, *Cavia porcellus*, male or female, were served as the subjects. The inclusion criteria include clean, intact, infection-free external ears and sensitive pinnae reflex. The subjects were kept in the Laboratory Animal Unit at constant temperature (22ºC) and on a regular 12-hour light/dark cycle. All experiments were conducted in compliance with the *Principles of Laboratory Animal Care* (NIH publication no. 86-23, revised 1985) and the ethical principles of The Hong Kong Polytechnic

University. All experimental protocols were approved by the Animal Subjects Ethics Sub-Committee of The Hong Kong Polytechnic University.

3.2.1.2 Animal preparation

Anesthesia was initially administrated with a combination of ketamine/xylazine (100 and 10 mg/kg, i.p., Alfasan, Holland) or with pentobarbital sodium (Nembutal 35 mg/kg, i.p., Abott labs, Irving, TX), and maintained by regular administration of supplemental doses of the same anesthetics (33 mg/kg/hr; 3.3 mg/kg/hr for ketamine/xylazine; 5-10 mg/kg/hr for Nembutal) during the surgical preparations and recordings. Atropine sulphate (Sigma, 0.05 mg/kg initially and 0.01 mg/kg/hr, s.c.) was administrated 15 min before anesthesia and at regular intervals. The subjects were mounted on the stereotaxic device following the induction of anesthesia, and the body temperature was maintained at about 37.5°C with an electric thermo-blanket (Homeothermic Blanket Systems, Harvard Apparatus, South Natick, MA). A midline incision was made in the scalp, and craniotomies were performed to enable us to vertically access the AC and MGB or other sensory cortex and thalamus in the right (both) hemisphere(s). The dura mater was removed above the auditory cortex and at a position vertically above the auditory thalamus. Cerebrospinal fluid was released through the foramen magnum. Occasionally, artificial respiration was applied to the animal, muscles were relaxed after administration of gallamine triethiodide (Sigma, 50 mg/kg initially 10 mg/kg/hr regularly, i.p.), and the end-tidal carbon dioxide was monitored.

In some experiments, ablation of AC was performed by suction after complete exposure of the AC, including part of the visual cortex and barrel cortex.

3.2.2 Acoustic stimuli

The subject was placed in a double-walled soundproof room (NAP, Clayton, Australia). Acoustic stimuli were generated digitally by a MALab system (Kaiser Instruments, Irvine, CA, USA) (Semple and Kitzes, 1993; Achermann and Borbély, 1997b), or by TDT auditory physiology workstation (Tucker-Davis Technologies, Alachua, FL). Acoustic stimuli were delivered through sealed acoustic system using a calibrated earphone (Bayer DT-48, Bayer, Wuppertal, Germany or EC1, TDT) to left or both ears. The sound pressure level (SPL) of the earphone was calibrated over the white noise and a frequency range of 100 Hz to 35 kHz under the control of a computer by using a condenser microphone (1/4 inch, Brüel and Kjær, Norcross, GA).

Noise bursts with frequencies ranging from 100 Hz to 35 kHz and pure tones (duration: 50/100 ms, rise/fall time: 5/10 ms, repetitive rate: 3 Hz to 0.25 Hz) were employed. In some experiment, simplified visual stimuli were given by using the custom-made LED matrix, triggered by the TDT auditory physiology workstation.

3.2.3 Pharmacology: Drug Applications

All drugs were bought from Sigma (US) or Tocris (UK), unless otherwise specified. A series of pilot experiments were performed to determine the optimal

dose of various drugs, including bicuculline methobromide (BIM) ($GABA_A$ receptor antagonist), kainic acid (KA, an excitatory neurotoxin), antagonists for different glutamate receptor types: AP-V(for NMDA receptor), CNQX (for non-NMDA receptor), LY367385 (for metabotropic receptor mGlu1α), L-glutamate, acetylcholine (Ach), GABA. Micro-injections were made through a Hamilton microinjection syringe which was connected to a grass pipette of 25-30-μm diameter. Saline, unless otherwise specified, was used as the internal vehicle control.

3.2.3.1 BIM injection in AC

BIM (15mM in 0.9% NaCl) was used here to activate the auditory cortex (or visual and somatosensory cortex). Normally, a volume of 0.2-0.3 μl was used (Sun et al., 2007). A minimum of 0.1μl was enough for local activation of injection cortices, and a maximum of 0.4μl was used for wide activation. The injection needle was perpendicular to the AC, and the tip of the needle was positioned in the primary auditory cortex (the exact steretaxic coordinates of the injection site were 4.5mm caudal to the bregma, and 4mm below the interface of parietal bone and temporal bone on the temporal lobe) at a depth of 1.0 mm from the cortical surface, aiming at the deep layers. The injection speed was about 3 min/μl. For vehicle control, two subjects were used in which the same dose of saline (0.9% NaCl) was injected into the corresponding site in the AC. In other subjects, the strategy of internal control was applied, and saline was injected into AC contralateral to the BIM injection.

The subjects survived for 1-1.5 hr after BIM injection in the AC, and then they were sacrificed for Fos immunohistochemistry.

3.2.3.2 Direct excitation of MGB neurons

Either L-glutamate (0.3 μl, 100 mM, pH 7-8, n= 7 subjects) or Ach (0.3 μl, 100 mM, pH 4.0, n=3 subjects) was administered for a direct activation of MGB neurons. The injections were consecutively made for 2-4 times with an interval of 5-10 minutes. Kainic acid (KA) used in the present study served for two purposes (McGeer et al., 1978; Steriade et al., 1985; Descheenes and Hu, 1990): one was to directly activate MGB neurons within a short period (<2 hr), and the other one was to lesion the TRN neurons after a long time action (> 20 hr). Two subjects were injected with KA(100 mM, 0.1μl) in the MGB.

In these cases, the subjects survived for 1-1.5 hr after glutamate/ Ach/KA injection in the MGB before they were sacrificed for Fos immunohistochemistry.

3.2.3.3 Injection of glutamate receptor antagonist

Nine subjects were injected respectively with three different kind of glutamate receptor antagonist: AP-V (100 mM, pH 8.0, n=3 subjects), CNQX (1 mM, pH 8.5, n=3 subjects) and LY367385 (0.5 mM, pH 7.4, n=3 subjects), three for each group. A total volume of 0.3 μl was consecutively injected for four times at 20-minute interval in MGB, starting before the AC was bilaterally activated with BIM till the sacrifice of subject. The same dose of saline (0.3 μl, 0.9% NaCl) was injected into the contralateral MGB as vehicle control for all subjects.

The exact stereotaxic coordinates of the injection sites in MGB were 5.5-5.8 mm caudal to the bregma, 3.3 mm lateral to the midline and 4.6-4.9 mm in depth.

3.2.3.4 Lesion of TRN with KA

Eight subjects were injected with KA (100 mM, 0.3 μl) in the TRN for a selective lesion of the TRN neurons two to seven days before BIM injection in the AC, this survival period being enough to verify histologically the efficacy and extent of TRN lesions (Steriade et al., 1985; Descheenes and Hu, 1990). Briefly, prior to any invasive procedures, the shaved area of the animals and the surgery apparatus were cleaned with 70% alcohol solution. KA was injected in small amounts (usually 0.05-0.06 μl) at two-six different sites to avoid seizures over a period of 60-90minutes. The exact stereotaxic coordinates of the injection sites in TRN were 3.2-3.8 mm caudal to the bregma, 3.6 mm lateral to the midline and 4.3-5.5 mm in depth. Finally, the bony cavity was packed with absorbable gelatin sponge and the wound was sutured and treated with lidocaine (Astra GmbH, Wedel, Germany). For postoperative care, antibiotic ointment (Furacin, SmithKline Beecham Pharmaceuticals, Johannesburg) was administered daily to the skin wound. To examine the effectiveness of the KA in selectively damaging the TRN neurons, coronal sections containing the TRN cut at 60μm were processed with Nissl staining.

3.2.4 Extracellular Recordings

The gross EEG was recorded monopolarly by means of a screw inserted into the bone over the cortical pericruciate area, served as monitoring the anesthetic level of the subject. The subject was mounted in a stereotaxic device following the induction of anesthesia. Body temperature was maintained between 37.5 and 38.5°C. Before the left ear was freed from the ear bar, the head was fixed with two stainless steel bolts together with acrylic resin to an extended arm of the stereotaxic frame. These ensured that the subject's head remained fixed to the stereotaxic device without movement (He, 1997; He et al., 2002).

Two types of electrodes were used to recording the cortical and thalamic neuronal activity extracellularly: (1) array of four/six/eight tungsten microelectrodes in constant inter-electrode distance of 0.2/0.5 mm, with an impedance of 1-2/5-6 MΩ (FHC Inc., Bowdoin, ME); (2) a single tungsten microelectrode (impedance: 1-2/5-6MΩ) attached to a glass micropipette of diameter of 30-40 μm, which was used for drug application.

The electrodes were advanced using a stepping micro-motor，that was controlled outside the sound-proof room. A preliminary mapping experiment was carried out to confirm the MGB and AC with acoustic responses. Penetrations were made according to the rat atlas (Paxinos and Watson, 1998), also referring to the topography of brain surface vessel (Figure 4.1), perpendicularly to the surface of the AC and vertically from the top of the brain to the MGB. Normally, the recording electrode array was placed in thalamus targeting the MGv with two/three electrodes of the matrix. Briefly, the electrodes were vertically

penetrated into the MGB, and after recording the first acoustic response, the electrodes were further advanced by 400-600μm. The MGv neurons are characterized with short latencies and easy-defined CF. The cortical electrodes were placed at a depth of 700 to 1100 μm targeting at Layers V and VI. The vertical coordinate of the electrode was determined at a point slightly above the cortical surface at the first penetration, was kept throughout each experiment for AC and thalamus respectively (He, 2003a). Spontaneous activities or acoustic responses of multi-units were simultaneously recorded in the MGB and AC, before, during and after BIM injection into the AC.

Signals were A/D-converted (Axon Digital 1440, Axon Instruments, Union City, CA) and filtered (300 Hz-5 kHz) before stored in a computer for off-line analysis. Spikes of single unit were detected with home-made software: time-amplitude window-discriminator.

For anatomical confirmation of recording sites, a small lesion was made passing a current of 1.0-2.0 μA through a recording electrode at the end of the last recording penetration in some subjects.

3.2.5 Electrical stimulation

Electrical stimuli, a train of 1 to10 monophasic (or biphasic) electric pulses (50-200 μA, 0.2-ms duration, 10/20-ms interval), were delivered through a either bipolar low-impedance electrode (He, 2003a; Yu et al., 2004a).

3.2.6 Histology

3.2.6.1 *C-fos* immunohistochemistry

After electrophysiological recordings, All subjects were deeply anesthetized with an overdose of pentobarbital sodium (0.1 ml/100 g, 60 mg/ml, i.p.) and perfused transcardially with 200 ml 0.9% NaCl, followed by ice-cold 4% paraformaldehyde in 0.1 M phosphate buffer (PB, pH 7.4). The brains were quickly removed from the skull and post-fixed for 4 hrs in the same fixative. After post-fixation, the brains were cryoprotected in 30% sucrose in PB (0.1 M, pH 7.4) for 2 days at 4°C. Coronal sections (with a thickness of 40 μm) were cut with a freezing microtome. Three serial sections were collected in phosphate-buffered saline (PBS, 0.01 M): one series was processed for *c-fos* expression, one series for Nissl staining, and the last one as reserve.

For *c-fos* expression, the series of sections were pretreated with a 0.3% hydrogen peroxide solution, followed by 1% sodium borohydride solution to remove peroxidase and aldehyde groups left in tissue after fixation with paraformaldehyde (Lai et al., 2004; Lai et al., 2006). The sections were then incubated in primary Fos antibody (1:4,000; rabbit polyclonal against a synthetic N-terminal fragment at residues 4-17 of human Fos; PC38; Calbiochem, La Jolla, CA) in PBS with 2% normal goat serum (NGS) and 0.3% Triton X-100 overnight at room temperature or 48 hrs at 4°C. After incubation with primary antibody, the sections were placed in biotinylated goat anti-rabbit IgG secondary antibody (Vector; 1:200; in PBS with 2% NGS and 0.3% Triton X-100) for 2 hrs at room temperature, and avidin-biotin peroxidase complex (ABC, Vector; 1:100

diluted by PBS) for 1 hr at room temperature.

In between steps, the sections were rinsed three times with KPBS (5 min/rinse) and then sections were agitated on a rotator during each step. Finally, an intensified diaminobenzidine tetrahydrochloride (DAB) reaction (DAB, 0.02% w/v; H_2O_2, 0.002% v/v; in KPBS; Vector, Burlingame, CA, USA) was carried out for 10 minutes at room temperature (Lai et al., 2004). The reaction was stopped by washing with KPBS (3 times). Control and experimental tissues from each group were processed in parallel. No staining was observed on brain sections with the omission of either the primary or secondary antibody. The sections were then mounted on gelatin-coated slides and were allowed to air dry at room temperature. They were dehydrated in a series of different concentration of ethanol: 50% ethanol (10 min), 70% ethanol (10 min), 90% ethanol (10 min), absolute ethanol (2 x 10 min) and then in toluene (2 x 10 min). Finally, the sections were mounted in DPX (BDH chemicals) and covered by glass coverslips.

Fos-positive neurons in subcortical auditory nuclei including the MGB were examined under a light microscope (Axioplan 2 imaging, Zeiss) and captured with a CCD camera (Spot; Diagnostic Instrument). Images of captured files were assembled using Adobe Photoshop 6.0.

3.2.6.2 Nissl staining

Nissl staining was used to confirm the selective lesion of TRN with KA, ablation of AC. Sub-divisions of the MGB were parceled based on the Nissl staining ,

referring to the atlases of Paxinos (1998).

3.2.6.3 Cell counting and Statistical Analysis.

Numerical results are expressed as means ± standard deviation (SD). Fos-positive neurons were analyzed in terms of density, cells per unit area, which allowed the contribution of cells from different animals to be normalized in case the animals are different sizes or different numbers of sections are used in different animals. Moreover, the labeling in different subdivisions of MGB would not be related to the size of the subdivisions. The total number of Fos-positive neurons of each anatomically demarcated nucleus of MGB (i.e. MGv, MGd and MGm) in each section was counted under a brightfield microscope at 100X magnification. The nomenclature of cell groups was in conformity with that described in the brain atlas of adult rats (Paxinos et al., 1998; Paxinos and Watson, 1998). Only cells in which the level of DAB reaction product in the nucleus was significantly higher than the tissue background levels were counted. This was based on an average gray level cutoff of 130 units (of 255) when the labeled neurons were analyzed with the digital image analysis system (Image version 1.61, W. Rasband, NIH; Lai et al., 2004). To facilitate the counting and to ensure the scientificity, the MGB was divided into three sub-areas: rostral, middle and caudal. Two or Three sections per sub-area and at least two animals per group were included, and the density of Fos-positive neurons was calculated by averaging those of all the selected sections. A student's *t-test* was used to examine the differences between two groups.

Analysis of variance (ANOVA) was used to examine the differences among three or above groups. The confidence level was taken at 95% ($P<0.05$).

Synchrony among different recording channels was quantified through cross-correlogram. For some descriptive analysis, a representative sample of the raw data was included.

Chapter 4

Corticothalamic Synchronization Leads to *c-fos* Expression in the Auditory Thalamus

4.1 Introduction

The thalamus relays sensory information to the cerebral cortex with an exception of olfaction, and in return, receives massive feedback projections from the cortex (Jones, 1985; Winer and Larue, 1987; Ojima, 1994; Steriade et al., 1997). Corticothalamic projections are suggested to provide a gain-control mechanism on the transmission of sensory information (Murphy and Sillito, 1987; Villa et al., 1991; He, 2003a) and to play an important role in the generation of neural oscillations (Steriade et al., 1993a; Golshani and Jones, 1999; Bal et al., 2000). In the auditory system, high frequency oscillation can be generated in the cortex, evoked by acoustic stimuli, and modulated by thalamic stimulation (Barth and MacDonald, 1996). A slow oscillation of < 1 Hz and a spindle-like oscillation of 5-10 Hz have also been described recently in the auditory thalamus (He, 2003b). The thalamic reticular nucleus (TRN) is situated between the cerebral cortex and the dorsal thalamus, playing an important role in controlling the flow of information between them, and is particularly well suited for the generation of spindle oscillations (7–14 Hz) that characteristically appear during early stages

of sleep. Moreover, the TRN has been proposed as a bridge linking the specific and non-specific pathways, leading to a large-scale coordination of neuronal processes (Llinás and Pare, 1997) by virtue of intranuclear connections through dendrodendritic GABAergic synapses (Steriade et al., 1985; Fuentealba et al., 2004) and electrical coupling (Landisman et al., 2002; Fuentealba et al., 2005).

Neuronal expression of Fos protein following novel physiological input constitutes a useful marker for polysynaptic activation, allowing subpopulations of neurons in specific neuronal circuits to be identified (Morgan et al., 1987; Sagar et al., 1988). Fos-immunoreactivity has been used to identify functionally activated neurons in the ascending auditory system (Keilmann and Herdegen, 1997; Luo et al., 1999; Saint Marie et al., 1999; Zhang et al., 2003; Sun et al., 2007). *C-fos*, however, did not express in the ventral and dorsal divisions of the MGB when the animal was exposed to acoustic stimulation in isolation (Zhang et al., 2003; Sun et al., 2007).

GABA is the major inhibitory neurotransmitter in cerebral cortex (Curtis and Johnston, 1974; Winer, 1992) where it acts on $GABA_A$-and $GABA_B$-receptors (Bormann, 2000; Chebib and Johnston, 1999). $GABA_A$-receptors mediate fast inhibitory postsynaptic potentials (Metherate, 1998; Li et al., 1996) which are particularly well-suited to generate or sharpen receptive field properties of cortical neurons (Sillito, 1975a, 1975b). Injections of bicuculline, an antagonist of $GABA_A$-receptors, into the sensory cortex can block the inhibitions on the cortical neurons and thus induce cortical hyperactivity (Sillito, 1975a; 1975b;

Johnson and Seutin, 1997; Sun et al., 2007).In an attempt to study the contribution of the corticofugal projection to thalamic neurons in the ascending auditory circuitry using Fos as an activity marker, we ascertained for the first time, the present of dense Fos-positive neurons in the ventral division (MGv) of medial geniculate body (MGB) after the auditory cortex (AC) was activated by injection of bicuculline methobromide (BIM), even though the acoustic stimuli are not present. We further investigated the relationship between *c-fos* expression in the MGB and corticofugal activation, as well as its pathway and related neurotransmitter- receptor types.

4.2 Materials and methods

Please refer to Chapter 3 for details about the animal preparation, application of drugs, multi-channel extracellular recording and histological procedures. All data in this chapter came from SD rats. EEG was recorded from the pericruciate area unless otherwise noted.

In this part, the following questions will be answered.

For the *c-fos* expressions in MGB:

1) What is the role of AC in inducing the *c-fos* expression in MGB (AC→MGB)? Can the same results be observed in other sensory systems in the corticothalamic network, e.g., the visual cortex (VC) →the lateral geniculate nucleus (LGN), and the somatosensory cortex (SC)→ the ventrobasal nucleus (VB)?
2) What are the related transmitters and receptors, excitatory glutamate, modulatory Ach or inhibitory GABA?
3) TRN neurons also expressed Fos protein. What is the role of TRN? Which corticothalamic pathway is involved, the direct excitatory one or the indirect inhibitory one via TRN?

For neuronal activities associated with *c-fos* expression in MGB:

1) What happened inside the corticothalamic network, which maybe underlie the *c-fos* expression in MGB after BIM injection in AC?
2) Which factor(s) is (are) more related with *c-fos* expression in MGB, the firing intensity or the firing pattern?

4.3 Results

4.3.1 Primary mapping in MGv and AC

The tonotopic organizations of the AC and MGB, especially the primary auditory area (AI) and MGv, were roughly mapped by using extracellular recording over several animals (four for AC, three for MGB) to identify the recording sites, injection sites and stimulation sites. For the MGB, sections stained with Nissl method were superimposed on the physiology map, by using the electrode penetration tracks and the electrical lesion as guidance. For the AC, the brain surface vessels were served as the landmark to superimpose the recording results from different animals.

We found that AI was identified in the posteriolateral neocortex in temporal lobe (Figure 4.1 showing the location and tonotopic organizations of AI, data from three animals), characterized by short latency responses to noise bursts and tonotopic organization with high frequencies represented rostrally and low frequencies caudally. Cells of similar characteristic frequencies formed the isofrequency contours in a dorsoventral orientation. These observations were well consistent with previous studies (Sally and Kelly, 1988; Gaese and Ostwald, 1995). Moreover, we found visual neurons located caudal and dorsal to the AC and somatosensory neurons, responding to the touch of the contralateral whiskers, within an area rostral and dorsal to the AC, namely barrel cortex.

Neurons in MGv were characterized with short latency(less than 10ms) and easily-defined characterized frequency (CF). The tonotopic organization of MGv

was impressive with low frequency represented dorsally and high frequency ventrally (Figure 4.2). From the histological and electrophysiological results, we knew that the MGB extended about 1.7 mm (6.4-4.7 mm caudal to bregma) in caudorostral orientation, 1.3 mm or so (2.7-4.0 mm lateral to the midline) lateromedially, and about 1.5 mm ventrodorsally, and that the MGv is the principal nucleus which takes up the large majority of MGB.

4.3.2 *C-fos* expression in the MGB is specific to the corticothalamic activation

4.3.2.1 No Fos expressed in MGv and MGd neurons activated by ascending inputs in isolation

Acoustic stimuli elicited no *c-fos* expression in the MGv and MGd of anesthetized animals. Various acoustic stimuli, including pure tones of different frequencies and noise bursts with repetitive rates of 1-3 Hz (60-75 dB SPL), were applied to the animals for 1-4 hrs. Although *c-fo*s expression was found in the cochlear nucleus, superior olivary complex and inferior colliculus (Figure 4.3, lower panel)，only a few Fos-positive neurons were detected in the MGB, with no labeling in the MGv and only sporadically scattered labeling in the MGm (Figure 4.3, upper panel).

Moreover, a variety of electrical stimulation strategies were adopted to either the inferior colliculus or the MGB, and no Fos-positive neurons could be detected in

MGv and MGd (data not shown).

4.3.2.2 C-fos expression in the MGB triggered by cortical activation

By contrast, the MGv and MGd showed extensive *c-fos* expression following cortical BIM (a $GABA_A$ antagonist) injection (Figure 4.4). Both MGv and MGd were most strongly labeled, extending along the rostrocaudal dimension. Control saline injections did not result in cortical and thalamic *c-fos* expression (data not shown). Furthermore, *c-fos* expression following unilateral cortical BIM injection was restricted to the ipsilateral MGB and cortex (Figure 4.4). Similar results were also observed in other sensory systems. The activation of the specific sensory cortex, e.g. VC (n=2 subjects) and SC, with BIM injection, resulted in *c-fos* expression in the related primary (lemniscal) dorsal thalamic nuclei, e.g. the dorsal division of LGN (dLGN, Figure 4.5) and VB (Figure 4.6).

In Figure 4.5, a small volume (0.1μl) of BIM was injected in the primary visual cortex. *C-fos* was expressed mainly in the dorsal division of LGN (dLGN) and the visual sector of TRN, when compared with the contralateral side. No Fos-positive neurons were found in other sensory thalamic relay nucleus, e.g. MGB and VB, and the auditory sector of the TRN with a small volume (0.1μl) of BIM injection in VC.

In another example (Figure 4.6), a larger volume (0.3 μl) of BIM was injected in the somatosensory barrel cortex, where neurons could respond to the touch of the contralateral whiskers. Fos-positive neurons were remarkably detected in the

VB nucleus and TRN (Figure 4.6A and B). *C-fos* expression was also found in other sensory thalamus (Figure 4.6B and C) when compared with the small volume (0.1μl), e.g. MGB, the auditory sector and visual sector of TRN. However, there were few Fos-positive neurons found in the dLGN. It is noteworthy that BIM injection in barrel cortex was much easier to induce *c-fos* expression in MGB than that in visual cortex with the same dose.

4.3.2.3 AC is an indispensable component in the cortically-induced c-fos expression in the MGv

Although we found that MGB neurons could express Fos protein after BIM injection in the barrel cortex, we could not rule out the active role of AC in this process. In the following experiments (Figure 4.7), we extensively ablated the AC before BIM (0.3 or 0.4μl) was injected in the barrel cortex (n=3 subjects). No Fos-positive neurons were detected in the MGv when compared with that of un-ablated animals (Figure 4.7 C and D), indicating that AC is indispensable for the *c-fos* expression in the MGv. However, *c-fos* expression was still detected in the auditory sector of TRN (Figure 4.7 B), implying that the activations of MGB and AC neurons is not the only way that could induce the *c-fos* expression in the auditory sector of TRN, and that the TRN intranuclear connections might also contribute it.

4.3.3 *C-fos* expression is mediated by glutamate and its receptors

4.3.3.1 C-fos expression is elicited by glutamate but not acetylcholine

To understand the dependence of *c-fos* expression on neurotransmitters that are related to descending and ascending projections, we injected glutamate (excitatory neurotransmitters, n=7 subjects), Ach (neuromodulator in the forebrain, n=3 subjects) and GABA (inhibitory neurotransmitters, n=3 subjects) in the MGB.

Direct injection of glutamate in the auditory thalamus could elicit *c-fos* expression in MGB neurons, while injection of Ach did not evoke *c-fos* expression in the MGv (Figure 4.8A). And glutamate-induced *c-fos* expression was also widely distributed, about 0.8 mm (n=3 subjects) in caudorostral orientation, reflecting of a population activity of neurons, though its range was much smaller than that derived from the BIM injection in AC. No Fos-positive neurons were envisioned in the MGv and MGd after GABA injection in the MGB (data not shown).

The induction of *c-fos* expression in the MGB by glutamate injection, however, depended on the level of anesthesia (Figure 4.8B). Animals (n=3) that were not administered with further anesthetic after glutamate injection procedure showed *c-fos* expression as in Figure 4.8, while those (n=4) which were supplemented with ketamine/xylazine to maintain their anesthesia level as normally during their survival period showed no *c-fos* expression in the MGB (Figure 4.8B, right panel). In both conditions, Fos-positive neurons were found in the AC, reflecting of the activation of the AC neurons and the efficacy of the glutamate injection in

MGB (Figure 4.8B).

4.3.3.2 Cortically-induced c-fos expression can be blocked by glutamate receptor antagonists

Then the next questions came up. What glutamate receptor types are involved in *c-fos* expression in the MGB? After BIM injection in the auditory cortex, we respectively injected three antagonists for different glutamate receptor types-APV (for NMDA receptor, n=3 subjects), CNQX (for AMPA receptor, n= 3 subjects) and LY367385 (for metabotropic glutamate receptor, mGluR1α, n=3 subjects) in the MGB. The results (Figure 4.9) showed that all of the three antagonists had a strong suppressive effect on the *c-fos* expression elicited by corticofugal activation (BIM injection in the auditory cortex).

Figure 4.9B-D illustrates that the spread of injection demarcated by mixing of the antagonist with pontamine skyblue (1%). In the approximate areas of the injection sites in the MGB, the suppressive effects were even more obvious. For example, the injection of CNQX, shown in Figure 4.9C, was locally restricted to the caudal MGB so that the suppression of *c-fos* expression in the middle and rostral MGB was relatively weaker than that produced by the injection of NMDA and mGluR1 receptor antagonists that spread more rostrally (Figure 4.9B and D). All of the three antagonist types for glutamate receptors had an effect in diminishing c-*fos* expression in the MGv.

4.3.4 Activation of the auditory cortex triggers the synchronized corticothalamic oscillations

4.3.4.1 Activation of the auditory cortex triggers the corticothalamic synchronization

To find out what happened to the MGB and AC neurons after BIM injection in the AC, and the physiological relationship between them, we simultaneously monitored neural activities in the thalamus and cortex through multi-channel extracellular recordings. We found an increased spontaneous activity and rhythmic burst firings in MGB neurons, which were synchronized with that in the AC. Figure 4.10A showed multi-channel extracellular recordings from the MGB (MGB1-4) and the auditory cortex (AC) before, during, and after BIM injection in the auditory cortex. Spontaneous neuronal activities were observed in all recordings in the MGB and the auditory cortex. These activities were not well synchronized before BIM injection in the cortex (Figure 4.10A, left panel). The auditory cortex started a rhythmic activity during the course of BIM injection into the cortex (Figure 4.10A, middle panel).

Corticothalamic synchrony developed 6.8 ± 3.9 min (n=13 subjects) after cortical BIM injection. The right panel of Figure 4.10A shows neuronal activities of the thalamus and cortex 12 min after BIM injection. In this case, the cortex and thalamus developed a highly synchronized activity with a rhythm of 2.8 Hz and a lag time of less than 50 ms. From the expanded traces (right panel

of Figure 4.10A), it was found that bursts in the cortex occurred before those of the thalamus. The cross-correlograms (bottom row of Figure 4.10A) revealed that there were no obvious correlations between the cortical and thalamic events before BIM injection. Rhythmic activity and the synchrony between the MGB and AC started during BIM injection (middle panel) and fully developed after BIM injection (right panel) with the AC preceding the MGB. This phenomenon was confirmed in all animals with a rhythmic oscillation of 0.3-3 Hz after BIM injection in the AC.

4.3.4.2 The strong association between c-fos expressions and the synchronized corticothalamic activities

The Fos-immunohistochemical results showed that there were no Fos-positive neurons in the MGB contralateral to injections site (Figure 4.4), so we simultaneously recorded the neuronal activities from the bilateral MGB after BIM injection (Figure 4.11A). Consistent with the histology, no synchronized activity was observed between bilateral MGB neurons, and no such strong burst firings as that in the ipsilateral MGB neurons were perceived in the contralateral side.

Similarly, we could not find synchrony between the MGB neurons and VB neurons in animals (Figure 4.11B), the AC of which was ablated before BIM injection in the barrel cortex. The synchrony among the VB sites was in line with the histological results that Fos protein was detected here (Figure 4.7).

In Figure 4.11C, we injected BIM in the frontal cortex (5-6 mm rostral to bregma, n=2 subjects). We failed to find the increase of both intensity and synchrony in the MGB and AC neuronal discharges. Histology also showed no *c-fos* expression herein.

In Figure 4.11D, a deep coronal section was made at 5.0 mm caudal to bregma from the brain surface deep into the rhinal sulcus (n=2 subjects), disconnecting the caudal MGB from the rostral MGB, TRN and the cerebral cortex (lower row). After that, BIM was injected into the AC. The synchronized corticothalamic oscillations were only observed in sites rostral to the section, where the cortical connections remained intact, not in the caudal MGB sites (up left), the acoustic responses of which were good (up right).

All in all, we found a strong association between the *c-fos* expressions and the occurrence of synchronized corticothalamic activities.

4.3.5 Firing patterns and *c-fos* expression

4.3.5.1 C-fos expression in the MGv is not a simply reflection of neuronal activity or the increment of neuronal activity

As *c-fos* is considered as a marker of incremental activity (Sagar et al., 1988; Morgan and Curran, 1991), the correlation between *c-fos* expression and neuronal activity was examined. Eighteen single units, eight recorded before and ten after BIM injection in the auditory cortex, were isolated from two BIM

(small volume)→AC animals. Eighteen other single units, eight recorded before and ten during the presentation of acoustic stimulus (AS, noise burst, 75dB SPL, 3 times/s), were isolated from two AS animals. Another eight single units, recorded at about ten min after the injection of kainic acid (KA) to the MGB, were isolated from two KA→MGB animals. KA, known to selectively destroy cells in the injected region but not axons coursing through the area (McGeer et al., 1978; Steriade et al., 1985; Descheenes and Hu, 1990), was used here to activate MGB neurons for a short period of 1.5 hr.

Figure 4.12A illustrated the raster displays of three single neurons, respectively from the three preparations listed above. The left column in Figure 4.12A shows the spontaneous neuronal activities before (control) and after BIM injection. The middle column shows spontaneous activities before (control) and after the delivery of repeated acoustic stimuli. The right column illustrates spontaneous activities after KA injection. It was obvious that the firing rates after BIM or KA injection in the auditory cortex and during acoustic stimulus were significantly higher than those under control conditions (Figure 4.12A and B). The spontaneous firing before KA injection can be assumed to be similar to the spontaneous firings shown in the other controls of the upper row.

The mean firing rates over 20 s was calculated for neurons and was summarized in Figure 12B. The means of all controls were similar (BIM→AC: 1.10 ± 0.62 spikes/s; AS: 1.57 ± 0.67; $p>0.05$, ANOVA). The firing rate increased significantly in all experimental conditions compared with controls (BIM→AC:

4.77 ± 1.87 spikes/s; AS: 5.20 ± 1.42; $p<0.05$, t-test; KA: 4.79 ± 0.98; Figure 4.12B). However, there were no significant differences in neuronal firing rates among the different experimental groups ($p>0.05$, ANOVA). Despite that they showed comparable spikes per unit time, their temporal patterns of the rasters (Figure 4.12A, lower panel) were different: BIM→AC showed spontaneous synchronized burst-like firings (indicated by red underline), and the other two showed much more single spikes.

An example of *c-fos* expression in the MGB for each of the three conditions is shown in Figure 4.12C. In both conditions of AS and KA→MGB, no *c-fos* expression was elicited in the MGv. *C-fos* expression was only detected in the MGv of BIM→AC animals. Considering that all three conditions had similar firing rates or increments in firing rate, the result that only BIM→AC animals had *c-fos* expression in the MGB could lead to the conclusion that *c-fos* expression in the MGv was not a simply reflection of neuronal activity or the increment of neuronal activity.

4.3.5.2 Burst firings associated with c-fos expressions are different from those in spindle oscillations

As we known, it is the hyperpolarizations derived from the activities of TRN that activate a hyperpolarization-activated inward current (I_h)(Pape and McCormick, 1989), which in turn, depolarizes the membrane potential of the TC neurons toward threshold for a Ca^{2+}-dependent low-threshold spike (LTS)

crowned by a burst of Na^+ fast spikes (LTS burst firings), eventually generating the spindle oscillations in the thalamocortical network. Spontaneous spindle oscillations recurred when the animals were anesthetized with either ketamine/xylazine or pentobarbital. In many cases of ketamine/xylazine (Figure 4.13), the firing rates of MGB neurons were as high as that of BIM-induced oscillations, or even stronger, and the firing patterns also showed burst discharges, which have been well documented in previous studies (Steriade et al., 1993a; Contreras and Steriade, 1996; Steriade et al., 1997; Sanchez-Vives and McCormick, 2000). However, we failed to find any Fos-positive neurons in the MGv and MGd of those animals (data not shown).

Moreover, the BIM-induced bursts showed a relative constant inter-spike intervals (ISI), which were different from the progressively increasing ISIs observed in the spindle bursts (Figure 4.13C; Hu and He, 2002; Hughes et al., 2004). In the latter experiments, we found that the BIM-induced burst firings remained nearly intact after the complete TRN lesion (for details, see 4.3.6), which, again, was different from the spindle bursts.

All these results led us to conjecture that burst firings associated with *c-fos* expressions after cortical BIM injection are different from those in spindle oscillations, and a high-threshold burst was more possibly involved(Jahnsen and Llinas, 1984c; Hughes et al., 2004).

However, further studies，especially intracellular arguments, are needed to prove our speculation that burst firings associated with *c-fos* expressions in MGv are

high-threshold calcium current dependent.

4.3.6 BIM-induced corticothalamic synchrony and thalamic *c-fos* expression do not depend on the TRN

4.3.6.1 C-fos expressions in the TRN neurons after BIM injection in the AC

We understand that the TRN is engaged in most corticothalamic oscillations. Strong TRN inhibition would cause a prolonged hyperpolarization of MGB neurons, which might lead to low-threshold calcium spikes or spike bursts (Steriade et al., 1993a; Golshani and Jones, 1999; Bal et al., 2000; Xiong et al., 2004) within spindle or delta rhythms. Our results also showed that Fos-positive neurons were obviously found in the TRN (Figure 4.5, 4.6, 4.7 and 4.13) ipsilateral to the BIM injection site.

On one hand, neurons in different TRN sectors showed modality-specific and a topographic connection with the dorsal thalamus and neocortex. For example, a small volume (0.1μl) of BIM injections local in the primary visual cortex led to *c-fos* expressed only in visual sector of the TRN (Figure 4.5).

On the other hand, TRN also exhibited the cross-modality features in *c-fos* expressions. As mentioned above (Figure 4.6 and 4.7), BIM injection in the barrel cortex could not induce *c-fos* expressions in the MGv after AC ablation. The TRN, however, still could find Fos-positive neurons, which might be due to the intranuclear interaction within the TRN, or the widespread projections from

the barrel cortex to the TRN of different modality. The TRN has been proposed as a bridge linking the specific and non-specific pathways, leading to a large-scale coordination of neuronal processes (Llinás and Pare, 1997) by virtue of intranuclear connections through dendrodendritic GABAergic synapses (Steriade et al., 1985; Fuentealba et al., 2004) and electrical coupling (Landisman et al., 2002; Fuentealba et al., 2005).

We had already known that the BIM-induced corticothalamic activation was mediated by glutamate and its receptors, and so far we also have known that TRN neurons were also activated by the cortical BIM injection, it was, however, unknown whether the corticothalamic synchrony and the *c-fos* expressions caused by cortical BIM injection depended on the TRN, and to what extent the TRN played a role herein. To examine this problem, one of the strategies is separate the corticofugal direct effects from those mediated by the collateral activation of TRN neurons by removal or selectively lesion of the TRN (McGeer et al., 1978; Steriade et al., 1985; Descheenes and Hu, 1990).

4.3.6.2 Complete lesion of the auditory sector of the TRN

We injected with kainic acid in the TRN for a selective lesion of the TRN neurons two to seven days before the detection section (n=8 subjects), this survival period being enough to verify histologically the efficacy and extent of TRN lesions (Steriade et al., 1985; Descheenes and Hu, 1990). Histological

results showed that, there was a complete damage of the TRN neurons (Figure 4.14), extending widely along the caudorostral axis, which almost covered the whole TRN region. KA injections resulted in nearly complete cell loss in the right TRN. In Figure 4.14A, the perikarya of lesioned TRN neurons disappeared with only some dusty Nissl substance perceived (right). In contrast, Nissl bodies in the control side were well-defined (left, indicated by the arrow head). Dorsal thalamic damage was observed in the ventroposterolateral nucleus (VPL, a nucleus of VB, adjacent to the TRN) of some animals.

The animals were injected with BIM in the AC two-seven days after the TRN lesion. No Fos-positive neurons could be detected in the auditory sector of the TRN after lesion (Figure 4.14B, right), also confirming that the auditory TRN neurons were damaged.

4.3.6.3 TRN lesion does not abolish the BIM-induced corticothalamic synchrony and thalamic c-fos expression.

Although almost the whole TRN, especially the auditory sector of the TRN was completely lesioned, *c-fos* expression in the MGv (Figure 4.15Aa, left) was almost unaffected when compared with those without TRN lesion, indicating that the indirect pathway of AC-TRN-MGB did not exert a decisive effect on *c-fos* expression in the MGB. A parallel experiment, in which GABA was directly injected to the MGB before BIM injection in the AC (Figure 4.15Aa, right), had no qualitatively positive effect on the *c-fos* expression in the MGB.

Both experiments demonstrated that the TRN has no obvious effect on *c-fos* expression in the MGB.

Figure 4.15B showed the effect of TRN lesion on the BIM-induced synchronization in the corticothalamic network. TRN lesion did not destroy the synchrony between the AC and MGB (Figure 4.15B), with no changes in the oscillation frequencies and the firing patterns of both the AC and MGB neurons. This indicated that the direct corticofugal pathway prevailed over the indirect pathway in producing this synchrony in the MGB.

4.3 Discussions

By combining the multi-channel extracellular recordings with Fos immunohisto-chemical methods, the present study illustrated a cortically BIM-induced synchronized oscillation in the corticothalamic network in *vivo* and its triggered *c-fos* expression in the primary thalamic nucleus, e.g. MGv. Five major findings are reported here. (1) We ascertained for the first time, that the MGv neurons can express Fos protein when AC is activated with cortical BIM (a $GABA_A$ receptor antagonist) injections (Figure 4.4, 4.6, 4.9A, 4.14B, 4.12 left, 4.15A), no matter whether acoustic stimuli are present or not. Instead, the corticothalamic inputs are critical (Figure 4.4-4.7, 4.12). (2) The BIM-induced synchronized corticothalamic oscillations with burst firing patterns are proposed to lead to the *c-fos* expression in the MGv (Figure 4.4-4.7, 4.10-4.12, 4.15). The association of *c-fos* expression and the synchronized corticothalamic oscillations is also observed in the other sensory corticothalamic network (Figure 4.5-4.6, 4.11), suggesting a common principle behind. (3) The *c-fos* expression in the MGB and the synchronized corticothalamic oscillations triggered by the BIM-induced cortical activation are elicited through a direct excitatory corticothalamic pathway, not by the indirect inhibitory pathway via the TRN (Figure 4.9, 4.14, 4.15). However, the present study can not rule out the active role of the TRN in this process. (4) The BIM-induced *c-fos* expressions in the TRN show both specific and cross–modality features (Figure 4.5, 4.7). (5) The BIM-induced burst discharges of the thalamocortical neurons are different from the

spindle-related LTS burst firings (Figure 4.13-4.15). The present results conclude that *c-fos* expression was not simply associated with firing rate, but rather with the firing pattern.

4.3.1 *C-fos* expression in the auditory pathway

Neuronal expression of Fos protein following novel physiological input constitutes a useful marker for polysynaptic activation, allowing subpopulations of neurons in specific neuronal circuits to be identified (Morgan et al., 1987; Sagar et al., 1988). Fos-immunoreactivity has been used to identify functionally activated neurons in the ascending auditory system (Keilmann and Herdegen, 1997; Luo et al., 1999; Saint Marie et al., 1999; Zhang et al., 2003; Sun et al., 2007).

In the present study, we could not elicit *c-fos* expression in the MGv with an acoustic stimulus, repeated electrical stimulation of the inferior colliculus, or direct KA injection in the MGB. Physiological experiments have shown that the MGB neurons responded to sound stimuli even in the anesthetized condition. The present results demonstrate that the corticofugal projection is crucial to elicit *c-fos* expression in MGv. Another implication of these results is that the descending cortical projection in the thalamus is much more physiologically powerful than the ascending projection from the inferior colliculus.

Previous studies have shown that cochlear nuclear neurons and inferior

colliculus neurons express *c-fos* upon activation by acoustic stimulus (Rouiller et al., 1992; Adams, 1995; Carretta et al., 1999; Saint Marie et al., 1999) as well as cortical neurons (Scheich and Zuschratter, 1995; Zuschratter et al., 1995). In the MGB, Fos-positive neurons were restricted to the medial divisions (MGm) while the ventral division (MGv) neurons, alternatively, showed no *c-fos* expression in response to acoustic stimuli (Saint Marie et al., 1999; Zhang et al., 2003; Sun et al., 2007), Figure 4.3). Only one other experiment has shown *c-fos* expression in the MGv (Newton et al., 2004). In that experiment, *c-fos* expression was elicited in the MGB after the animal acquired a visually cued conditioned fear. The authors concluded that the *c-fos* expression was elicited by a newly established pathway from the retina directly to the MGB. This was a highly speculative explanation, as there was no anatomical proof for the formation of such a circuit, and it was unclear whether the new circuit could be formed within 14 weeks. Additionally, there was no report that the ascending pathway could activate *c-fos* expression in the MGv. It is more likely that the fear conditioning caused an activation of the corticothalamic projection, which in turn activated the MGB by a process similar to that observed in the present study.

4.3.2 Neuronal activity and *c-fos* expression

Generally, *c-fos* has been considered as a marker of neuronal activity or a marker

of the increment of neuronal activity at certain conditions (Sagar et al., 1988; Morgan and Curran, 1991; Saint Marie et al., 1999; Mouritsen et al., 2004). Although similar firing rates were observed in MGB neurons after (i) BIM injection to the AC, (ii) receiving a fast-repetitive acoustic stimulus, or (iii) direct kainic acid injection to the MGB, only BIM injection to the AC produced dense *c-fos* expression in the MGB (Figure 4.12).

Kainic acid is an excitotoxic agent that increases spontaneous neuronal activity within 2-4 hr and damages neurons morphologically after 20 hr (Steriade et al., 1985; Lee et al., 1994). In the present study, Hyperactivity in the MGB was recorded after kainic acid was injected into the MGB, and the animal was sacrificed 1.5 hr after injection. Although we could not exclude the possibility of neuronal damage by kainic acid injection, the high firing rate of the MGB neurons gave evidence for their functionality.

It was necessary to activate the corticofugal pathway in order to induce *c-fos* expression in the MGv. Cortical activation caused synchronized burst firings in the MGB, suggesting that *c-fos* expression in the MGB may be linked to the burst firing pattern rather than the firing rate.

4.3.3 *C-fos* expression in the thalamus

In animals exploring for a new environment, Montero and colleagues showed that *c-fos* expression in the TRN and LGN was elicited by the corticofugal pathway (Montero, 1997; Montero et al., 2001). The sensory thalamic nuclei

received both ascending inputs from the brainstem and descending projections from the cortex, and meanwhile were modulated by acetylcholine release from the brainstem or the basal forebrain (Steriade et al., 1997). Corticothalamic terminals activate the TC neurons that expressed NMDA and non-NMDA ionotropic receptors, as well as mGluR receptors (Jones, 1985) (Scharfman et al., 1990; McCormick and von Krosigk, 1992; Turner et al., 1994; Golshani et al., 1998; Tennigkeit et al., 1999), while the ascending sensory terminals activated thalamocortical neurons that expressed only NMDA and AMPA ionotropic receptors (Salt and Eaton, 1996; Steriade et al., 1997).

Direct injection of acetylcholine did not elicit *c-fos* expression, while glutamate elicited dense *c-fos* expression in the MGv (Figure 4.8). The present result proposes that *c-fos* expression in the MGv is related to the corticothalamic inputs mediated by AMPA, NMDA and mGluR receptors. *C-fos* expression has been proposed to link with calcium influx, which then triggers a cascade of Ca^{2+}-sensitive gene expression (Sheng et al., 1988; Sheng et al., 1990; Lerea et al., 1992; Jinnah et al., 2003). Extracellular Ca^{2+} influx can occur through various channels, such as NMDA receptors and T-type and L-type voltage-operated Ca^{2+} channels. The mGluR1 receptor can also affect Ca^{2+} homeostasis and can trigger Ca^{2+}-sensitive gene transcription in neurons. The present results show that all of the three glutamate receptor types are involved in *c-fos* expression in MGv.

4.3.4 Thalamocortical oscillations and *c-fos* expression

Neurons in the thalamus and cerebral cortex showed spontaneous synchronized activities also before the cortex was injected with BIM. The $GABA_A$ antagonist can activate the auditory cortex. The interplay between the cortical and thalamic neurons (possibly including the TRN neurons) caused a rhythmic oscillation at a frequency of 0.3-3 Hz. This oscillation gradually spread from the auditory cortex to the thalamus, resulting in a synchrony between them.

The generation of the oscillation in the present study seemed not to depend on the TRN, since TRN inhibition only applied to the thalamus, and the cortex could develop the oscillation of similar rhythm before the thalamus. To further confirm whether the thalamic oscillation was directly driven by the corticothalamic projections or by the rebound from hyperpolarization derived from the TRN, we selectively destroyed the TRN neurons, with little effects on the fibers coursing through the TRN (McGeer et al., 1978; Steriade et al., 1985; Descheenes and Hu, 1990), and found that the MGB still showed the synchronized oscillation as that in the AC (Figure 4.15B). Using a similar preparation, Timofeev and colleagues (1998) concluded that thalamic neurons reflected cortical events as a function of the membrane potential in TRN/TC neurons and the degree of synchronization in cortical neuronal network. The present result indicates that the synchronized oscillation in the MGB could be generated without the participation of the TRN. In addition, the frequency and duration of the firing bursts in the thalamus did not change in TRN-lesioned

animals.

As we known, low-threshold-spike (LTS) burst firings of the thalamocortical neurons, underlying the generations of the spindle oscillations, arise from the hyperpolarizations, which were derived from the activities of TRN. However, we failed to find any Fos-positive neurons in the MGv of those animals, even though the firing rates of MGB neurons were as high as that of BIM-induced oscillations, or even stronger, and the LTS burst discharges were also synchronized with the cortical activity.

All these results led us to conjecture that burst firings associated with *c-fos* expressions after cortical BIM injection was different from those in spindle oscillations, and a high-threshold (HT) burst was more possibly involved (Jahnsen and Llinas, 1984c; Hughes et al., 2004).

However, further studies，especially intracellular arguments, are needed to prove our speculation that burst firings associated with *c-fos* expressions in MGv are high-threshold calcium current dependent. Our result from the *in-vivo* preparation showing that thalamocortical oscillations could occur without the participation of the TRN is a great addition to our present understanding that most thalamocortical oscillations need the inhibitory interaction of the TRN neurons (Steriade et al., 1993a; Destexhe et al., 1996a; McCormick and Bal, 1997; Guillery and Sherman, 2002; Timofeev et al., 2002).

The association between *c-fos* expression in the principle thalamic nuclei and the slow synchronized oscillations in the corticothalamic network was also applied

to other sensory corticothalamic circuitry, e.g. visual and somatosensory system.

Another striking finding is that the cortex started the oscillatory spontaneous activity before the thalamus (Figure 4.10). By suppressing the $GABA_A$ receptors after the cortical BIM injection, the cerebral cortex would be excitotoxically activated, as shown in the *c-fos* expression in the cortex (Figure 4.4, 4.6 and 4.7), especially in the deep layers, when compared with animals without *c-fos* expression in the primary thalamic nuclei (Figure 4.5). The hyperactivity of the cortex may activate the MGv directly via the projection neurons in layer VI of the auditory cortex (Rouiller and Welker, 1991; Ojima, 1994; He, 2003b). In contrast, the contralateral auditory cortex showed no *c-fos* expression (Figure 4.4A, left). A very weak synchrony was detected in the electrodes that were implanted in the contralateral cortex (data not shown). This indicates that there is a much stronger interaction between the cortex and thalamus within the same hemisphere than that between the cortices of the two hemispheres.

In summary, *c-fos* expression in the MGB triggered by cortical activation was elicited via a direct corticothalamic pathway, not by the pathway through the TRN. *C-fos* expression in the MGB had a link to glutamate receptors (viz. NMDA, AMPA and mGluR receptors), but not to acetylcholine receptors. The present results conclude that *c-fos* expression was not simply associated with firing rate, but rather the firing pattern. Burst firings of possibly high- threshold calcium spikes, which synchronized with the cortical oscillation, are proposed to

lead to *c-fos* expression in the MGB. The present results also imply that the corticothalamic projection is much stronger than the ascending collicular projection to the thalamus, and is much stronger than the commissural projection between the two hemispheres.

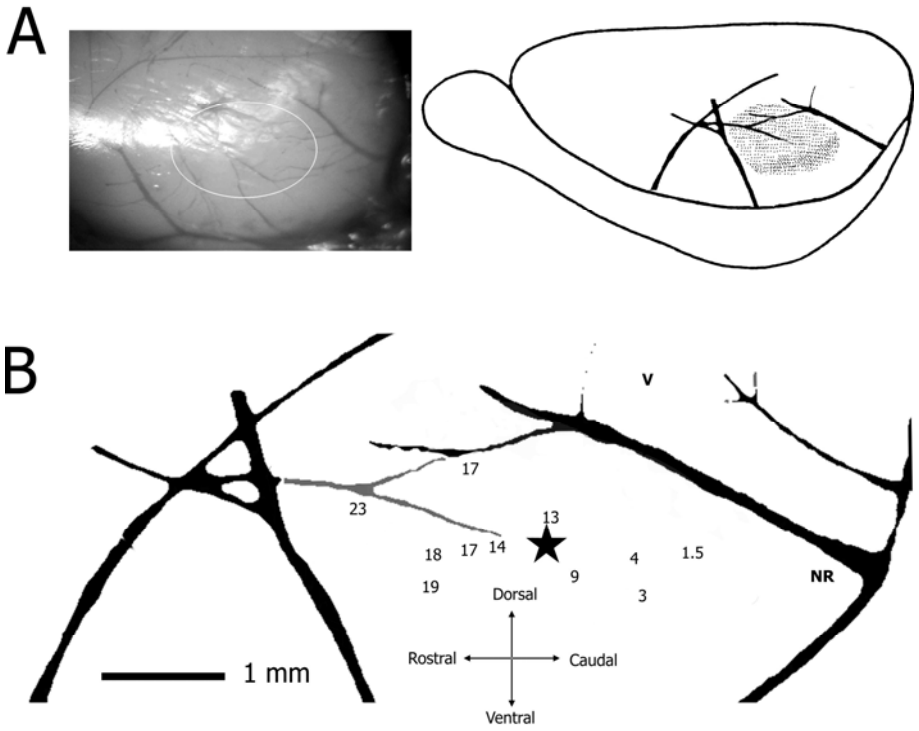

Figure 4.1 The location and tonotopic organizations of the primary auditory cortex (AI) in rats. (A) The brain surface vessels in the temporal lobe, AI indicated by dotted area. (B) The brief tonotopic map of AI with high frequencies represented rostrally and low frequencies caudally, data from three animals, superimposed according to the surface vessels. Numbers indicate neuronal characteristic frequencies (in kHz), and pentacle indicates the bicuculline injection site in the AC.

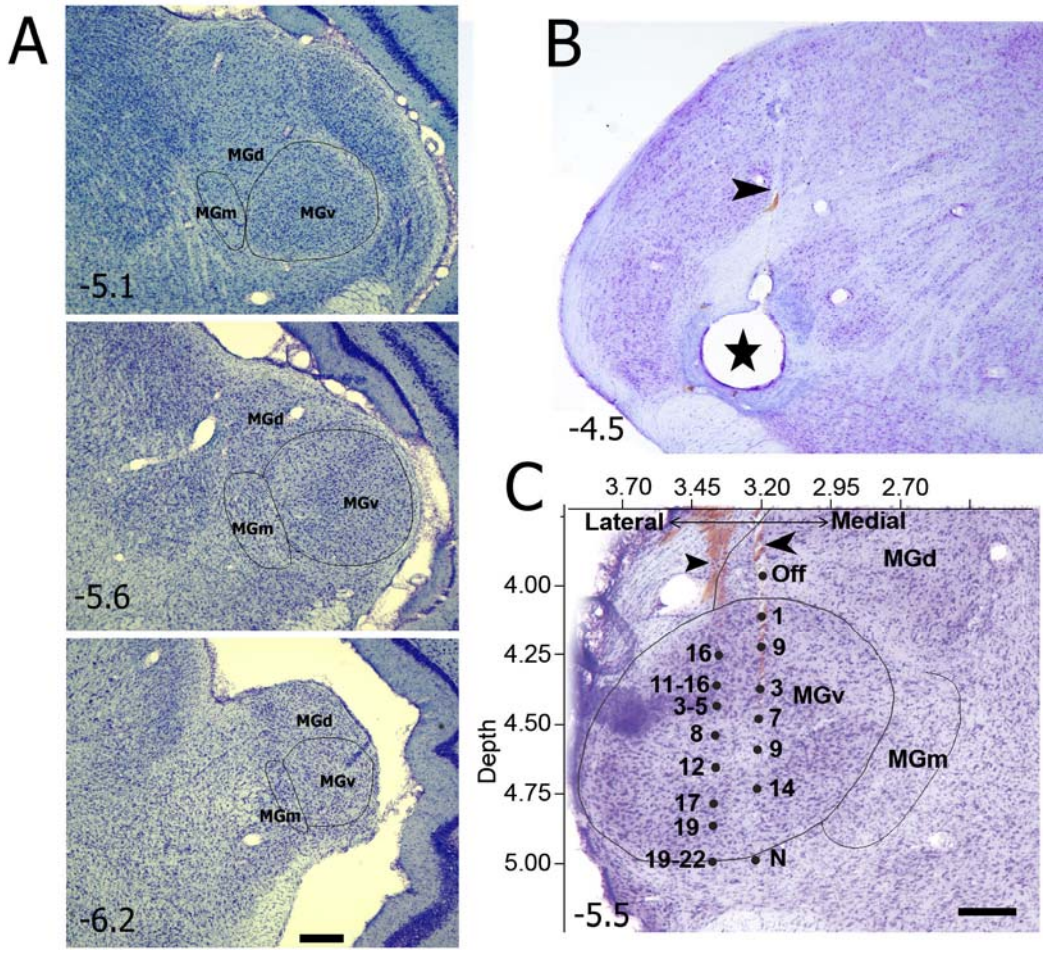

Figure 4.2 Coronal sections with Nissl staining showing the location and tonotopic feature of the medial geniculate body (MGB) in rats. (A)-(C) Number on the down-left corner of each section denotes the distance from bregma (-: caudal to bregma, in mm). This convention here applies to the following figures unless otherwise noted. (A) Series sections from the same animal showing the sub-divisions of the MGB. (B)-(C) from another animal. Two recording penetrations are shown in (C). Vertical coordinate indicates the depth from the cortical surface. Horizontal coordinate indicates the lateromedial distance from midline (in mm). Numbers beside the black circles indicate the characteristic frequency (CF, in kHz). The coordinate is re-constructed based on the electrical lesion area (marked with pentacle) and the electrode tracks (marked with arrow head). MGv: the ventral division of MGB, MGm: the medial division of MGB , MGd: the dorsal division of MGB. The conventions apply to the following figures. Scale bar: 400 µm.

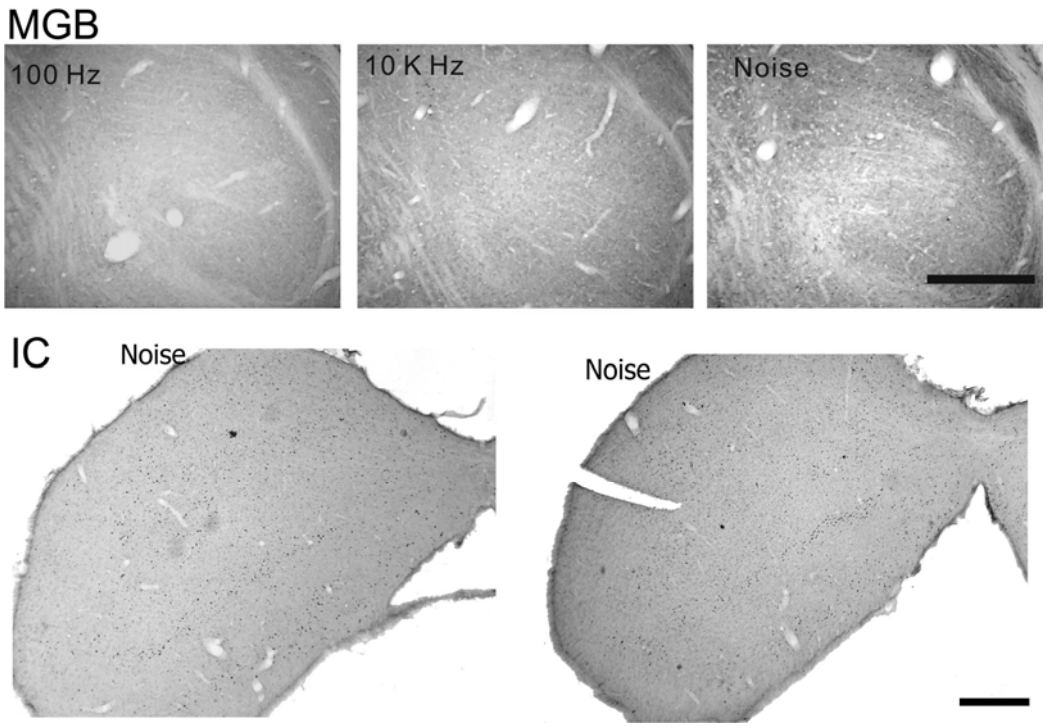

Figure 4.3 *C-fos* expressions in the inferior colliculus (IC) and MGB with acoustic stimulation in isolation. Upper: Acoustic stimuli evoked no Fos labeling in the MGB. Stimuli included pure tones (100 Hz and 10 kHz) and noise bursts. Lower: Noise burst induced *c-fos* expression in the IC, with bands-pattern distributions of Fos-positive neurons. Scale bar: 400 μm.

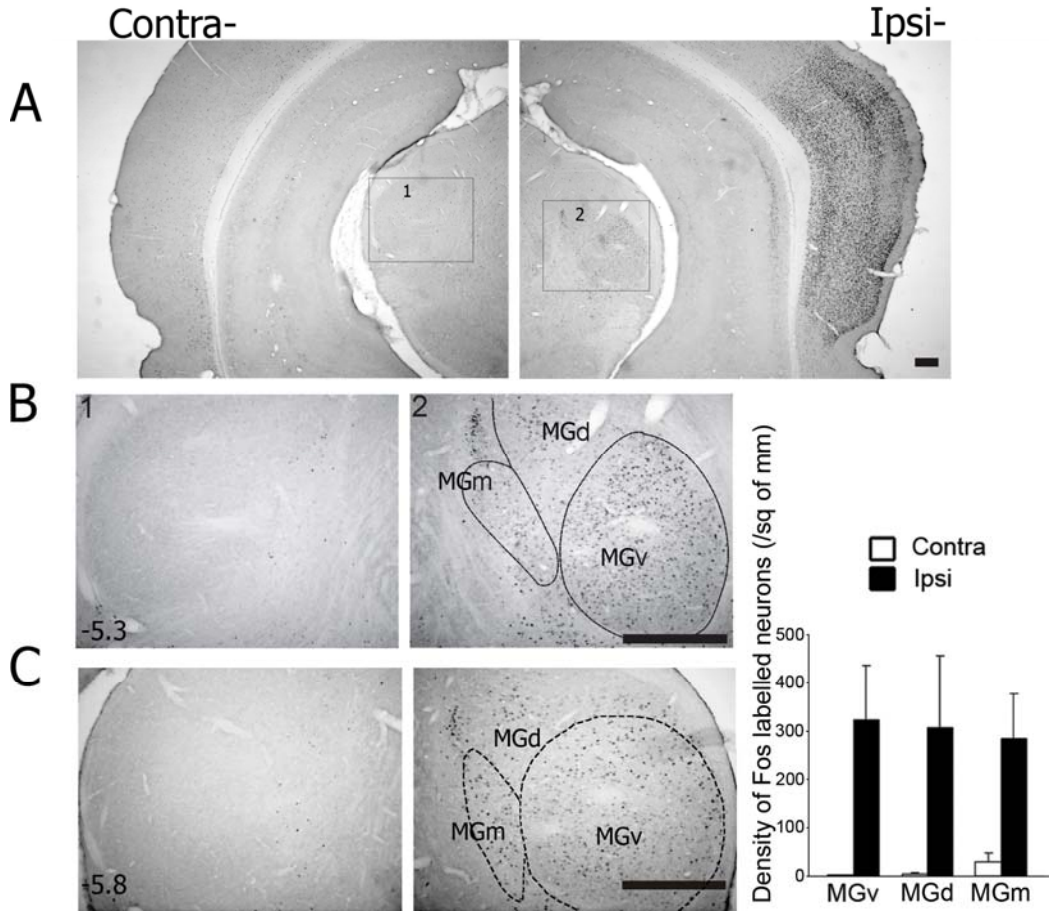

Figure 4.4 *C-fos* expressions in the bilateral AC and MGB after unilateral BIM injection in AC. (A) Photomicrographs of the bilateral AC and MGB at low-power magnification. (B)-(C) Two different caudorostral levels at high-power magnification. Regions in (A) marked with 1 and 2 were depicted in (B). Histogram shows the densities of Fos-positive neurons in the different MGB divisions. Significant differences ($P<0.01$, paired t-test) were found in different MGB divisions between bilateral sides. Scale bars: 400μm.

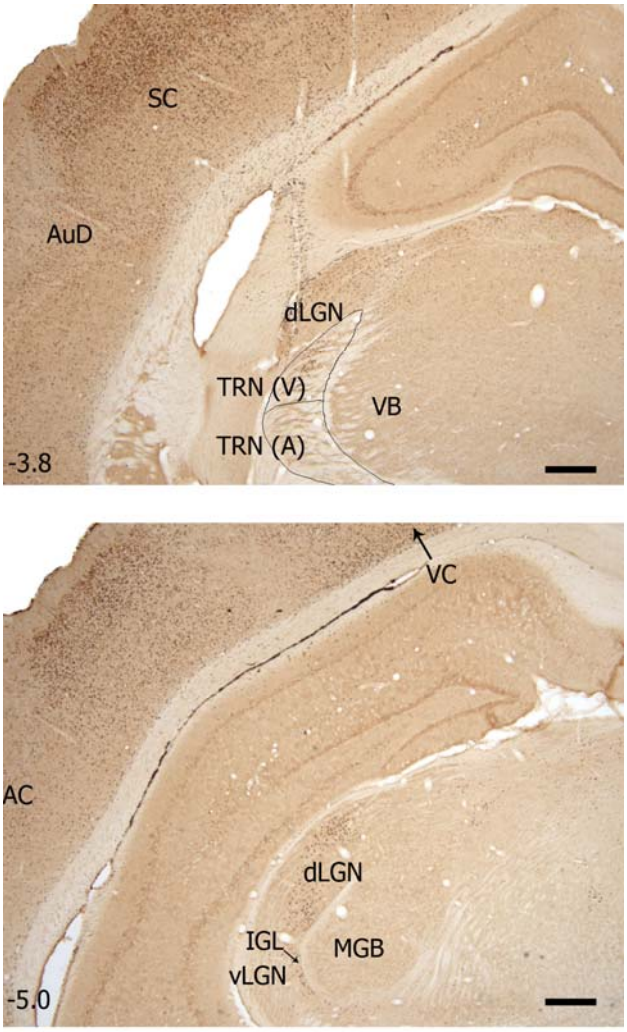

Figure 4.5 *C-fos* expressions in the dLGN and TRN(V) in two coronal sections at different caudorostral levels after a small volume (0.1 µl) of BIM injection in the primary VC (the exact stereotaxic coordinates of the injection site were 6.3 mm caudal to the bregma and 3.2 mm lateral to midline). SC: somatosensory cortex, VB: ventrobasal nucleus, LGN: lateral geniculate nucleus, vLGN: ventral division of LGN, dLGN: dorsal division of LGN, AuD: secondary auditory cortex, TRN: thalamic reticular nucleus, TRN(A): auditory TRN, TRN(V): visual TRN, IGL: intergeniculate leaf, VC: visual cortex. The conventions apply to the following figures. Scale bars: 400µm.

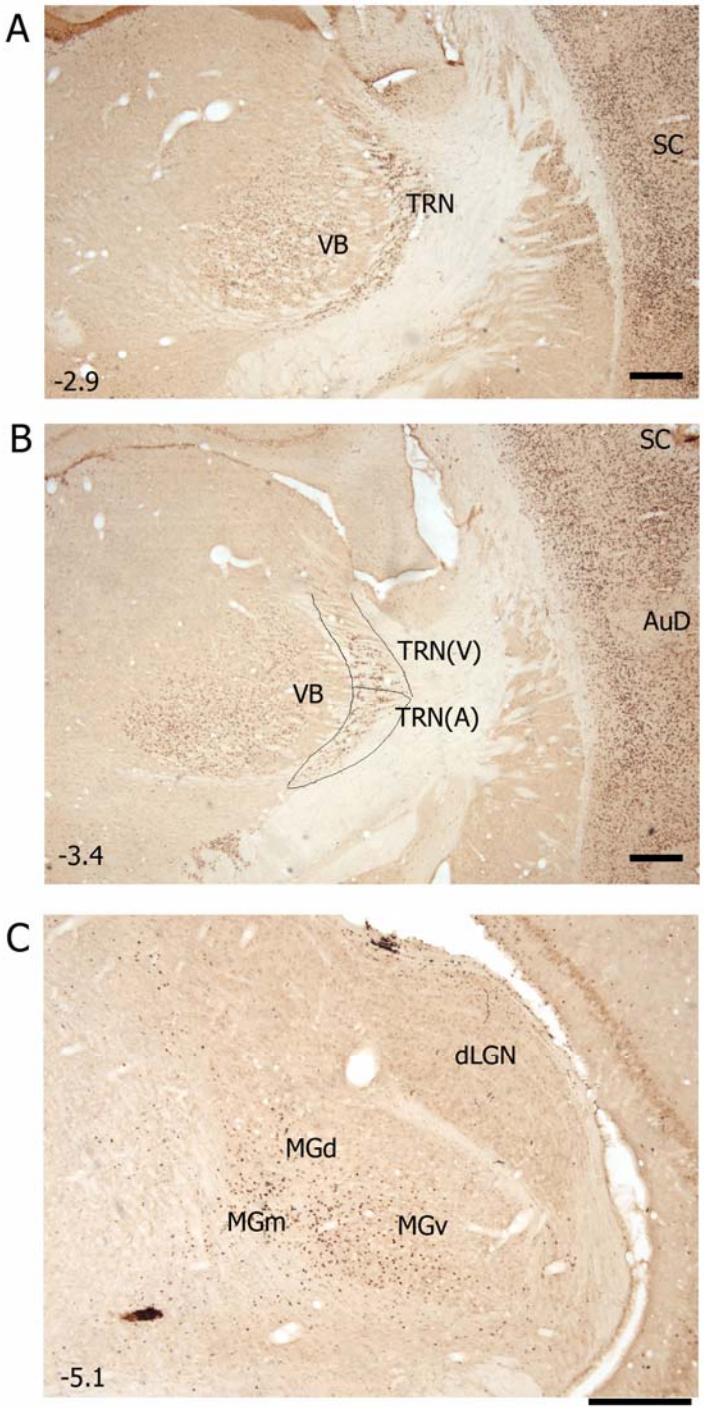

Figure 4.6 *C-fos* expressions in the VB, MGB and TRN in three coronal sections at different caudorostral levels after a large volume (0.3 µl) of BIM injected in the SC (the exact stereotaxic coordinates of the injection site were 2.5 mm caudal to the bregma and 5.2 mm lateral to midline) . Scale bars: 400µm.

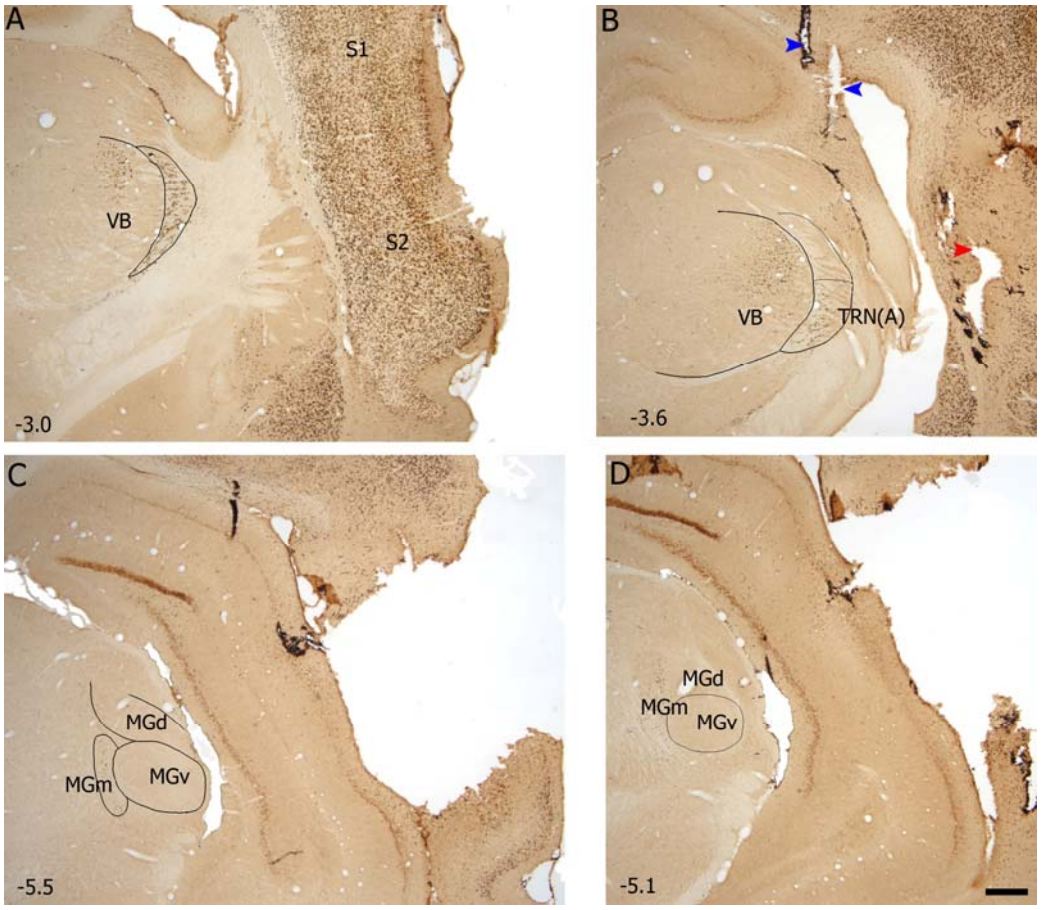

Figure 4.7 *C-fos* expressions in the VB, MGB and TRN in four coronal sections at different caudorostral levels. The AC was extensively ablated (B-D) before a large volume (0.4µl) of BIM injected in the SC (the exact stereotaxic coordinates of the injection site were 2.5 mm caudal to the bregma and 5.2 mm lateral to midline). Scale bars: 400µm.

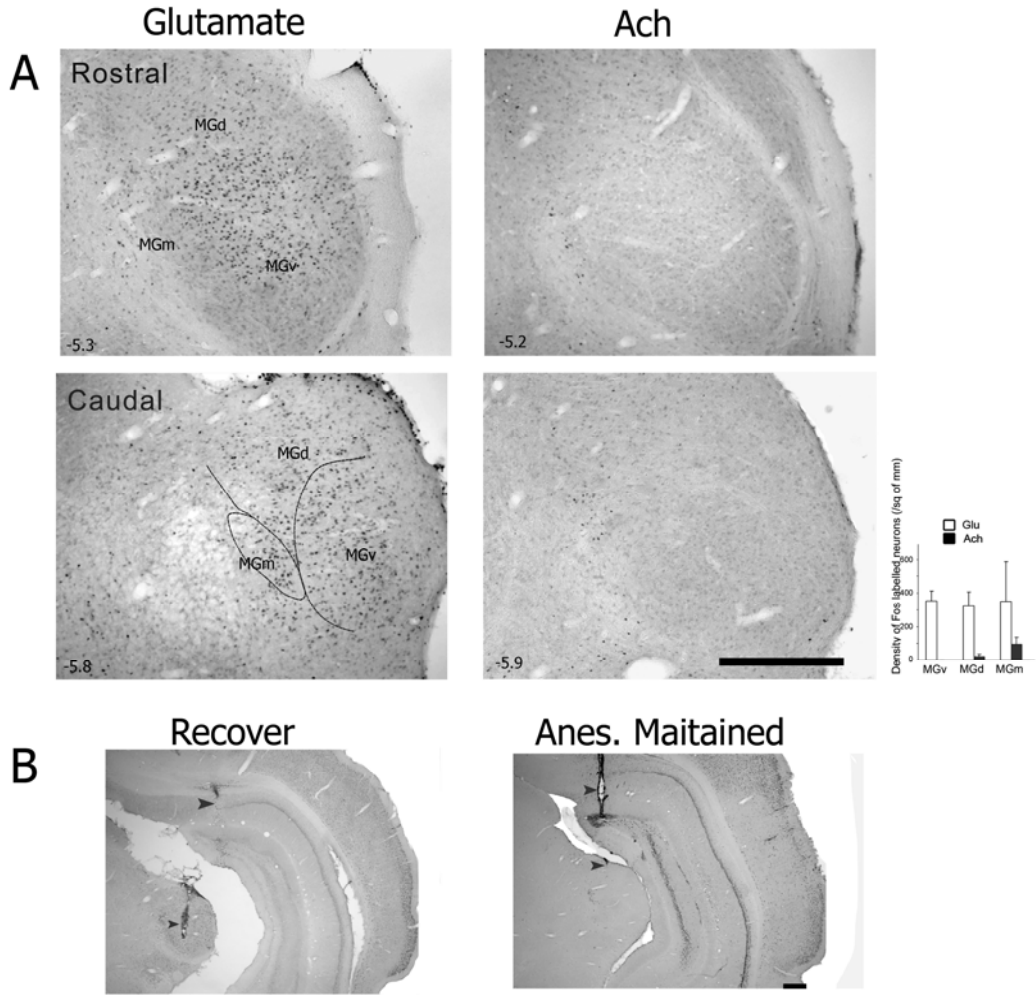

Figure 4.8 *C-fos* expressions in the MGB after injection of glutamate or acetylcholine in the MGB. (A) *C-fos* expressions in two coronal sections at different caudorostral levels after injection of glutamate (left) or acetylcholine (right) in the MGB. Histogram shows the densities of Fos-positive neurons in the different MGB divisions. Significant differences ($P<0.01$, paired t-test) were found in different MGB divisions between the two groups. (B) *C-fos* expressions in the MGB after injection of glutamate in the MGB. Left: No further anesthetic was administered after glutamate injection procedure. Right: Anesthesia level was maintained as normally during their survival period. Scale bars: 400μm.

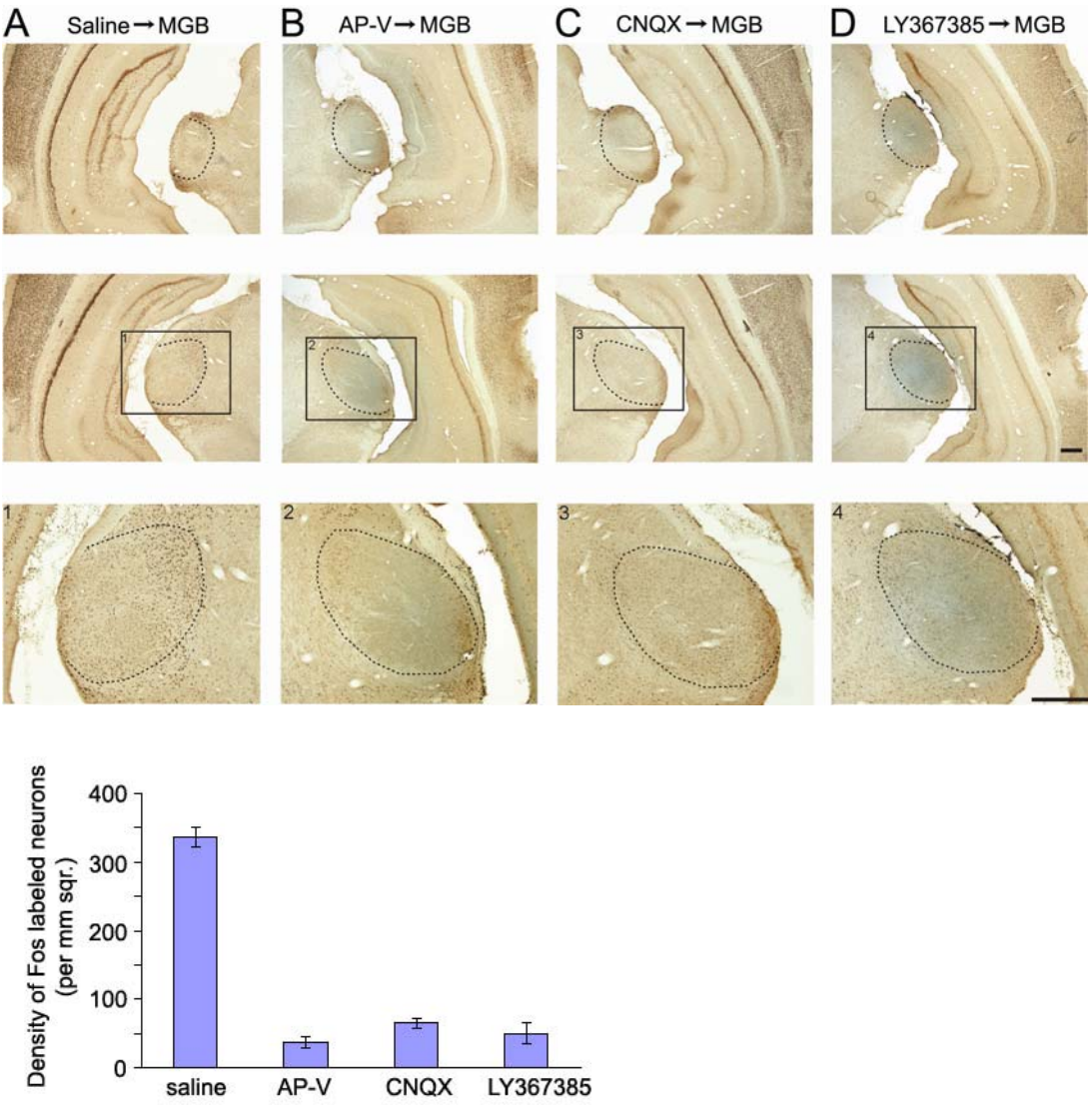

Figure 4.9 Suppression of *c-fos* expressions in the MGB by glutamate receptor antagonists. The MGB was injected with saline (A) or with antagonists of NMDA receptor, AP-V (B), antagonist of AMPA receptor, CNQX (C), and antagonist of metabotropic glutamate receptor, LY367385 (D) before and after BIM injection in AC. The upper two rows show two coronal sections at different rostrocaudal levels. Regions marked with 1, 2, 3, and 4, in the middle row are shown in the lower row with a higher magnification. The boundary of MGB is indicated with dotted lines. Scale bars: 400 µm. Histogram in the bottom panel shows the densities of Fos-positive neurons in MGv under these different conditions. Significant differences ($P<0.01$, one-way ANOVA followed by post hoc Tukey) were found between the saline control group and the antagonist applied groups.

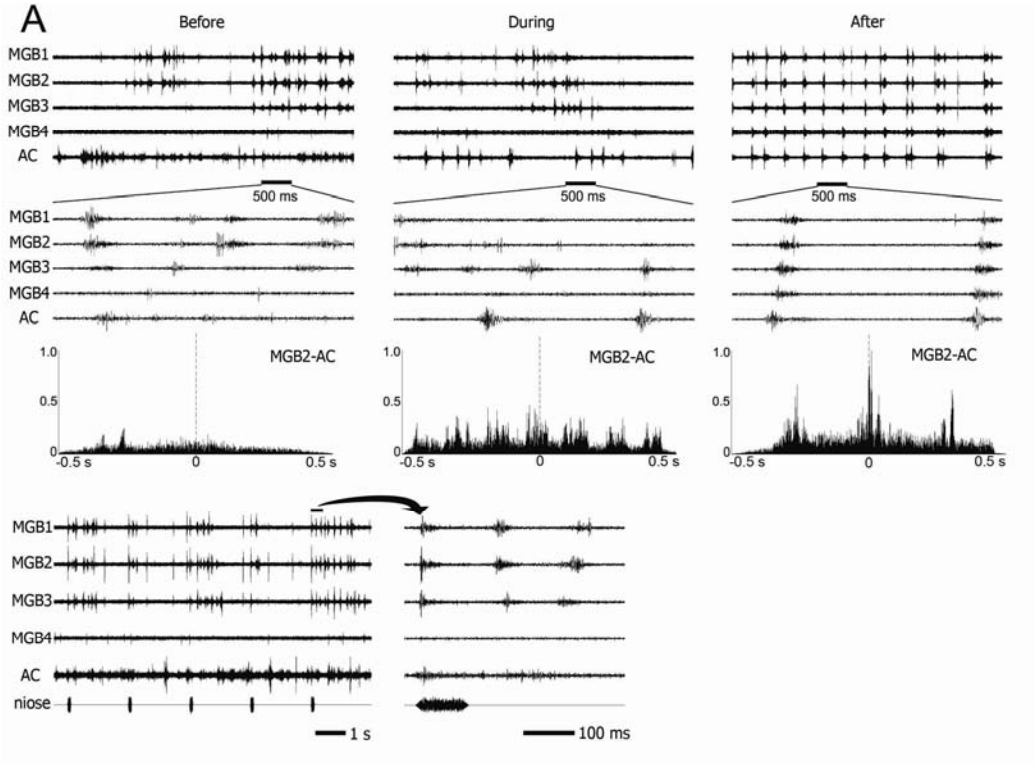

Figure 4.10 Multi-channel recordings of neuronal activities in the MGB and AC. (A) Recordings before, during, and after BIM injection in the AC. MGB1-4: 5.9, 5.4, 5.0, 4.5 mm caudal to bregma, 4500μm in depth. AC: 0.8 mm in depth, upper row showing the neuronal activities in a long time scale; middle row showing those in short time scale. The lower row showing the cross-correlograms between the recordings of MGB2 and the AC. Cross-correlogram was computed from 5 consecutive epochs with a time window of 500 ms. The center vertical dashed representing zero phase lag. (B) Neuronal responses to repeated noise-burst stimuli in the same recording sites as in (A). Recordings were carried out before the BIM injection to confirm MGB and AC. The marked episode in the left panel is expanded in the right panel.

The conventions apply to the following figures.
The recording sites are denoted on the left of each trace.
EEG recorded from the pericruciate area unless otherwise noted.
EEG(A), EEG(V): EEG recorded from the AC, VC.
Th: thalamic sites, but neither MGB nor VB, or can not confirmed.
AC(1,2…), MGB(1, 2…),VB (1,2…), etc: signals (local field potential or neuronal discharge) from extracellular recording electrode in the AC, MGB, VB, etc.

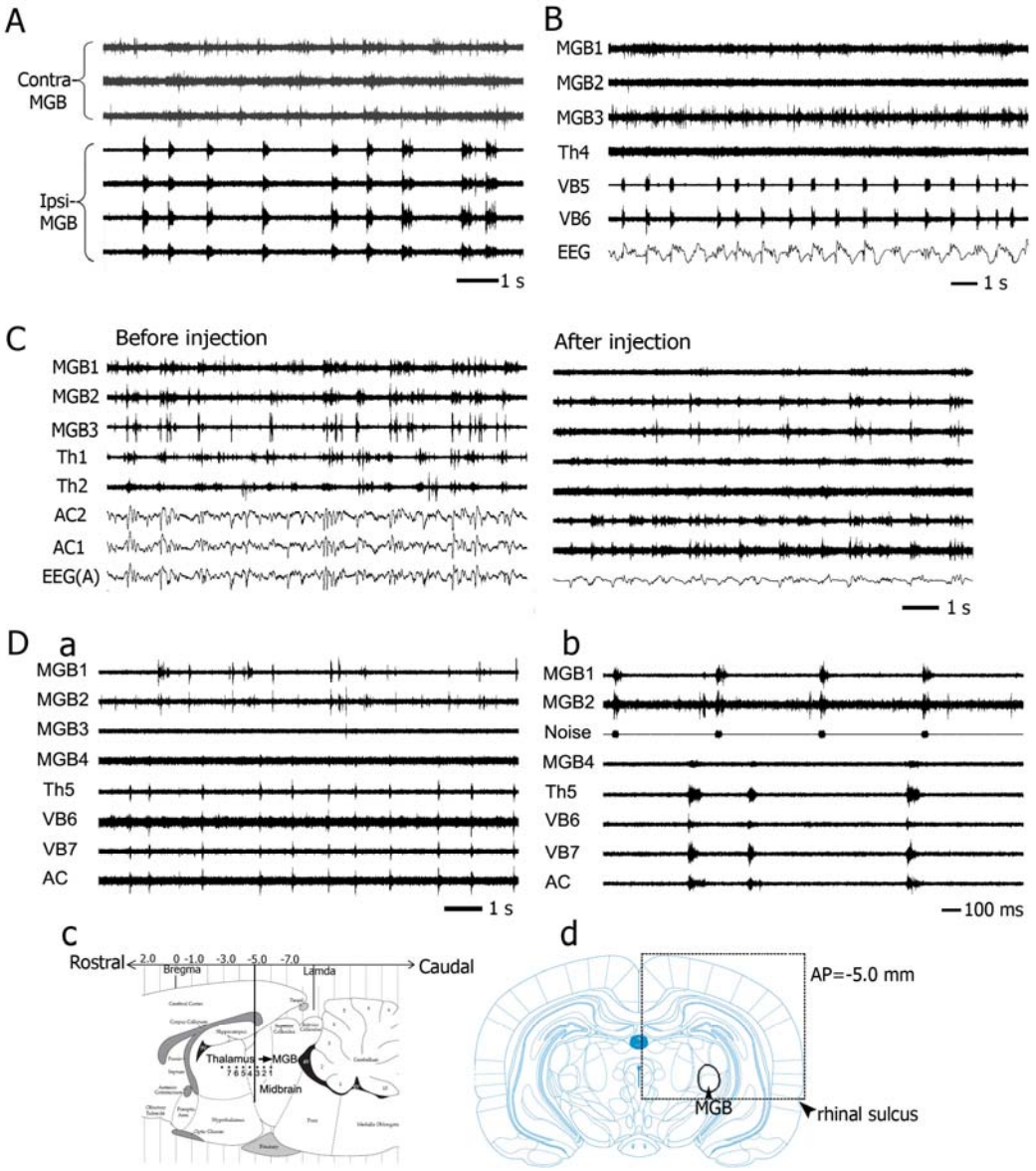

Figure 4.11 Multi-channel recordings of neuronal activities in the thalamus and cortex under four different conditions. (A) Recordings from the bilateral MGB after unilateral BIM injection in the AC. Upper three traces from the contralateral side of the injection site and lower four from the ipsilateral side. (B) The AC was extensively ablated before BIM injection in SC. (C) Recordings before and after BIM injection in the frontal cortex. (D) A deep coronal section performed to separate the caudal MGB from the TRN and AC before the BIM injection in the AC. (a) Spontaneous activity after section. (b) Acoustic response after section. (c) The locations of the recording thalamic sites are indicated with dots marked with 1-7. Section was made between electrode 3 and 4, at 5.0 mm caudal to bregma. (d) The rectangle denotes the range of section from the brain surface deep into the level of rhinal sulcus.

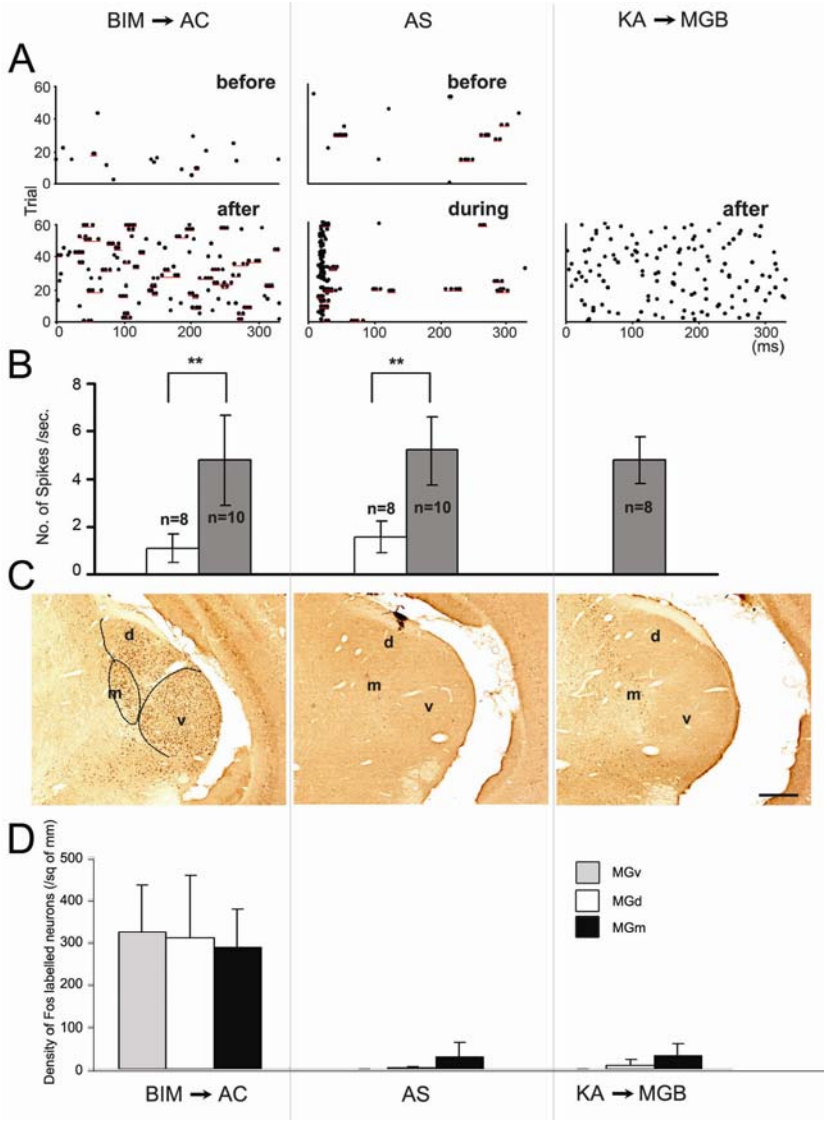

Figure 4.12 Neuronal activities and *c-fos* expressions in the MGB under three different conditions. (A) Raster displaying show spontaneous firing before and after the BIM injection in the AC (BIM→AC, left panel), spontaneous firing and neuronal response to acoustic stimulus (AS, middle panel), and the spontaneous firing after KA injection into the MGB (KA→MGB, right panel). Raster displays show spontaneous activities or auditory responses of neurons for 20 s (60 trails of 333 ms). (B) Bar chart showing the mean firing rate in different conditions as shown in (A). Comparisons between the mean firing rates before and after BIM→AC, and the mean firing rates before and during AS, were significantly different (**P <0.01, t-test). Comparison between the mean firing rates before BIM→AC and before AS, and comparisons among the means of firing rates after BIM→AC, during AS, and after KA→MGB, were not significant (ANOVA, P> 0.05). n indicating the number of isolated single cells (C) Photomicrographs showing *c-fos* expression under the three conditions. (D) Histogram showing the densities of Fos-positive neurons in the different divisions of MGB after BIM→AC, after AS, and after KA→MGB. Significant differences (P<0.01) were found among them. Scale bar: 400 µm.

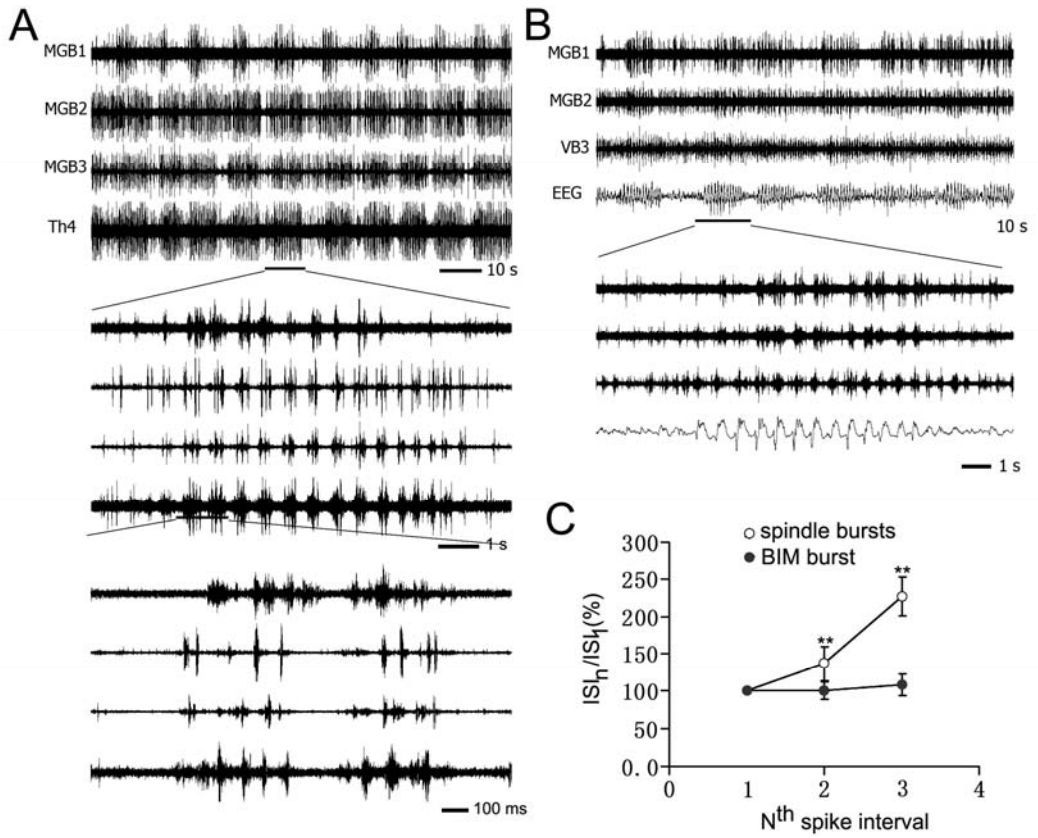

Figure 4.13 Spontaneous spindle activities grouped within slow oscillations (~1 Hz) in animals anesthetized with ketamine/xylazine. (A) Synchronized spindle oscillations in the thalamus. (B) Synchronized spindle oscillations in the cerebral cortex and thalamus. The firing rate was as high as that of BIM-induced oscillations, or even higher, however, no Fos protein was detected in these animals. (C) Plots of inter-spike interval (ISI) showing the difference between the spindle bursts and the BIM-induced burst. The intervals are normalized by taking the 1st ISI as 100%.

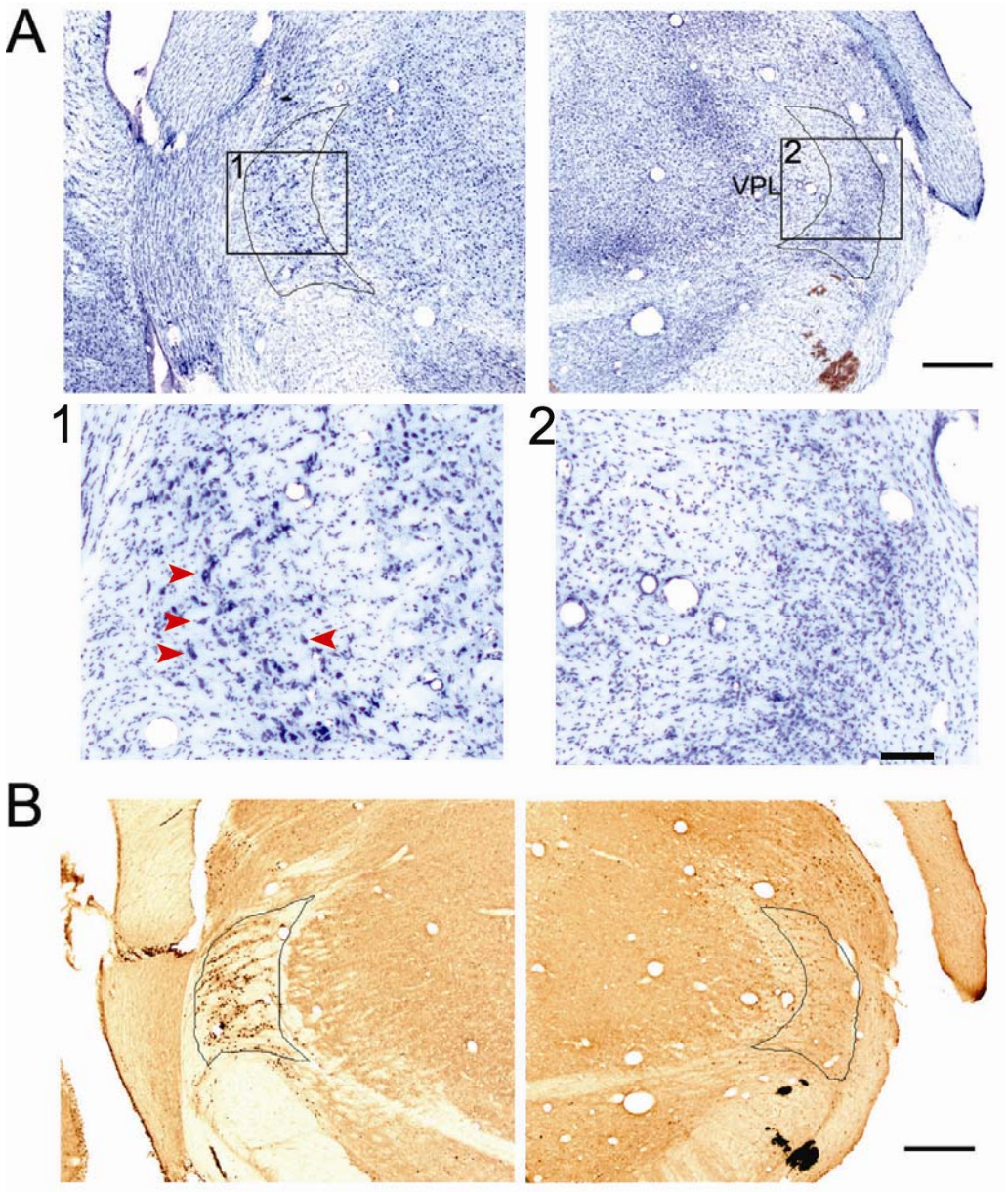

Figure 4.14 Selective lesion of TRN neurons with kainic acid injection 2 days before the cortical BIM injection. (A) Photomicrographs of Nissl-stained coronal sections of the TRN from the control side (left) and kainic acid-lesioned side (right) of the same animal. Note nearly total neuronal loss on the lesioned side (right). In contrast, Nissl bodies in the control side were well-defined (left), indicated by arrow head. (B) *C-fos* expressions in the TRN from the same animal as (A). No Fos detected on the lesioned side. Scale bar: 400 µm.

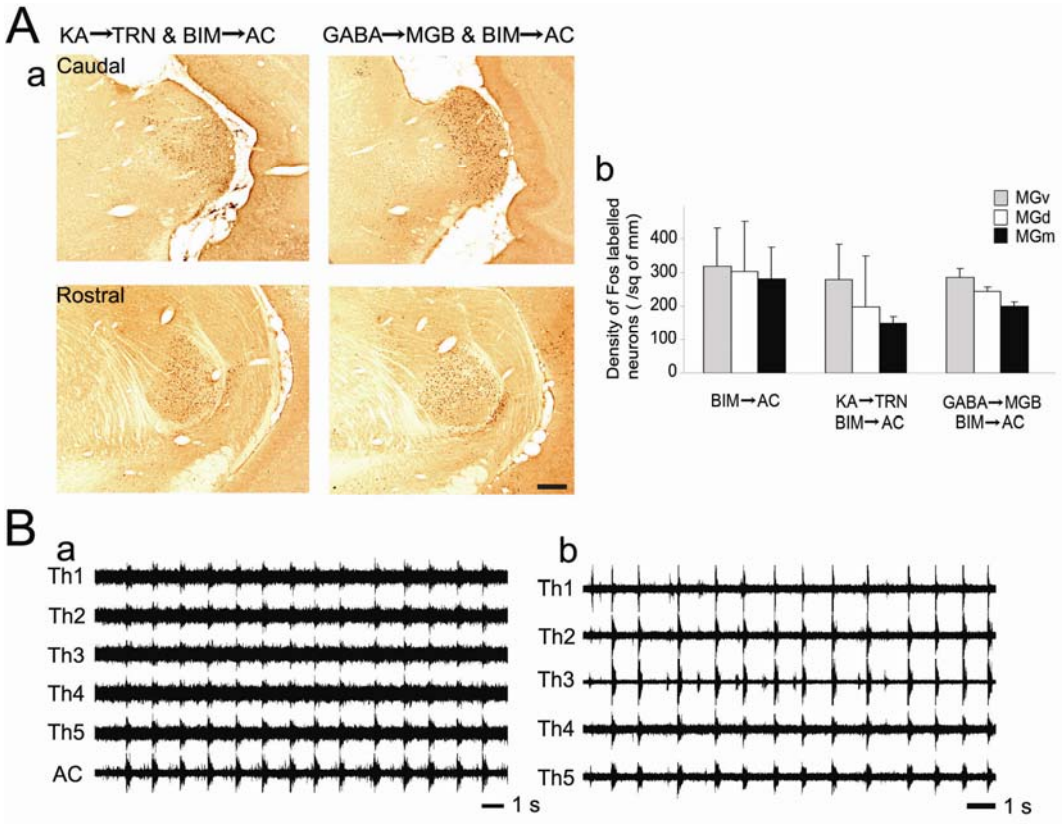

Figure 4.15 *C-fos* expressions and spontaneous neuronal activities after BIM injection in the AC of the TRN-lesioned animals. (Aa) Photomicrographs show *c-fos* expressions in different coronal levels of the MGB after BIM injection in the AC of the TRN-lesioned animal (left), and after GABA injection in the MGB followed by BIM injection in the AC (right). Scale bar: 400 µm. (Ab) Histogram showing densities of Fos-positive neurons in different divisions of MGB after BIM → AC, TRN lesion group, and GABA→MGB group. No significant differences (P> 0.05) in the MGv and MGd were found among them. (B) Spontaneous oscillations in the thalamus and AC after BIM injection in the AC of the TRN-lesioned animals (a and b).

Chapter 5

Corticothalamic and Intrathalamic Distributions of Slow Oscillations (<15 Hz) *in vivo*

5.1 Introduction

Oscillatory active ities in neural networks, especially in the corticothalamic network, have been intensively studied over the past years. Neuronal oscillations have been suggested as the basis of many different behavioral patterns, as well as the perception and attention mechanisms. While some cellular mechanisms underlying these neuronal oscillations have already been reported (von Krosigk et al., 1993; Bal et al., 1995a, 1995b), the distribution, coherence and recurrence of oscillations are far more complicated and elusive than we had thought. Nevertheless, neural maps of slow oscillations may provide a functionally useful probe in studying the highly integrative brain functions. The propagation of correlated activities or oscillations along neural pathways has also been implicated in synaptic development (Meister et al., 1991), synaptic consolidation (Steriade and Timofeev, 2003) and spike-timing-dependent synaptic plasticity (Abbott and Nelson, 2000).

Previous studies regarding the propagation of neuronal oscillations showed a

great discrepancy. Some reported a high degree of spatiotemporal variability from one spindle sequence to the next, while others demonstrated that spindle sequences occurred nearly simultaneously even in distant cortical fields. In lateral geniculate-perigeniculate slice of ferrets, clear-cut propagation of spindle sequences was observed (Kim et al., 1995). In *in vivo* preparations of both animals (anesthetized or conscious) and humans, however, Contreras and colleagues (1997) revealed a simultaneity of spontaneous spindle sequences in the intact brain, but could not find propagations of spontaneous spindle. In addition, the spontaneous spindle oscillations throughout the thalamus were less organized in decorticated animals (Contreras et al., 1996, 1997). These results lead to a conclusion that the strong corticothalamic projections played a great role in the synchronization of the spindles. Another study in humans using high-density EEG recordings, demonstrated each cycle of the slow oscillations was a traveling wave during natural NREM sleep. Each cycle was characterized with a definite originate and a continuous pathway of propagation over the scalp, which probably varied from one cycle to the next. Waves originated more frequently in prefrontal-orbitofrontal regions and traveled in an anterioposterior direction (Massimini et al., 2004).

In the present study, we investigated the propagations of spontaneous slow rhythms *in vivo* in the corticothalamic network within a given modality (e.g. auditory) and across different modalities. To compare the spatiotemporal dynamics of the slow oscillations, sleep- or anesthesia-related slow rhythms

(<15Hz, mainly spindle oscillations) and the bicuculline-induced slow oscillations were considered in the present study. Both rats and guinea pigs were studied in the present investigation to determine whether the pattern of slow oscillation propagation was comparable across species. We found that in different preparations studied slow oscillations typically propagated along the rostrocaudal direction in the thalamus within given modalities or across modalities. Such spatiotemporal patterns of the slow oscillations were highly reproducible across subjects of different species. The present results would propose that common principles probably governed the spatiotemporal patterns of different oscillation types, thus providing the framework for functional studies on the efficacy of connectivity in the corticothalamic network.

5.2 Materials and methods

Please refer to Chapter 3 for details about the animal preparation, application of drugs, multi-channel extracellular recording and histological procedures. Both SD rats and guinea pigs were used in this experiment. And the penetrations and cell parcellations in guinea pigs were performed according to atlas of (Rapisarda and Bacchelli, 1977) and previous accumulations of our laboratory (He et al., 2002; Xiong et al., 2004; Yu et al., 2004b, 2004a; Zhang et al., 2007).

For electrophysiological recordings, local field potential (LFP) was also obtained at the extracellular recording electrodes with a bandpass of 0.1-40 Hz. Additionally, recordings of local EEG were also performed at the surface or depth of motor, somatosensory, visual, and/or auditory cortices with monopolar low-impedance electrodes.

5.3 Results

5.3.1 Propagation of BIM-induced oscillations in the corticothalamic network

Extracellular multiunit recordings revealed that the BIM-induced oscillations (0.3-3 Hz) propagated within the corticothalamic network (Figure 5.1). After BIM injection in the primary AC, the corticothalamic synchronization in the thalamus was first observed in the MGB sites, where neurons probably were tonotopically matched with the cortical injection site (not confirmed). Sequentially, the synchronized oscillations traveled bidirectionally along the caudorostral axis. A full corticothalamic synchrony developed 6.8 ± 3.9 min (n=13 subjects) after cortical BIM injection. Although a certain degree (about 15-25%) of irregular epochs (see epoch 1, Figure 5.1) were observed amongst the synchronized oscillations, examination of tens of consecutive epochs revealed a preferential propagation direction from the rostral to the caudal in the thalamus. The burst discharges in the AC preceded the oscillations of all the thalamus sites, irrespective of their different modality attributions, e.g. MGB (for the auditory) and VB (for the somatosensory) in Figure5.1.

Furthermore, when we looked into the details of the irregular epochs (epoch 1), purely-thalamic short burst jitters were always found in MGB sites, but never in the ventrobasal nucleus (VB) site in this case. Accordingly, the time order between AC and VB maintained constant even in the irregular epochs. It is

reasonable to postulate that the short thalamic jitters were the reason behind the abnormal distributions of oscillation in the MGB. Another noteworthy observation was that jitters only disrupted the preferential propagation direction when they occurred shortly before next BIM-induced oscillation. If they occurred long before (epoch 3) or after the BIM-induced oscillations (epoch 2), the preferred propagation would still continue.

5.3.2 Propagation of slow oscillations (<15 Hz) in the corticothalamic network

To investigate whether the slow oscillation (<15 Hz) also traveled in a preferential direction in anesthetized animals without BIM injection, similar experiments were conducted in rats or guinea pigs anesthetized with pentobarbital or ketamine/xylazine. Barbiturate anesthesia produced spindle oscillations (7-15 Hz) with a waxing and waning pattern, recurring once every 3-10 s (see for example Figure 5.4 and 5.5A). Ketamine/xylazine, however, produced a coalescence of slow oscillations (~1 Hz) with spindle rhythms, which was more likely prevalent in deep sleep (Figure 5.5B).

5.3.2.1 Spindle oscillations propagate in the same preferential direction as BIM-induced oscillations in the AC and MGB

Similar to the BIM-induced oscillations, the spindle oscillations were also found to propagate caudally along the rostrocaudal axis (Figure 5.2).

Representative data illustrating the propagation of 8 consecutive spindle waves obtained from a pentobarbital-anesthetized guinea pig were shown in Figure 5.2. Spontaneous spindle oscillations regularly recurred approximately once every 3-5 s in both MGB and AC. Recordings from four AC sites (with an inter-electrode distance of 0.5mm) revealed a high degree of spindle synchrony, with nearly equal inter-burst intervals at different sites. The positive deflection in the local field potential (LFP) at AC4 corresponded to burst discharges at AC1, AC2 and AC3, which was more obvious in the late stage of a spindle sequence (low panel). In the thalamus, however, a spatiotemporal distribution pattern was observed in three MGB sites with an inter-electrode distance of 0.5 mm. Spindle oscillations were propagating from rostral to caudal in about 70% of the total epochs, which is a much higher rate than would be predicted by chance. Furthermore, the activities of AC sites were found to precede the oscillations of MGB neurons. The results were confirmed in other experiments.

In Figure 5.3, two TRN, four MGB and four AC sites were simultaneously monitored. Spindle oscillations were found propagating from rostral to caudal in the MGB (the third epoch marked as 1 in Figure 5.3A and expanded in Figure 5.3B). The AC showed a nearly simultaneity of spindle rhythms (neuronal firings in AC1; and LFPs in AC2, AC3 and AC4). Neuronal spindle discharges of two TRN sites (top two traces) were also found grouped within slow waves. However, no synchrony between the TRN and AC-MGB was envisioned, which may be due to their different modality attributions. While acoustic responses

were observed in AC and MGB recording sites, no response was found in TRN sites. However, the cross-modality interactions were observed in these two TRN sites, where the TRN neurons responded to the electrical stimulation of the AC (Figure 5.3D, stimulus indicated by the up arrow). The present results indicated that the distribution of slow oscillations, to some extent, was modality-specific, i.e. spindle oscillations in different modality nuclei could occur independently or in a semi-independent manner, to a certain extent.

5.3.2.2 The distribution of spindle oscillations, to a certain extent, is modality-dependent

Experiments were further conducted to further confirm the spatial restriction or modality specificity of spindle distribution. Figure 5.4 illustrated spontaneous recurrence of spindle oscillations in the somatosensory and auditory systems. A well-defined synchronization was observed respectively, between the AC and MGB, as well as between the somatosensory cortex (SC) and somatosensory thalamus, namely ventrobasal nucleus (VB). However, the inter-spindle frequencies for the auditory system and somatosensory system were different (~0.1 Hz for auditory system *vs.* ~0.16 Hz for somatosensory system). This implies that spindle rhythms recurred independently in the auditory and somatosensory systems. Such a difference could not be attributed to the occurrence of local components (see Figure 5.5, LSC, indicated by rectangle) or

the loss of some epochs resulting from the discrepancy of refractory periods in individual neurons.

In contrast, this modality-specific asynchrony was seldom observed among the TRN sites of different modalities, indicating strong intranuclear connections within the TRN. TRN has been proposed as a bridge linking the specific and non-specific pathways, leading to a large-scale coordination of neuronal processes (Llinás and Pare, 1997) by virtue of intranuclear connections through dendrodendritic GABAergic synapses (Steriade et al., 1985; Fuentealba et al., 2004) and electrical coupling (Landisman et al., 2002; Fuentealba et al., 2005).

It should be mentioned that in some cases, synchrony was observed in widespread thalamic and cortical territories, as two examples shown in Figure 5.5. In Figure 5.5A, EEG signals simultaneously recorded from different cortical regions on the bilateral hemispheres, showed a highly coherence among all recording sites by the virtue of intracortical, cortico-thalamo-cortical and callosal connections, Occasionally, a more local spindle sequence could be discerned, as an example shown in the somatosensory cortex of the left hemisphere (Figure 5.5A, LSC, indicated by rectangle). In Figure 5.5B, spontaneous neuronal discharges were recorded from three cortical sites (two VC and one SC), while EEG were recorded from the pericruciate area of the ipsilateral hemisphere. Clearly, signals from all channels exhibited highly coherence despite the long physical distance between the recording sites.

The next question to be addressed is whether the preferential direction of the spindle propagation is common in other modalities or even across modalities when the whole forebrain operates as an entity.

5.3.2.3 Spindle oscillations propagate from rostral to caudal across thalamic nuclei of different modalities

Data were obtained from simultaneous recordings in the TRN, the dorsal thalamus and cortical region of different modalities.

In Figure 5.6, extracellular signals from five TRN sites were recorded. Electrodes TRN5 to TRN1 were arranged in a rostrocaudal fashion with an inter-electrode distance of 200 μm. Only two sites (TRN2 and TRN3) responded to acoustic stimuli. Although signals recorded from TRN 4 and TRN5 were weak, a rostrocaudal propagation of spindles could still be observed across the five TRN sites. The propagation continued into MGB sites, which were situated caudally to the TRN. Consequently, the spindle oscillations propagated caudally across the TRN sectors of different modalities and the MGB in the thalamus.

In another example shown in Figure 5.7, the spindle oscillation sequentially traveled in a rostral to caudal fashion across two TRN sites, both of which showed no acoustic response, and two MGB sites, irrespective of the modalities they represented (two epochs depicted in B and C). In this case, both the local field potentials (LEP: recorded from TRN3 and MGB2 sites) and EEG signals (two from AC; two from motor cortex, MC) faithfully reflected cellular events

of local neuronal populations (Figure 5.7D). The positive deflections of the MGB2 corresponded to the burst discharges of the same electrode. It seemed like that the large-scaled LFP signals were as useful as the fine neuronal firing signals in the study of propagations of the oscillations. Technically, the former is much easier to be obtained than the latter.

Unfortunately, that the LFPs in the thalamus faithfully reflected cellular events of local neuronal populations was not commonly encounted in our recordings.

5.3.3 LFPs in the thalamus show a relatively low fidelity to the cellular events of local neuronal populations

In most of our recordings, both EEG and the LFPs in cerebral cortex were found to faithfully reflect the cellular events of local neuronal populations (two examples were shown in Figure 5.8, also see Figure 5.9). This became particularly obvious when neuronal discharges developed into burst firing. In Figure 5.8A and B, the cortical LFPs and the multiunit discharges were recorded from the same electrode, showing that the negative deflections in LFPs corresponded to burst discharges.

However, the thalamic LFP showed a relatively low fidelity to the local cellular events of neuronal populations. A representative case was illustrated in Figure 5.9 which showed the relationships between LFP and neuronal discharges of the cerebral cortex and thalamus. The AC continuously showed a stereotyped delta rhythm (AC1-4, ~4 Hz) interpolated with short spindles (AC2), while the

thalamus exhibited spindle oscillations (MGB1, Th2-6, 6-7 Hz). The LFPs at AC2 were coherent with the neuronal discharges at an adjacent electrode AC1 with the negative deflection corresponding to the burst firings, especially when all of the three AC sites came into synchrony (epoch 2). The waves of LFPs at both MGB1 and Th3, however, shared great similarity with that of the cortical LFP (AC2), though some small deflections could be discerned to superimpose on the cortically-derived big waves when the spindle oscillation occurred in local thalamic sites (epoch 1 and 2). The association between the positive/negative deflections and the neuronal spindle bursts in the thalamus were too weak to be identified, even when they were recorded from the same electrode (Th3, epoch 1 and 2).

A possible factor, which might also contribute to the difference between local cellular discharges and LFPs, is volume conduction (Massimini et al., 2004; Kawakubo et al., 2007). Hence, the different thalamic nuclei could operate as an entity, and therefore have the same LFPs. This factor is also tenable in the cerebral cortex, however, there is no such a powerful input to the cortex just like the corticothalamic volley to the thalamus.

In the light of these results, we propose that due to the high impact of the corticothalamic projections on the thalamus, the thalamic LFPs could not always faithfully reflect cellular events of local neuronal populations. Although highly speculative, such a notion was reasonable, since the principle underlying the LFP is the postsynaptic potentials. Therefore, the great simultaneity of thalamic

LFPs at different sites probably did not represent the highly coherence of the thalamic neuronal activity, but indicated a strong external impact on them.

5.4 Discussions

By using multi-channel extracellular recordings in large thalamic and cortical territories of *in vivo* preparations, we have reported five major findings. (1) Both bicuculline-induced slow oscillations and sleep- or anesthesia-related slow oscillations (<15 Hz) propagated in the same preferential direction from rostral to caudal in the thalamus within a given modality and across modalities (Figure 5.1-5.3, 5.6, 5.7, 5.9). (2) When synchronized, the activity in cerebral cortex precedes that of the thalamic sites, at least within the same modality (Figure 5.1-5.4, 5.6-5.8). The results would propose that common principles probably governed the spatiotemporal patterns of different oscillation types. (3) The slow oscillations could be of global distributions, showing nearly-simultaneous EEG or burst discharges in the bilateral hemispheres (Figure 5.5), or more local events of modality-dependence (Figure 5.4), recurring independently in different modality systems. (4) However, this modality-specific asynchrony was seldom observed among the TRN sites of different modalities. (5) LFPs in the thalamus showed a relatively low fidelity to the cellular events of local neuronal populations (Figure 5.9), due to the high impact of the corticothalamic volleys on the thalamus.

5.4.1 Propagations of slow oscillations in the corticothalamic network

Our present results of rostrocaudal propagation of thalamic slow oscillations that were preceded by those of the cortex agreed with a prediction of the wave generation model put forth by Andersen and Andersson (Andersen and Andersson, 1968) that the successive recruitment of neighboring neurons into the spindle wave should appear as propagation wave through the neural network. The waxing pattern of spindle waves was proposed to result, at least partially, from the recruitment of more and more cells into the synchronized oscillations. The propagation of spindle waves was previously reported in various thalamic nuclei of cats with both *in vivo* (Andersen et al., 1966) and *in vitro* preparations (Kim et al., 1995). Some earlier experiments in anesthetized or naturally sleeping monkeys also occasionally observed spindle waves propagate though the thalamus (Verzeano and Negishi, 1960; Verzeano et al., 1965). Our results, based on multi-site extracellular recordings, in rats and guinea pigs would support the notion that oscillations propagate in the thalamus of mammals.

Moreover, in present study, both bicuculline-induced slow oscillations and sleep- or anesthesia-related slow oscillations (including the thalamic spindles and the cortically-generated slow oscillations (~1 Hz)) propagated in the same preferential direction from rostral to caudal in the thalamus within a given modality and across different modalities. The results would propose that common principles probably governed the spatiotemporal patterns of different types of oscillation in the corticothalamic network.

5.4.2 Contribution of the corticothalamic volleys to the spindle synchronizations

Contreras and colleagues (1997) reported that spindle oscillations, triggered by low intensity electrical cortical stimulation, propagated in the anterioposterior axis of thalamus. Increasing the intensity of the stimulation, however, induced spindle wave simultaneously started in all leads. In decorticated animals, the thalamic propagations were also suggested to be possible. Obviously, by presenting this result, the authors tried to explain the near simultaneity of spindle waves as the result of strong corticothalamic inputs, and tried to find the bridge between the near simultaneity and propagation of the spindle oscillation described by others.

Indeed, investigations of patterns of spindle oscillation in the anesthetized animals demonstrated that spindles were strongly influenced by the occurrence of other spontaneous oscillations. Corticothalamic volleys are highly effective in triggering and potentiating the generation of spindles in the thalamus (Steriade et al., 1993d; Contreras and Steriade, 1995, 1996; Steriade et al., 1997; Meeren HKM et al., 2002). Cortical-generated slow oscillations play a decisive role in pacing thalamic spindles and determining their patterns (Contreras et al., 1996; Timofeev and Steriade, 1996; Destexhe et al., 1999a; Destexhe et al., 1999b).In fact, almost in all our experiments, the oscillations in cortical sites were found to precede those in thalamic sites, at least when they were within the same modality. It should be emphasized that the degree of

synchronization of the cortical-generated slow oscillations is far higher than that of spindle (Contreras and Steriade, 1997). Similar result was also illustrated in our experiments: the stronger the cortical-generated slow oscillations (~1 Hz), the smaller the time dispersion of the thalamic-generated spindles (Figure 4.13, 5.5B *vs.* other figures).

Nevertheless, time-lag between different cortical sites during slow oscillations was also unraveled. *In vivo* studies from cats showed that neighboring cortical cells discharged closely, and that oscillatory waves traveled in a posterior-to-anterior direction (Amzica and Steriade, 1995a). Propagations of slow oscillations were also observed on the human scalp (Hughes, 1995; Massimini et al., 2004). It is noteworthy that our preliminary results also showed propagation in a preferential direction occasionally appeared in cerebral cortex (Guo et al., unpublished observation, also see Figure 5.5B).

5.4.3 Contribution of the rostral TRN sector to the spindle synchronizations

Another possible mechanism that may contribute to the highly coherence of spindle oscillations, is the divergent connections between the rostral part of TRN and the dorsal thalamus (Steriade et al., 1984). In the present study, the asynchronies between both cortical and thalamic sites of different modalities were never observed in different TRN sectors of different modalities, by virtue of intranuclear connections through dendrodendritic GABAergic synapses (Steriade et al., 1985; Fuentealba et al., 2004) and electrical coupling

(Landisman et al., 2002; Fuentealba et al., 2005). In decorticated conditions, the projections from the rostral TRN sectors may account for some propagation phenomenon (Contreras et al., 1997). TRN projections to the intralaminar and midline thalamic nuclei are much more diffuse than those to specific dorsal thalamic nuclei (Kolmac and Mitrofanis, 1997). The difference between the relatively topographically organized connectivity linking TRN and thalamocortical cells and the more diffuse connectivity link TRN and intralaminar thalamic nuclei might explain the different results due to different thalamic sectors investigated. In our experiments, spindle propagations occurred in the TRN sites, especially in caudal TRN, an area known to be related to primary sensory modalities, including auditory, visual and somatosensory modalities.

In summary, the slow oscillations (<15 Hz) could be of global distributions, or more local events of modality-dependence, recurring independently in different modality systems. Both bicuculline-induced slow oscillations and sleep- or anesthesia-related slow oscillations propagated in the same preferential direction from rostral to caudal in the thalamus within a given modality and across different modalities. When synchronized, the activity in cerebral cortex preceded that of the thalamic sites, at least within the same modality. However, modality-specific asynchrony was seldom observed among the TRN sites of different modalities, indicating strong intranuclear connections within the TRN.

The results would propose that common principles probably governed the spatiotemporal patterns of different oscillation types. All in all, experimental evidence provided by the present study would further our understanding on the shaping and propagation of synchronized excitability within the corticothalamic network of specific modality and across modalities.

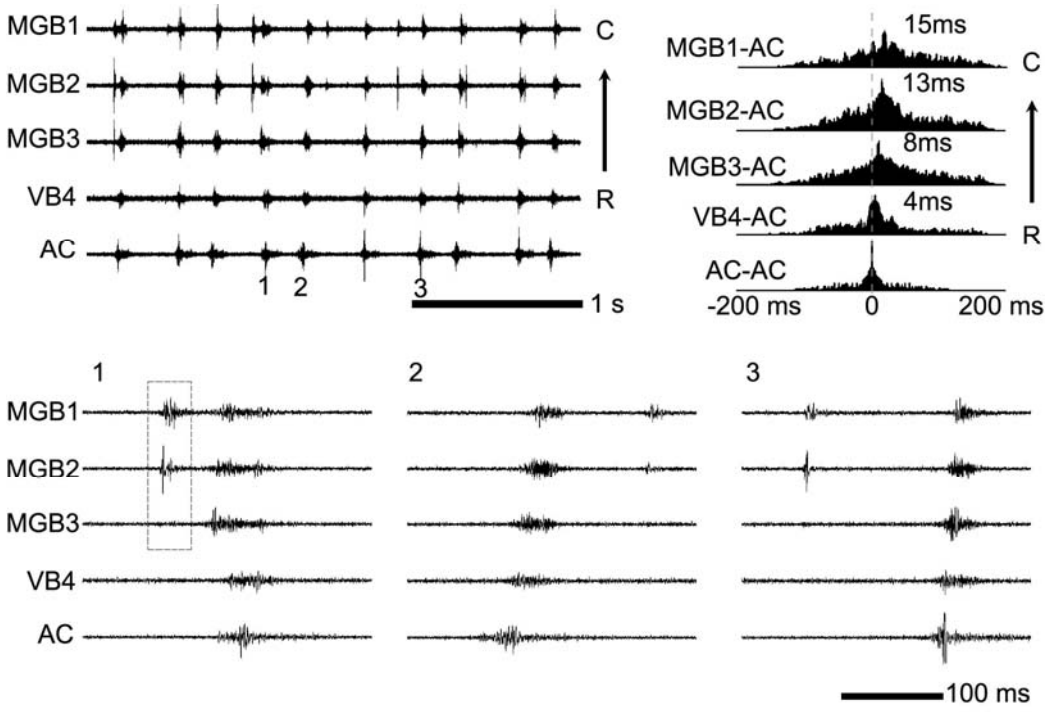

Figure 5.1 Propagation of BIM-induced slow oscillations across the AC and thalamic sites after the corticothalamic synchronization fully developed. Three epochs marked with 1, 2, 3 are expanded below. The auto-correllogram of the AC activity and the cross-correlograms between the recordings of each thalamic (MGB1-3, VB4) site and the AC site are shown in the upper right panel. Correlogram was computed with a time window of 200 ms. The center vertical dashed line represents the zero time lag, the time above each correlogram denotes the time lag, computed from 3 consecutive epochs. R→C denotes the arrangement of the thalamic electrodes with an inter-electrode distance of 0.5 mm (R: rostral, C: caudal). These conventions apply to the subsequent figures, unless otherwise stated. Note that the activities of AC preceded those of all the thalamic sites. The dashed rectangle denotes the purely thalamic components, as these short jitters occurred before the bursts of the AC, indicating their independence of activities of the AC. Data obtained from SD rat.

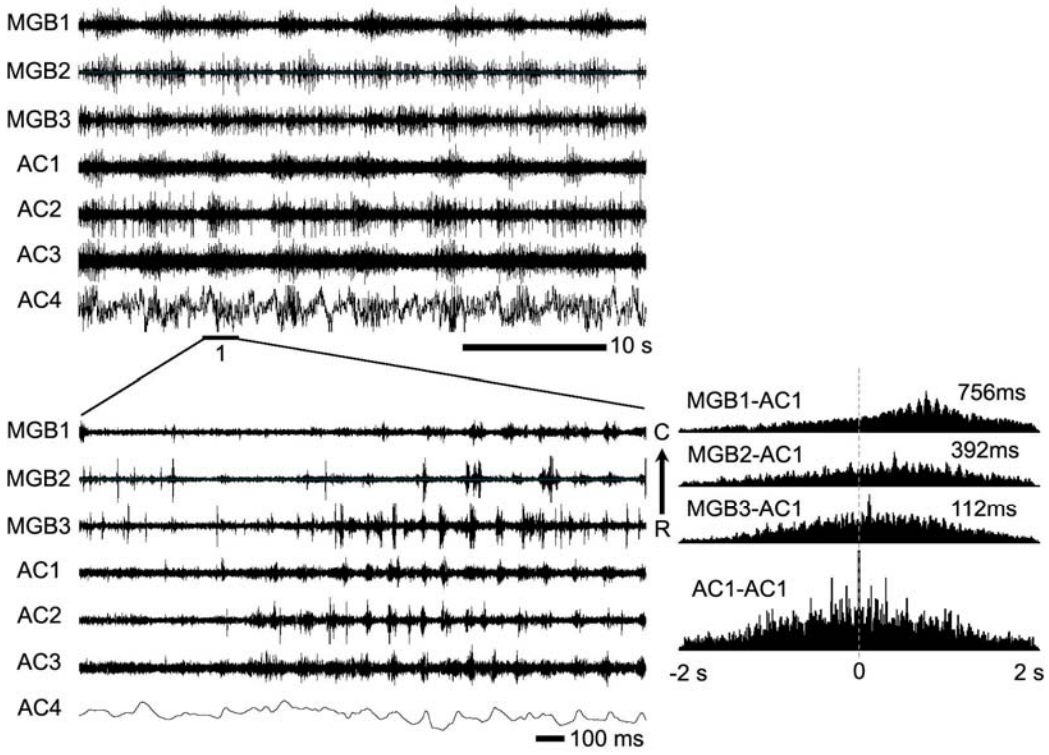

Figure 5.2 Propagation of spontaneous spindle oscillations across the AC and MGB. The epoch marked with 1 is expanded below. Animal was anesthetized with pentobarbital. Spindle sequences recurred once every ~5 s. The right panel shows the auto-correllogram of the AC activity and the cross-correlograms between the recordings of each thalamic (MGB1-3) site and the AC site. Correlogram was computed with a time window of 2 s. The spindles propagated from rostral to caudal in the MGB, with the AC sites preceding the MGB sites, similar to the cortically BIM-induced slow oscillations. Data obtained from **guinea pig**.

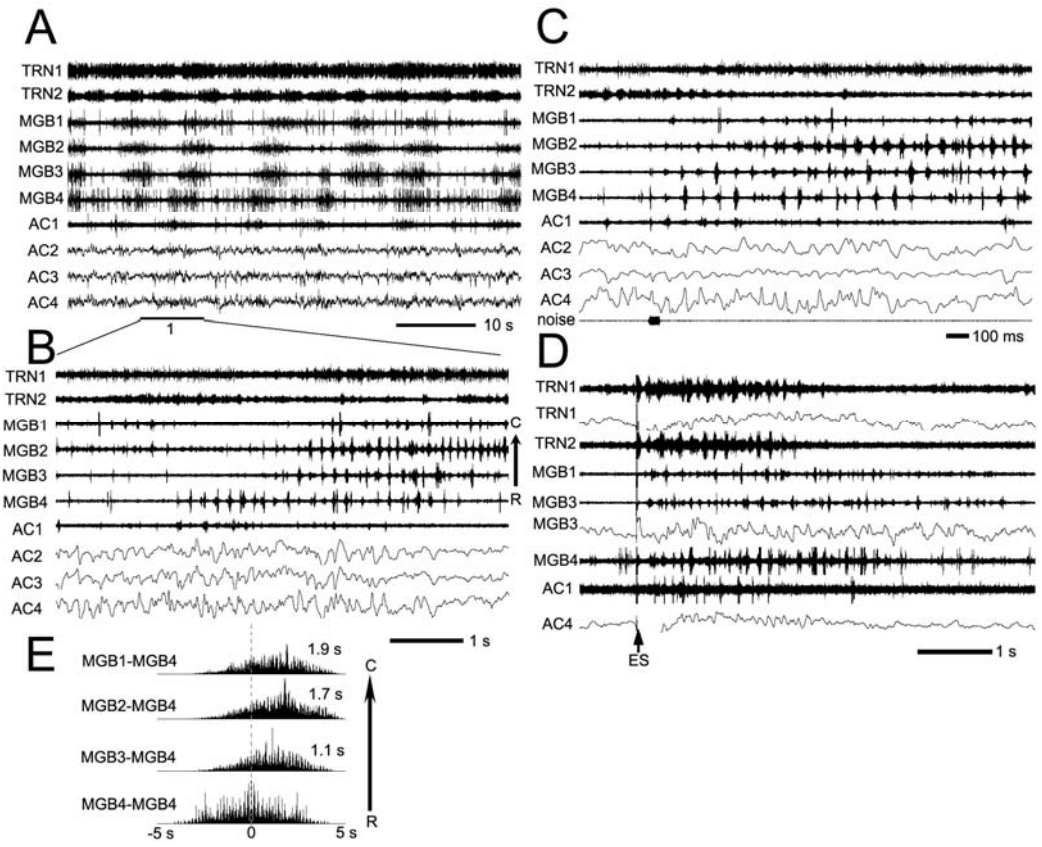

Figure 5.3 Propagation of spontaneous spindle oscillations across the AC, MGB and TRN (non-auditory). The epoch marked with 1 is expanded below (B). Animal was anesthetized with pentobarbital. Spindle sequences recurred once every ~5 s. The spindles are revealed to propagate from rostral to caudal in the MGB, with the AC sites preceding the MGB sites. No synchrony was observed between the TRN (non-auditory) and AC-MGB. (C) No acoustic responses to noise, were found in both TRN sites. (D) Responses to electrical stimulation of the AC (indicated by the upward arrow). (E) Auto-correllogram of the MGB4 activity and the cross-correlograms between the recordings of MGB1-3 and MGB4 sites. Correlogram was computed with a time window of 5 s. Data obtained from guinea pig.

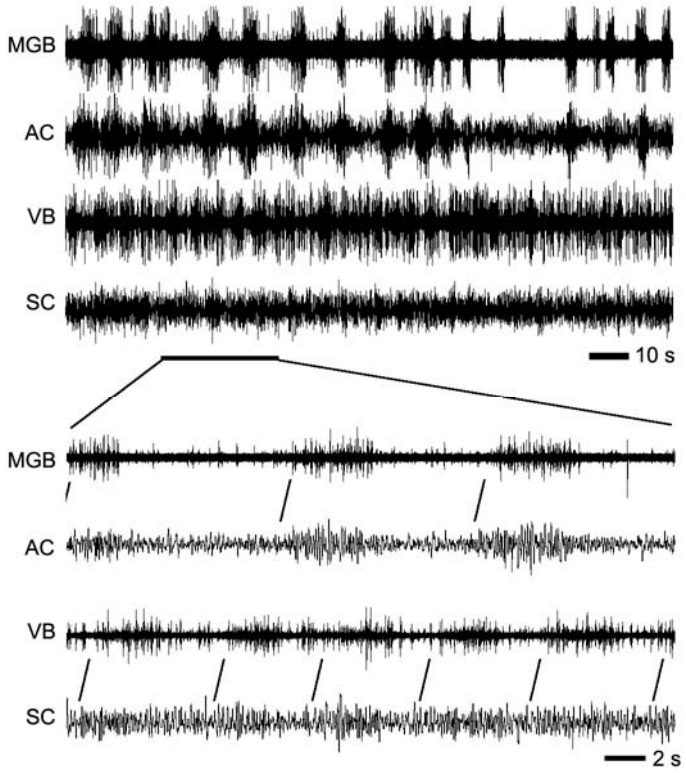

Figure 5.4 Spatially restricted distributions of spindle oscillations in different modalities (auditory *vs.* somatosensory). Animal was anesthetized with pentobarbital. Part marked by the horizontal line is expanded below. The oblique lines denote the correspondences of the epochs between AC and MGB, as well as between SC and VB. The inter-spindle frequencies for the auditory system and somatosensory system are different (~0.1 Hz for auditory system *vs.* ~0.16 Hz for somatosensory system), i.e., spindle rhythms recurred independently in the auditory and somatosensory systems. Data obtained from SD rat.

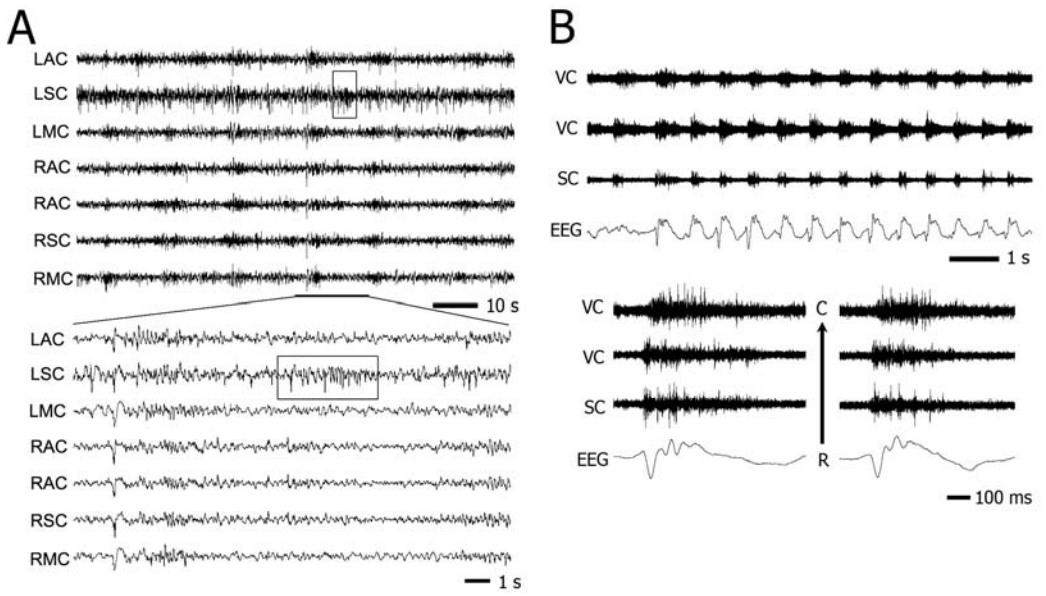

Figure 5.5 Global distributions of spindle oscillations in cerebral cortex across different modalities. Animals were anesthetized respectively with pentobarbital (A) and ketamine/xylazine (B). (A) Part marked by the horizontal line is expanded below. All signals were EEG, recorded from bilateral hemispheres. LAC: left auditory cortex, RAC: right auditory cortex, LMC: left motor cortex, etc. A more local spindle sequence in LSC is denoted by rectangle. Data obtained from guinea pig. (B) Neuronal discharges of VC and SC, as well as the pericruciate EEG were from the same hemisphere. Data obtained from SD rat.

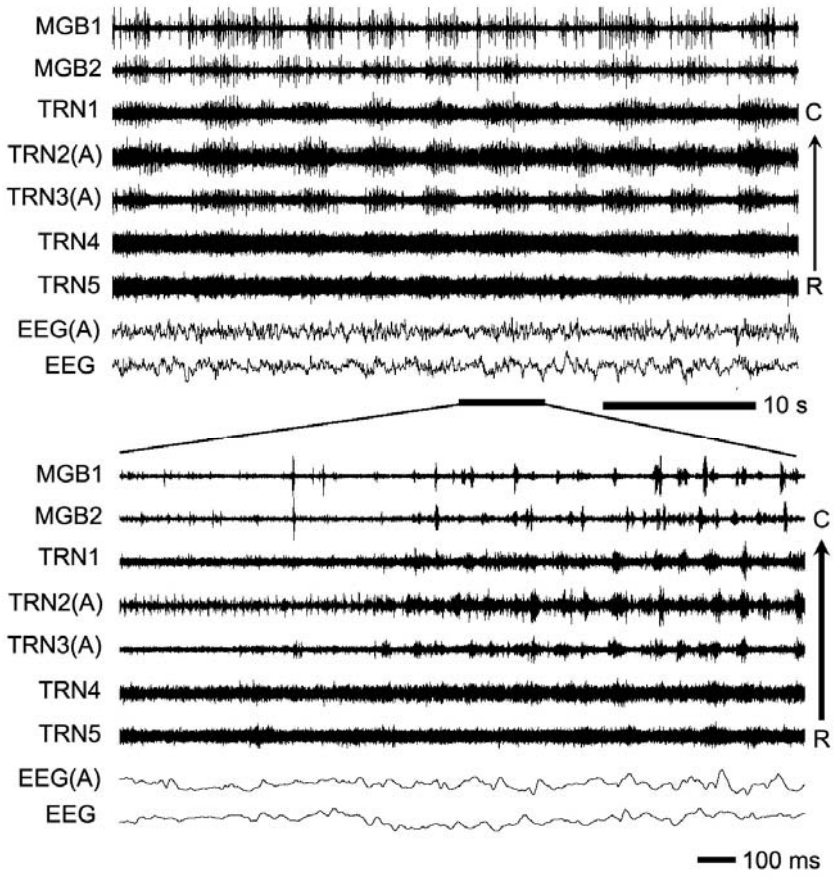

Figure 5.6 Propagation of spontaneous spindle oscillations across different modalities. Electrodes TRN5 to TRN1 were arranged from rostral to caudal with a inter-electrode distance of 200 μm. Only TRN2 and TRN3 responded to acoustic stimuli. A rostrocaudal propagation of spindles can be observed across the five TRN sites of different modalities. The propagation continued onto MGB sites, which are situated caudally to the TRN. MGB1 and MGB2 are in the same coronal section. Data obtained from guinea pig.

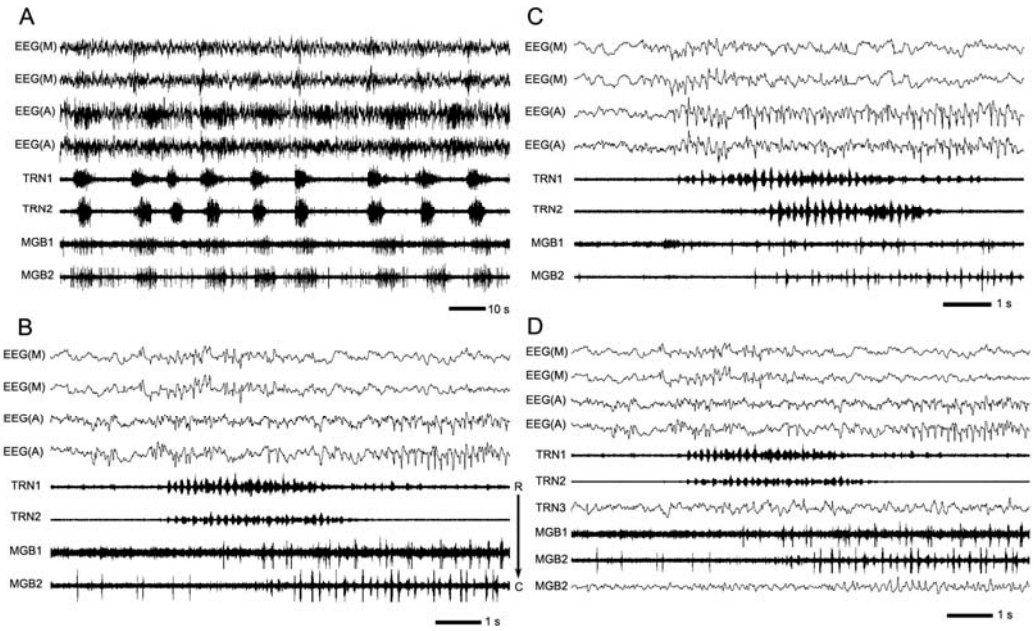

Figure 5.7 Propagation of spontaneous spindle oscillations across different modalities. The spindle oscillation travelled sequentially in a rostral to caudal fashion across two TRN sites (non-auditory) and two MGB sites, despite their different modalities. Two epochs are expanded in (B) and (C). (D) Local field potentials (LFP) from TRN3 and MGB2 also included. These local field potentials (including four EEG signals) faithfully reflected cellular events of local neuronal populations. Note that the positive deflections of the MGB2 corresponded to the burst discharges of the same electrode. Data obtained from guinea pig.

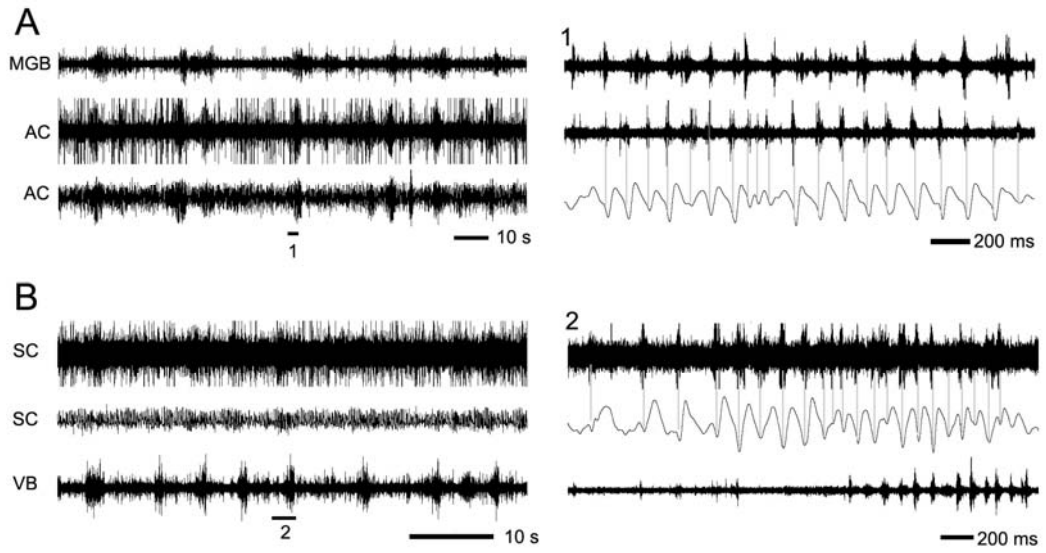

Figure 5.8 High fidelity of cortical LFPs to the local cellular events of neuronal populations. Two examples are shown in (A) and (B). (A) Synchronized spindle oscillation in the MGB and AC. The lower two traces (multiunit discharge and LFP, respectively) were recorded from the same electrode in the AC. (B) Synchronized spindle oscillation in the VB and SC, The upper two traces (multiunit discharge and LFP, respectively) were recorded from the same electrode in the SC. Parts marked with 1 and 2 are expanded on the right panel. The gray vertical lines denote the correspondences of the negative deflections in LFP to the burst discharges. Data obtained from SD rats.

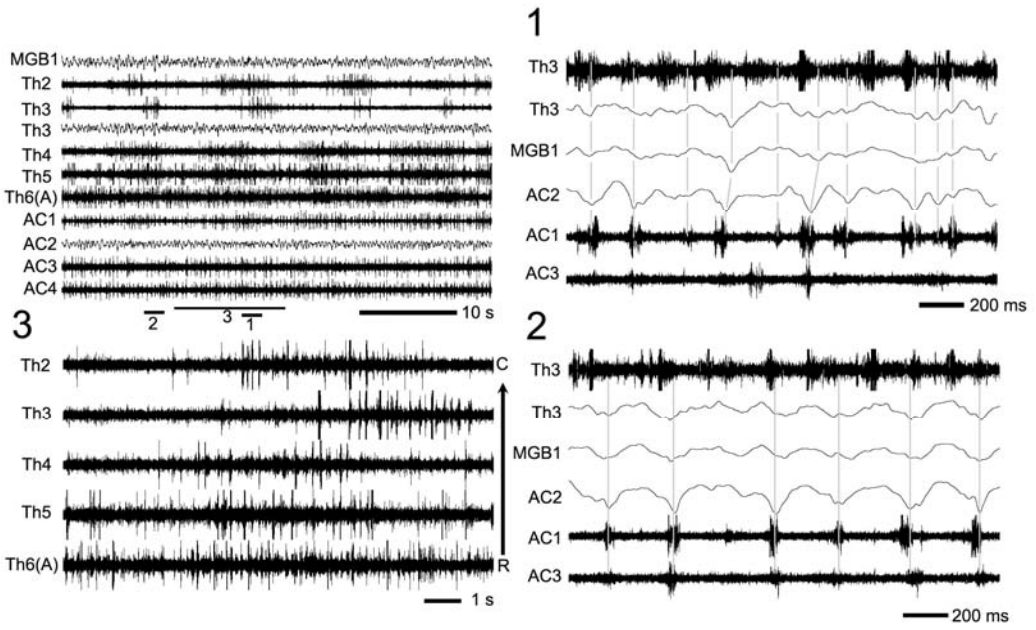

Figure 5.9 Correspondence of LFPs to the local cellular events of neuronal populations in the cerebral cortex and thalamus. Parts marked by 1, 2, 3 are expanded. The LFPs at AC2 were coherent with the neuronal discharges at an adjacent electrode AC1 with the negative deflection corresponding to the burst firings (epoch 1 and 2). The waves of LFPs at both MGB1 and Th3 shared great similarity with that of the cortical LFP (AC2), though some small deflections could be discerned to superimpose on the cortically-derived big waves when the spindle oscillation occurred in local thalamic sites (epoch 1 and 2). The correspondence between the positive/negative deflections and the neuronal spindle bursts in the thalamus, however, was too weak to be identified, even though they are recorded from the same electrode (Th3, epoch 1 and 2). Data obtained from SD rat.

Chapter 6

Summary of findings and conclusions

The present study investigated the mechanisms underlying the generation, synchronization, and propagation of the spontaneous slow rhythms in the corticothalamic network within a given modality and across different modalities in animals under anesthesia by using multi-channel extracellular recordings and immunohistochemical method.

Our results in Chapter 4 illustrated a cortically BIM-induced synchronized oscillation in the corticothalamic network and its triggered *c-fos* expression in the MGv. Five major findings are reported here. (1) We ascertained for the first time, that the MGv neurons can express Fos protein when AC is activated with cortical BIM (a $GABA_A$ receptor antagonist) injections, no matter whether acoustic stimuli are present or not. Instead, *c-fos* expression in the MGv is specific to the corticothalamic activation. (2) The BIM-induced corticothalamic synchronized oscillations of burst firing patterns are proposed to lead to the *c-fos* expression in the MGv. The association of *c-fos* expression and the corticothalamic synchronized oscillations is also envisioned in the other sensory corticothalamic network, suggesting a common principle behind. (3) The *c-fos* expression in the MGB and the corticothalamic synchronized oscillations triggered by the BIM-induced cortical activation are elicited through a direct

excitatory corticothalamic pathway, not by the indirect inhibitory pathway via the TRN. (4) The present study can not rule out the active role of TRN in this process, and the BIM-induced *c-fos* expressions in the TRN show both specific and cross–modality features. (5) BIM-induced burst discharges of the thalamocortical neurons are different from the spindle-related LTS burst firings. The present results conclude that *c-fos* expression is not simply associated with firing rate, but rather the firing pattern.

Our results in Chapter 5 demonstrated the propagations of slow rhythms in the corticothalamic network *in vivo* within a given modality (auditory) and across modalities in terms of BIM-induced and sleep or anesthesia-related slow oscillations. Four major findings are reported here. (1) Both bicuculline-induced slow oscillations and sleep- or anesthesia-related slow oscillations (<15 Hz) propagate in the same preferential direction from rostral to caudal in the thalamus within modality and across modalities. (2) When synchronized, the activity in cerebral cortex precedes that of the thalamic sites, at least within the same modality. (3) The slow oscillations can be of global distributions, showing nearly-simultaneous EEG or burst discharges in the bilateral hemispheres, or more local events of modality-dependence, recurring independently in different modality systems. (4) However, this modality-specific asynchrony is seldom observed among the TRN sites of different modalities, indicating strong intranuclear connections within the TRN. The results would propose that common principles probably governed the spatiotemporal patterns of different

oscillation types.

As a whole, the thesis can deepen our present understanding of the mechanisms for the generation, synchronization and propagation of the spontaneous activity in the corticothalamic network. Our result from the *in vivo* preparation showing that thalamocortical oscillations could occur without the participation of the TRN is a great addition to our present understanding that most thalamocortical oscillations need the inhibitory interaction of the TRN neurons. A study across different modalities can offer a more general view on the brain rhythms, suggesting that common principles probably govern the spatiotemporal patterns of different oscillation types. All in all, experimental evidence provided by the present study would further our understanding on the generation and propagation of synchronized excitability within the corticothalamic network of specific modality and across modalities.

References

Abbott LF, Nelson SB (2000) Synaptic plasticity: taming the beast. Nat Neurosci 3 Suppl:1178-1183.

Achermann P, Borbély A (1997a) Low-frequency (<1 Hz) oscillations in the human sleep EEG. Neuroscience 81: 213-222.

Achermann P, Borbély A (1997b) Low-frequency (<1 Hz) oscillations in the human sleep EEG. Neuroscience 81:213-222.

Adams JC (1995) Sound stimulation induces Fos-related antigens in cells with common morphological properties throughout the auditory brainstem. J Comp Neurol 361:645-668.

Alitto HJ, Usrey WM (2003) Corticothalamic feedback and sensory processing. Curr Opin Neurobiol 13:440-445.

Amzica F, Steriade M (1995a) Short- and long-range neuronal synchronization of the slow (< 1 Hz) cortical oscillation. J Neurophysiol 73:20-38.

Amzica F, Steriade M (1995b) Disconnection of intracortical synaptic linkages disrupts synchronization of a slow oscillation. J Neurosci 15:4658-4677.

Amzica F, Steriade M (1997) The K-complex: its slow (<1-Hz) rhythmicity and relation to delta waves. Neurology 49:952-959.

Andersen P, Andersson SA (1968) Physiological basis of the alpha rhythm. New York: Appleton-Century-Crofts.

Andersen P, Andersson SA, Lomo T (1966) Patterns of spontaneous rhythmic activity within various thalamic nuclei. Nature 211:888-889.

Andersen RA, Knight PL, Merzenich MN (1980) The thalamocortical and corticothalamic connections of AI, AII, and the anterior auditory field (AAF) in the cat: evidence for two largely segregated systems of connections. J Comp Neurol 194:663-701.

Arcelli P, Frassoni C, Regondi MC, De Biasi S, Spreafico R (1997) GABAergic neurons in mammalian thalamus: a marker of thalamic complexity. Brain

Res Bul 42:27-37.

Bal T, von Krosigk M, McCormick DA (1995a) Synaptic and membrane mechanisms underlying synchronized oscillations in the ferret lateral geniculate nucleus in vitro. J Physiol 483 (Pt 3):641-663.

Bal T, von Krosigk M, McCormick DA (1995b) Role of the ferret perigeniculate nucleus in the generation of synchronized oscillations in vitro. J Physiol 483 (Pt 3):665-685.

Bal T, Debay D, Destexhe A (2000) Cortical feedback controls the frequency and synchrony of oscillations in the visual thalamus. J Neurosci 20:7478-7488.

Barth DS, MacDonald KD (1996) Thalamic modulation of high-frequency oscillating potentials in auditory cortex. Nature 383:78-81.

Bazhenov M, Timofeev I, Steriade M, Sejnowski TJ (2002) Model of thalamocortical slow-wave sleep oscillations and transitions to activated States. J Neurosci 22:8691-8704.

Blumenfeld H, McCormick DA (2000) Corticothalamic inputs control the pattern of activity generated in thalamocortical networks. J Neurosci 20:5153-5162.

Bormann J (2000) The ‘ABC’ of GABA receptors. Trends Pharmacol. Sci. 21 (1), 16–19.

Buzsaki G (1991) Network properties of memory trace formation in the hippocampus. Boll Soc Ital Biol Sper 67:817-835.

Calford MB (1983) The parcellation of the medial geniculate body of the cat defined by the auditory response properties of single units. J Neurosci 3:2350-2364.

Calford MB, Webster WR (1981) Auditory representation within principal division of cat medial geniculate body: an electrophysiology study. J Neurophysiol 45:1013-1028.

Carretta D, Herve-Minvielle A, Bajo VM, Villa AE, Rouiller EM (1999) c-Fos expression in the auditory pathways related to the significance of

acoustic signals in rats performing a sensory-motor task. Brain Res 841:170-183.

Chebib M, Johnston GA (1999) The ‘ABC’ of GABA receptors: a brief review. Clin. Exp. Pharmacol. Physiol. 26 (11), 937–940.

Clarey JC, Irvine DR (1990) The anterior ectosylvian sulcal auditory field in the cat: I. An electrophysiological study of its relationship to surrounding auditory cortical fields. J Comp Neurol 301:289-303.

Conley M, Kupersmith AC, Diamond IT (1991) The Organization of Projections from Subdivisions of the Auditory Cortex and Thalamus to the Auditory Sector of the Thalamic Reticular Nucleus in Galago. Eur J Neurosci 3:1089-1103.

Contreras D, Steriade M (1995) Cellular basis of EEG slow rhythms: a study of dynamic corticothalamic relationships. J Neurosci 15:604-622.

Contreras D, Steriade M (1996) Spindle oscillation in cats: the role of corticothalamic feedback in a thalamically generated rhythm. J Physiol 490 (Pt 1):159-179.

Contreras D, Steriade M (1997) Synchronization of low-frequency rhythms in corticothalamic networks. Neuroscience 76:11-24.

Contreras D, Destexhe A, Sejnowski TJ, Steriade M (1996) Control of spatiotemporal coherence of a thalamic oscillation by corticothalamic feedback. Science 274:771-774.

Contreras D, Destexhe A, Sejnowski TJ, Steriade M (1997) Spatiotemporal patterns of spindle oscillations in cortex and thalamus. J Neurosci 17:1179-1196.

Coulter DA, Huguenard JR, Prince DA (1989) Calcium currents in rat thalamocortical relay neurones: kinetic properties of the transient, low-threshold current. J Physiol 414:587-604.

Crabtree JW (1998) Organization in the auditory sector of the cat's thalamic reticular nucleus. J Comp Neurol 390:167-182.

Crabtree JW, Killackey HP (1989) The Topographic Organization and Axis of

Projection within the Visual Sector of the Rabbit's Thalamic Reticular Nucleus. Eur J Neurosci 1:94-109.

Crabtree JW, Isaac JT (2002) New intrathalamic pathways allowing modality-related and cross-modality switching in the dorsal thalamus. J Neurosci 22:8754-8761.

Crick F (1984) Function of the thalamic reticular complex: the searchlight hypothesis. Proc Natl Acad Sci U S A 81:4586-4590.

Crunelli V, Lightowler S, Pollard CE (1989) A T-type Ca2+ current underlies low-threshold Ca2+ potentials in cells of the cat and rat lateral geniculate nucleus. J Physiol 413:543-561.

Crunelli V, Haby M, Jassik-Gerschenfeld D, Leresche N, Pirchio M (1988) Cl- - and K+-dependent inhibitory postsynaptic potentials evoked by interneurones of the rat lateral geniculate nucleus. J Physiol 399:153-176.

Cunningham MO, Whittington MA, Bibbig A, Roopun A, LeBeau FE, Vogt A, Monyer H, Buhl EH, Traub RD (2004) A role for fast rhythmic bursting neurons in cortical gamma oscillations in vitro. Proc Natl Acad Sci U S A 101:7152-7157.

Curtis DR, Johnston GA (1974) Amino acid transmitters in the mammalian central nervous system. Ergeb. Physiol. 69 (0), 97–188.

De Gennaro L, Ferrara M (2003) Sleep spindles: an overview, Sleep Med Rev: 423-440.

Descheenes M, Hu B (1990) Electrophysiology and Pharmacology of the Corticothalamic Input to Lateral Thalamic Nuclei: an Intracellular Study in the Cat. Eur J Neurosci 2:140-152.

Deschenes M, Roy JP, Steriade M (1982) Thalamic bursting mechanism: an inward slow current revealed by membrane hyperpolarization. Brain Res 239:289-293.

Destexhe A (1998) Spike-and-wave oscillations based on the properties of GABAB receptors. J Neurosci 18:9099-9111.

Destexhe A, Contreras D, Steriade M (1999a) Cortically-induced coherence of a thalamic-generated oscillation. Neuroscience 92:427-443.

Destexhe A, Contreras D, Steriade M (1999b) Neocortical excitability controls the coherence of thalamic-generated oscillations through corticothalamic feedback. Neuroscience 92 427-443.

Destexhe A, Contreras D, Sejnowski TJ, Steriade M (1994) A model of spindle rhythmicity in the isolated thalamic reticular nucleus. J Neurophysiol 72:803-818.

Destexhe A, Bal T, McCormick DA, Sejnowski TJ (1996a) Ionic mechanisms underlying synchronized oscillations and propagating waves in a model of ferret thalamic slices. J Neurophysiol 76:2049-2070.

Destexhe A, Contreras D, Steriade M, Sejnowski TJ, Huguenard JR (1996b) In vivo, in vitro, and computational analysis of dendritic calcium currents in thalamic reticular neurons. J Neurosci 16:169-185.

Edeline JM (1990) Frequency-specific plasticity of single unit discharges in the rat medial geniculate body. Brain Res 529:109-119.

Edeline JM, Weinberger NM (1992) Associative retuning in the thalamic source of input to the amygdala and auditory cortex: receptive field plasticity in the medial division of the medial geniculate body. Behav Neurosci 106:81-105.

Fell J, Elfadil H, Roschke J, Burr W, Klaver P, Elger CE, Fernandez G (2002) Human scalp recorded sigma activity is modulated by slow EEG oscillations during deep sleep. Int J Neurosci 112:893-900.

Fleidervish IA, Gutnick MJ (1996) Kinetics of slow inactivation of persistent sodium current in layer V neurons of mouse neocortical slices. J Neurophysiol 76:2125-2130.

Fuentealba P, Timofeev I, Steriade M (2004) Prolonged hyperpolarizing potentials precede spindle oscillations in the thalamic reticular nucleus. Proc Natl Acad Sci U S A 101:9816-9821.

Fuentealba P, Timofeev I, Bazhenov M, Sejnowski TJ, Steriade M (2005)

Membrane bistability in thalamic reticular neurons during spindle oscillations. J Neurophysiol 93:294-304.

Gaese BH, Ostwald J (1995) Temporal coding of amplitude and frequency modulation in the rat auditory cortex. Eur J Neurosci 7:438-450.

Galarreta M, Hestrin S (1998) Frequency-dependent synaptic depression and the balance of excitation and inhibition in the neocortex Nat Neurosci 1:587-594.

Golshani P, Jones EG (1999) Synchronized paroxysmal activity in the developing thalamocortical network mediated by corticothalamic projections and "silent" synapses. J Neurosci 19:2865-2875.

Golshani P, Warren RA, Jones EG (1998) Progression of change in NMDA, non-NMDA, and metabotropic glutamate receptor function at the developing corticothalamic synapse. J Neurophysiol 80:143-154.

Golshani P, Liu XB, Jones EG (2001) Differences in quantal amplitude reflect GluR4- subunit number at corticothalamic synapses on two populations of thalamic neurons. Proc Natl Acad Sci U S A 98:4172-4177.

Guillery RW, Sherman SM (2002) Thalamic relay functions and their role in corticocortical communication: generalizations from the visual system. Neuron 33:163-175.

Meeren, HK, Pijn, JP, Van Luijtelaar, EL, Coenen, AM, Lopes da Silva FH (2002) Cortical focus drives widespread corticothalamic networks during spontaneous absence seizures in rats. J Neurosci 22: 1480-1495.

He J (1997) Modulatory effects of regional cortical activation on the onset responses of the cat medial geniculate neurons. J Neurophysiol 77:896-908.

He J (2003a) Corticofugal modulation on both ON and OFF responses in the nonlemniscal auditory thalamus of the guinea pig. J Neurophysiol 89:367-381.

He J (2003b) Slow oscillation in non-lemniscal auditory thalamus. J Neurosci 23:8281-8290.

He J, Yu YQ, Xiong Y, Hashikawa T, Chan YS (2002) Modulatory effect of cortical activation on the lemniscal auditory thalamus of the Guinea pig. J Neurophysiol 88:1040-1050.

Hirsch JC, Fourment A, Marc ME (1983) Sleep-related variations of membrane potential in the lateral geniculate body relay neurons of the cat. Brain Res 259:308-312.

Hoogland PV, Welker E, Van der Loos H (1987) Organization of the projections from barrel cortex to thalamus in mice studied with Phaseolus vulgaris-leucoagglutinin and HRP. Exp Brain Res 68:73-87.

Hu B, He J (2002) Differential distribution of burst and single-spike responses in auditory thalamus. J Neurophysiol 88:2152-2156.

Hu B, Senatorov V, Mooney D (1994) Lemniscal and non-lemniscal synaptic transmission in rat auditory thalamus. J Physiol 479 (Pt 2):217-231.

Hughes JR (1995) The phenomenon of traveling waves: a review. Clin Electroencephalogr 26:1-6.

Hughes SW, Lorincz M, Cope DW, Blethyn KL, Kekesi KA, Parri HR, Juhasz G, Crunelli V (2004) Synchronized oscillations at alpha and theta frequencies in the lateral geniculate nucleus. Neuron 42:253-268.

Huguenard JR (1996) Low-threshold calcium currents in central nervous system neurons. Annu Rev Physiol 58:329-348.

Huguenard JR, Prince DA (1994a) Intrathalamic rhythmicity studied in vitro: nominal T-current modulation causes robust antioscillatory effects. J Neurosci 14:5485-5502.

Huguenard JR, Prince DA (1994b) Clonazepam suppresses GABAB-mediated inhibition in thalamic relay neurons through effects in nucleus reticularis. J Neurophysiol 71:2576-2581.

Imig TJ, Morel A (1983) Organization of the thalamocortical auditory system in the cat. Annu Rev Neurosci 6:95-120.

Imig TJ, Morel A (1984) Topographic and cytoarchitectonic organization of thalamic neurons related to their targets in low-, middle-, and

high-frequency representations in cat auditory cortex. J Comp Neurol 227:511-539.

Jahnsen H, Llinas R (1984a) Voltage-dependent burst-to-tonic switching of thalamic cell activity: an in vitro study. Arch Ital Biol 122:73-82.

Jahnsen H, Llinas R (1984b) Electrophysiological properties of guinea-pig thalamic neurones: an in vitro study. J Physiol 349:205-226.

Jahnsen H, Llinas R (1984c) Ionic basis for the electro-responsiveness and oscillatory properties of guinea-pig thalamic neurones in vitro. J Physiol 349:227-247.

Ji D and Wilson MA (2007) Coordinated memory replay in the visual cortex and hippocampus during sleep.Nat Neurosci 10:100-107.

Jinnah HA, Egami K, Rao L, Shin M, Kasim S, Hess EJ (2003) Expression of c-FOS in the brain after activation of L-type calcium channels. Dev Neurosci 25:403-411.

Johnson SW, Seutin V (1997) Bicuculline methiodide potentiates NMDA-dependent burst firing in rat dopamine neurons by blocking apamin-sensitive Ca2+-activated K+ currents. Neurosci. Lett. 231 (1),13–16.

Jones EG (1975) Some aspects of the organization of the thalamic reticular complex. J Comp Neurol 162:285-308.

Jones EG (1985) The Thalamus. New York: Plenum.

Jones EG (2002) Thalamic circuitry and thalamocortical synchrony. Philos Trans R Soc Lond B Biol Sci 357:1659-1673.

Kawakubo Y, Kasai K, Okazaki S, Hosokawa-Kakurai M, Watanabe K, Kuwabara H, Ishijima M, Yamasue H, Iwanami A, Kato N, Maekawa H (2007) Electrophysiological abnormalities of spatial attention in adults with autism during the gap overlap task. Clin Neurophysiol 118:1464-1471.

Keilmann A, Herdegen T (1997) The c-Fos transcription factor in the auditory pathway of the juvenile rat: effects of acoustic deprivation and repetitive

stimulation. Brain Res 753:291-298.

Kim U, McCormick DA (1998) The functional influence of burst and tonic firing mode on synaptic interactions in the thalamus. J Neurosci 18:9500-9516.

Kim U, Bal T, McCormick DA (1995) Spindle waves are propagating synchronized oscillations in the ferret LGNd in vitro. J Neurophysiol 74:1301-1323.

Kolmac CI, Mitrofanis J (1997) Organisation of the reticular thalamic projection to the intralaminar and midline nuclei in rats. J Comp Neurol 377:165-178.

Lai CH, Tse YC, Shum DK, Yung KK, Chan YS (2004) Fos expression in otolith-related brainstem neurons of postnatal rats following off-vertical axis rotation. J Comp Neurol 470:282-296.

Lai SK, Lai CH, Yung KK, Shum DK, Chan YS (2006) Maturation of otolith-related brainstem neurons in the detection of vertical linear acceleration in rats. Eur J Neurosci 23:2431-2446.

Lancel M, van Riezen H, Glatt A (1992) The time course of sigma activity and slow-wave activity during NREMS in cortical and thalamic EEG of the cat during baseline and after 12 hours of wakefulness. Brain Res 596:285-295.

Landisman CE, Long MA, Beierlein M, Deans MR, Paul DL, Connors BW (2002) Electrical synapses in the thalamic reticular nucleus. J Neurosci 22:1002-1009.

LeDoux JE, Farb C, Ruggiero DA (1990) Topographic organization of neurons in the acoustic thalamus that project to the amygdala. J Neurosci 10:1043-1054.

Lee AK and Wilson MA (2002) Memory of sequential experience in the hippocampus during slow wave sleep. Neuron 36:1183-1194.

Lee SM, Friedberg MH, Ebner FF (1994) The role of GABA-mediated inhibition in the rat ventral posterior medial thalamus. I. Assessment of

receptive field changes following thalamic reticular nucleus lesions. J Neurophysiol 71:1702-1715.

LeMasson G, Marder E, Abbott LF (1993) Activity-dependent regulation of conductances in model neurons. Science 259:1915-1917.

Lerea LS, Butler LS, McNamara JO (1992) NMDA and non-NMDA receptor-mediated increase of c-fos mRNA in dentate gyrus neurons involves calcium influx via different routes. J Neurosci 12:2973-2981.

Leresche N, Lightowler S, Soltesz I, Jassik-Gerschenfeld D, Crunelli V (1991) Low-frequency oscillatory activities intrinsic to rat and cat thalamocortical cells. J Physiol 441:155-174.

Li XF, Armony JL, LeDoux JE (1996) GABAA and GABAB teceptors differentially regulate synaptic transmission in the auditory thalamo-amygdala pathway: An in vivo microiontophoretic study and a model. Synapse 24 (2), 115–124.

Liu XB, Warren RA, Jones EG (1995) Synaptic distribution of afferents from reticular nucleus in ventroposterior nucleus of cat thalamus. J Comp Neurol 352:187-202.

Llinas R, Jahnsen H (1982) Electrophysiology of mammalian thalamic neurones in vitro. Nature 297:406-408.

Llinás R, Pare D (1997) Coherent Oscillations in Specific and Nonspecific Thalamocortical Networks and Their Role in Cognition. In: Thalamus Vol. II (Steriade M JE, McCormick DA., ed), pp 501-516. New York: Plenum.

Luo L, Ryan AF, Saint Marie RL (1999) Cochlear ablation alters acoustically induced c-fos mRNA expression in the adult rat auditory brainstem. J Comp Neurol 404:271-283.

Massimini M, Amzica F (2001) Extracellular calcium fluctuations and intracellular potentials in the cortex during the slow sleep oscillation. J Neurophysiol 85:1346-1350.

Massimini M, Huber R, Ferrarelli F, Hill S, Tononi G (2004) The sleep slow

oscillation as a traveling wave. J Neurosci 24:6862-6870.

McCarley RW, Winkelman JW, Duffy FH (1983) Human cerebral potentials associated with REM sleep rapid eye movements: links to PGO waves and waking potentials. Brain Res 274:359-364.

McCormick DA (1993) Actions of acetylcholine in the cerebral cortex and thalamus and implications for function. Prog Brain Res 98:303-308.

McCormick DA, Prince DA (1986) Acetylcholine induces burst firing in thalamic reticular neurones by activating a potassium conductance. Nature 319:402-405.

McCormick DA, Prince DA (1987) Actions of acetylcholine in the guinea-pig and cat medial and lateral geniculate nuclei, in vitro. J Physiol 392:147-165.

McCormick DA, Pape HC (1990a) Properties of a hyperpolarization-activated cation current and its role in rhythmic oscillation in thalamic relay neurones. J Physiol 431:291-318.

McCormick DA, Pape HC (1990b) Noradrenergic and serotonergic modulation of a hyperpolarization-activated cation current in thalamic relay neurones. J Physiol 431:319-342.

McCormick DA, Wang Z (1991) Serotonin and noradrenaline excite GABAergic neurones of the guinea-pig and cat nucleus reticularis thalami. J Physiol 442:235-255.

McCormick DA, von Krosigk M (1992) Corticothalamic activation modulates thalamic firing through glutamate "metabotropic" receptors. Proc Natl Acad Sci U S A 89:2774-2778.

McCormick DA, Bal T (1997) Sleep and arousal: thalamocortical mechanisms. Annu Rev Neurosci 20:185-215.

McGeer EG, Olney JW, McGeer PL (1978) Kainic acid as a tool in neurobiology. New York: Raven Press.

Meister M, Wong RO, Baylor DA, Shatz CJ (1991) Synchronous bursts of action potentials in ganglion cells of the developing mammalian retina. Science

252:939-943.

Metherate R (1998) Synaptic mechanisms in auditory cortex function. Front. Biosci. 3d, 494–501.

Metherate R, Ashe JH (1993) Ionic flux contributions to neocortical slow waves and nucleus basalis-mediated activation: whole-cell recordings in vivo. J Neurosci 13:5312-5323.

Mitrofanis J, Guillery RW (1993) New views of the thalamic reticular nucleus in the adult and the developing brain. Trends Neurosci 16:240-245.

Molle M, Marshall L, Gais S, Born J (2002) Grouping of spindle activity during slow oscillations in human non-rapid eye movement sleep. J Neurosci 22:10941-10947.

Monckton JE, McCormick DA (2002) Neuromodulatory role of serotonin in the ferret thalamus. J Neurophysiol 87:2124-2136.

Montero VM (1997) c-fos induction in sensory pathways of rats exploring a novel complex environment: shifts of active thalamic reticular sectors by predominant sensory cues. Neuroscience 76:1069-1081.

Montero VM, Guillery RW, Woolsey CN (1977) Retinotopic organization within the thalamic reticular nucleus demonstrated by a double label autoradiographic technique. Brain Res 138:407-421.

Montero VM, Wright LS, Siegel F (2001) Increased glutamate, GABA and glutamine in lateral geniculate nucleus but not in medial geniculate nucleus caused by visual attention to novelty. Brain Res 916:152-158.

Morgan JI, Curran T (1991) Stimulus-transcription coupling in the nervous system: involvement of the inducible proto-oncogenes fos and jun. Annu Rev Neurosci 14:421-451.

Morgan JI, Cohen DR, Hempstead JL, Curran T (1987) Mapping patterns of c-fos expression in the central nervous system after seizure. Science 237:192-197.

Mouritsen H, Janssen-Bienhold U, Liedvogel M, Feenders G, Stalleicken J, Dirks P, Weiler R (2004) Cryptochromes and neuronal-activity markers

colocalize in the retina of migratory birds during magnetic orientation. Proc Natl Acad Sci U S A 101:14294-14299.

Mulle C, Madariaga A, Deschenes M (1986) Morphology and electrophysiological properties of reticularis thalami neurons in cat: in vivo study of a thalamic pacemaker. J Neurosci 6:2134-2145.

Murphy PC, Sillito AM (1987) Corticofugal feedback influences the generation of length tuning in the visual pathway. Nature 329:727-729.

Neckelmann D, Amzica F, Steriade M (1998) Spike-wave complexes and fast components of cortically generated seizures. III. Synchronizing mechanisms. J Neurophysiol 80:1480-1494.

Newton JR, Ellsworth C, Miyakawa T, Tonegawa S, Sur M (2004) Acceleration of visually cued conditioned fear through the auditory pathway. Nat Neurosci 7:968-973.

Nunez A, Amzica F, Steriade M (1992a) Intrinsic and synaptically generated delta (1-4 Hz) rhythms in dorsal lateral geniculate neurons and their modulation by light-induced fast (30-70 Hz) events. Neuroscience 51:269-284.

Nunez A, Curro Dossi R, Contreras D, Steriade M (1992b) Intracellular evidence for incompatibility between spindle and delta oscillations in thalamocortical neurons of cat. Neuroscience 48:75-85.

Ojima H (1994) Terminal morphology and distribution of corticothalamic fibers originating from layers 5 and 6 of cat primary auditory cortex. Cereb Cortex 4:646-663.

Pape HC, McCormick DA (1989) Noradrenaline and serotonin selectively modulate thalamic burst firing by enhancing a hyperpolarization-activated cation current. Nature 340:715-718.

Pare D, Steriade M, Deschenes M, Oakson G (1987) Physiological characteristics of anterior thalamic nuclei, a group devoid of inputs from reticular thalamic nucleus. J Neurophysiol 57:1669-1685.

Paxinos G, Watson C (1998) The Rat Brain in Stereotaxic Coordinates, Deluxe

Fourth Edition with CD-Rom. San Diego: Acacemic Press.

Pinault D, Bourassa J, Deschenes M (1995) The axonal arborization of single thalamic reticular neurons in the somatosensory thalamus of the rat. Eur J Neurosci 7:31-40.

Rasch B, Born J (2007) Maintaining memories by reactivation. Curr Opin Neurobiol 17:698-703.

Rasch B, Buchel C, Gais S, Born J (2007) Odor cues during slow-wave sleep prompt declarative memory consolidation. Science 315:1426-1429.

Rapisarda C, Bacchelli B (1977) The brain of guinea pig in sterotaxic coordinated. Arch Sci Biol 61:1-37.

Rouiller EM, Welker E (1991) Morphology of corticothalamic terminals arising from the auditory cortex of the rat: a Phaseolus vulgaris-leucoagglutinin (PHA-L) tracing study. Hear Res 56:179-190.

Rouiller EM, Wan XS, Moret V, Liang F (1992) Mapping of c-fos expression elicited by pure tones stimulation in the auditory pathways of the rat, with emphasis on the cochlear nucleus. Neurosci Lett 144:19-24.

Sagar SM, Sharp FR, Curran T (1988) Expression of c-fos protein in brain: metabolic mapping at the cellular level. Science 240:1328-1331.

Saint Marie RL, Luo L, Ryan AF (1999) Effects of stimulus frequency and intensity on c-fos mRNA expression in the adult rat auditory brainstem. J Comp Neurol 404:258-270.

Sally SL, Kelly JB (1988) Organization of auditory cortex in the albino rat: sound frequency. J Neurophysiol 59:1627-1638.

Salt TE, Eaton SA (1996) Functions of ionotropic and metabotropic glutamate receptors in sensory transmission in the mammalian thalamus. Prog Neurobiol 48:55-72.

Sanchez-Vives MV, McCormick DA (2000) Cellular and network mechanisms of rhythmic recurrent activity in neocortex. Nat Neurosci 3:1027-1034.

Scharfman HE, Lu SM, Guido W, Adams PR, Sherman SM (1990) N-methyl-D-aspartate receptors contribute to excitatory postsynaptic

potentials of cat lateral geniculate neurons recorded in thalamic slices. Proc Natl Acad Sci U S A 87:4548-4552.

Scheich H, Zuschratter W (1995) Mapping of stimulus features and meaning in gerbil auditory cortex with 2-deoxyglucose and c-Fos antibodies. Behav Brain Res 66:195-205.

Schwindt PC, Spain WJ, Crill WE (1989) Long-lasting reduction of excitability by a sodium-dependent potassium current in cat neocortical neurons. . J Neurophysiol 61:233-244.

Semple MN, Kitzes LM (1993) Binaural processing of sound pressure level in cat primary auditory cortex: evidence for a representation based on absolute levels rather than interaural level differences. J Neurophysiol 69:449-461.

Sheng M, McFadden G, Greenberg ME (1990) Membrane depolarization and calcium induce c-fos transcription via phosphorylation of transcription factor CREB. Neuron 4:571-582.

Sheng M, Dougan ST, McFadden G, Greenberg ME (1988) Calcium and growth factor pathways of c-fos transcriptional activation require distinct upstream regulatory sequences. Mol Cell Biol 8:2787-2796.

Sherman SM, Guillery RW (2001) Exploring the thalamus. San Diego: Academic press.

Shinonaga Y, Takada M, Mizuno N (1994) Direct projections from the non-laminated divisions of the medial geniculate nucleus to the temporal polar cortex and amygdala in the cat. J Comp Neurol 340:405-426.

Shosaku A, Sumitomo I (1983) Auditory neurons in the rat thalamic reticular nucleus. Exp Brain Res 49:432-442.

Shosaku A, Kayama Y, Sumitomo I (1984) Somatotopic organization in the rat thalamic reticular nucleus. Brain Res 311:57-63.

Shosaku A, Kayama Y, Sumitomo I, Sugitani M, Iwama K (1989) Analysis of recurrent inhibitory circuit in rat thalamus: neurophysiology of the thalamic reticular nucleus. Prog Neurobiol 32:77-102.

Sillito AM (1975a) The contribution of inhibitory mechanisms to the receptive field properties of neurones in the striate cortex of the cat. J.Physiol. 250 (2), 305–329.

Sillito AM (1975b) The effectiveness of bicuculline as an antagonist of GABA and visually evoked inhibition in the cat's striate cortex. J. Physiol. 250 (2), 287–304.

Simon NR, Mandshanden I, Lopes da Silva FH (2000) A MEG study of sleep Brain Res 860:64-76.

Steriade M (1990) [Cholinergic control of thalamic function]. Arch Int Physiol Biochim 98:A11-46.

Steriade M (2002) Cortical coupling in sleep and paroxysmal oscillations International Congress Series 1226:71-85

Steriade M (2006) Grouping of brain rhythms in corticothalamic systems. Neuroscience 137:1087-1106.

Steriade M, Deschenes M (1984) The thalamus as a neuronal oscillator. Brain Res 320:1-63.

Steriade M, Llinas RR (1988) The functional states of the thalamus and the associated neuronal interplay. Physiol Rev 68:649-742.

Steriade M, McCarley RW (1990) Brainstem control of wakefulness and sleep. New York: Plenum.

Steriade M, Amzica F (1996) Intracortical and corticothalamic coherency of fast spontaneous oscillations. Proc Natl Acad Sci U S A 93:2533-2538.

Steriade M, Amzica F (1998) Slow sleep oscillation, rhythmic K-complexes, and their paroxysmal developments. J Sleep Res 7 Suppl 1:30-35.

Steriade M, Contreras D (1998) Spike-wave complexes and fast components of cortically generated seizures. I. Role of neocortex and thalamus. J Neurophysiol 80:1439-1455.

Steriade M, Timofeev I (2003) Neuronal plasticity in thalamocortical networks during sleep and waking oscillations. Neuron 37:563-576.

Steriade M, Apostol V, Oakson G (1972) [Systems of regulation of spontaneous and evoked activities of neurons in the thalamic motor relay]. Rev Can Biol 31:Suppl:131-152.

Steriade M, Oakson G, Kitsikis A (1978) Firing rates and patterns of output and nonoutput cells in cortical areas 5 and 7 of cat during the sleep-waking cycle. Exp Neurol 60:443-468.

Steriade M, Parent A, Hada J (1984) Thalamic projections of nucleus reticularis thalami of cat: a study using retrograde transport of horseradish peroxidase and fluorescent tracers. J Comp Neurol 229:531-547.

Steriade M, Dossi RC, Nunez A (1991a) Network modulation of a slow intrinsic oscillation of cat thalamocortical neurons implicated in sleep delta waves: cortically induced synchronization and brainstem cholinergic suppression. J Neurosci 11:3200-3217.

Steriade M, McCormick DA, Sejnowski TJ (1993a) Thalamocortical oscillations in the sleeping and aroused brain. Science 262:679-685.

Steriade M, Nunez A, Amzica F (1993b) A novel slow (< 1 Hz) oscillation of neocortical neurons in vivo: depolarizing and hyperpolarizing components. J Neurosci 13:3252-3265.

Steriade M, Nunez A, Amzica F (1993c) Intracellular analysis of relations between the slow (< 1 Hz) neocortical oscillation and other sleep rhythms of the electroencephalogram. J Neurosci 13:3266-3283.

Steriade M, Contreras D, Amzica F (1994) Synchronized sleep oscillations and their paroxysmal developments. Trends Neurosci 17:199-208.

Steriade M, Amzica F, Contreras D (1996a) Synchronization of fast (30-40 Hz) spontaneous cortical rhythms during brain activation. J Neurosci 16:392-417.

Steriade M, Jones EG, McCormick DA (1997) Thalamus. Amsterdam: Elsevier.

Steriade M, Timofeev I, Grenier F (2001) Natural waking and sleep states: a view from inside neocortical neurons. J Neurophysiol 85:1969-1985.

Steriade M, Deschenes M, Domich L, Mulle C (1985) Abolition of spindle

oscillations in thalamic neurons disconnected from nucleus reticularis thalami. J Neurophysiol 54:1473-1497.

Steriade M, Domich L, Oakson G, Deschenes M (1987) The deafferented reticular thalamic nucleus generates spindle rhythmicity. J Neurophysiol 57:260-273.

Steriade M, Dossi RC, Pare D, Oakson G (1991b) Fast oscillations (20-40 Hz) in thalamocortical systems and their potentiation by mesopontine cholinergic nuclei in the cat. Proc Natl Acad Sci U S A 88:4396-4400.

Steriade M, Contreras D, Curro Dossi R, Nunez A (1993d) The slow (< 1 Hz) oscillation in reticular thalamic and thalamocortical neurons: scenario of sleep rhythm generation in interacting thalamic and neocortical networks. J Neurosci 13:3284-3299.

Steriade M, Contreras D, Amzica F, Timofeev I (1996b) Synchronization of fast (30-40 Hz) spontaneous oscillations in intrathalamic and thalamocortical networks. J Neurosci 16:2788-2808.

Steriade M, Amzica F, Neckelmann D, Timofeev I (1998) Spike-wave complexes and fast components of cortically generated seizures. II. Extra- and intracellular patterns. J Neurophysiol 80:1456-1479.

Sun X, Xia Q, Lai CH, Shum DK, Chan YS, He J (2007) Corticofugal modulation of acoustically induced Fos expression in the rat auditory pathway. J Comp Neurol 501:509-525.

Tennigkeit F, Schwarz DW, Puil E (1999) Effects of metabotropic glutamate receptor activation in auditory thalamus. J Neurophysiol 82:718-729.

Timofeev I, Steriade M (1996) Low-frequency rhythms in the thalamus of intact-cortex and decorticated cats. J Neurophysiol 76:4152-4168.

Timofeev I, Steriade M (1997) Fast (mainly 30-100 Hz) oscillations in the cat cerebellothalamic pathway and their synchronization with cortical potentials. J Physiol 504 (Pt 1):153-168.

Timofeev I, Grenier F, Steriade M (1998) Spike-wave complexes and fast components of cortically generated seizures. IV. Paroxysmal fast runs in

cortical and thalamic neurons. J Neurophysiol 80:1495-1513.

Timofeev I, Grenier F, Bazhenov M, Sejnowski TJ, Steriade M (2000) Origin of slow cortical oscillations in deafferented cortical slabs. Cereb Cortex 10:1185-1199.

Timofeev I, Grenier F, Bazhenov M, Houweling AR, Sejnowski TJ, Steriade M (2002) Short- and medium-term plasticity associated with augmenting responses in cortical slabs and spindles in intact cortex of cats in vivo. J Physiol 542:583-598.

Toldi J FO, Wolff JR: (1986) Sensory interactive zones in the rat cerebral cortex. Neuroscience 18: 461-465.

Tsodyks MV, Markram H (1997) The neural code between neocortical pyramidal neurons depends on neurotransmitter release probability. Proc Natl Acad Sci USA 94:719-723.

Turner JP, Leresche N, Guyon A, Soltesz I, Crunelli V (1994) Sensory input and burst firing output of rat and cat thalamocortical cells: the role of NMDA and non-NMDA receptors. J Physiol 480 (Pt 2):281-295.

Ulrich D, Huguenard JR (1996) Gamma-aminobutyric acid type B receptor-dependent burst-firing in thalamic neurons: a dynamic clamp study. Proc Natl Acad Sci U S A 93:13245-13249.

Verzeano M, Negishi K (1960) Neuronal activity in cortical and thalamic networks. J Gen Physiol 43(6)Suppl:177-195.

Verzeano M, Laufer M, Spear P, McDonald S (1965) [The activity of the neuronal networks of the thalamus of monkeys]. Actual Neurophysiol (Paris) 6:223-251.

Villa AE, Rouiller EM, Simm GM, Zurita P, de Ribaupierre Y, de Ribaupierre F (1991) Corticofugal modulation of the information processing in the auditory thalamus of the cat. Exp Brain Res 86:506-517.

Villablanca J, Salinas-Zeballos ME (1972) Sleep-wakefulness, EEG and behavioral studies of chronic cats without the thalamus: the 'athalamic' cat. Arch Ital Biol 110:383-411.

von Krosigk M, Bal T, McCormick DA (1993) Cellular mechanisms of a synchronized oscillation in the thalamus. Science 261:361-364.

von Krosigk M, Monckton JE, Reiner PB, McCormick DA (1999) Dynamic properties of corticothalamic excitatory postsynaptic potentials and thalamic reticular inhibitory postsynaptic potentials in thalamocortical neurons of the guinea-pig dorsal lateral geniculate nucleus. Neuroscience 91:7-20.

White EL, Hersch SM (1982) A quantitative study of thalamocortical and other synapses involving the apical dendrites of corticothalamic projection cells in mouse SmI cortex. J Neurocytol 11:137-157.

Winer JA (1992) The functional architecture of the medial geniculate body and the primary auditory cortex; in Webster DB, Popper AN, Fay RR (eds): The Mammaliam Auditory Pathway: Neuroanatomy. New York: Springer.

Winer JA, Morest DK (1983) The neuronal architecture of the dorsal division of the medial geniculate body of the cat. A study with the rapid Golgi method. J Comp Neurol 221:1-30.

Winer JA, Larue DT (1987) Patterns of reciprocity in auditory thalamocortical and corticothalamic connections: study with horseradish peroxidase and autoradiographic methods in the rat medial geniculate body. J Comp Neurol 257:282-315.

Winer JA, Diamond IT, Raczkowski D (1977) Subdivisions of the auditory cortex of the cat: the retrograde transport of horseradish peroxidase to the medial geniculate body and posterior thalamic nuclei. J Comp Neurol 176:387-417.

Wong RO, Meister M, Shatz CJ (1993) Transient period of correlated bursting activity during development of the mammalian retina. Neuron 11:923-938.

Xiong Y, Yu YQ, Chan Y-S, He JF (2004) Effects of cortical stimulation on auditory-responsive thalamic neurones in anaesthetized guinea pigs. J

Physiol (Lond) 560:207-217.

Yen CT, Conley M, Hendry SH, Jones EG (1985) The morphology of physiologically identified GABAergic neurons in the somatic sensory part of the thalamic reticular nucleus in the cat. J Neurosci 5:2254-2268.

Yu XJ, Meng XK, Xu XX, He SG, H J. Catchment Areas of Thalamic Reticular Neurons in terms of Cortical and Thalamic Inputs (submitted)

Yu YQ, Xiong Y, Chan YS, He J (2004a) Corticofugal gating of auditory information in the thalamus: an in vivo intracellular recording study. J Neurosci 24:3060-3069.

Yu YQ, Xiong Y, Chan YS, He J (2004b) In vivo intracellular responses of the medial geniculate neurones to acoustic stimuli in anaesthetized guinea pigs. J Physiol 560:191-205.

Zhang JS, Kaltenbach JA, Wang J, Kim SA (2003) Fos-like immunoreactivity in auditory and nonauditory brain structures of hamsters previously exposed to intense sound. Exp Brain Res 153:655-660.

Zhang Z, Yu YQ, Liu CH, Chan YS, He J (2007) Frequency tuning and firing pattern properties of auditory thalamic neurons: An in vivo intracellular recording from the guinea pig. Neuroscience.

Zuschratter W, Gass P, Herdegen T, Scheich H (1995) Comparison of frequency-specific c-Fos expression and fluoro-2-deoxyglucose uptake in auditory cortex of gerbils (Meriones unguiculatus). Eur J Neurosci 7:1614-1626.